ISSN: 2146-1414

MIRT

Molecular Imaging and Radionuclide Therapy

October 2017 Volume 26 Issue 3 www.tsnm.org

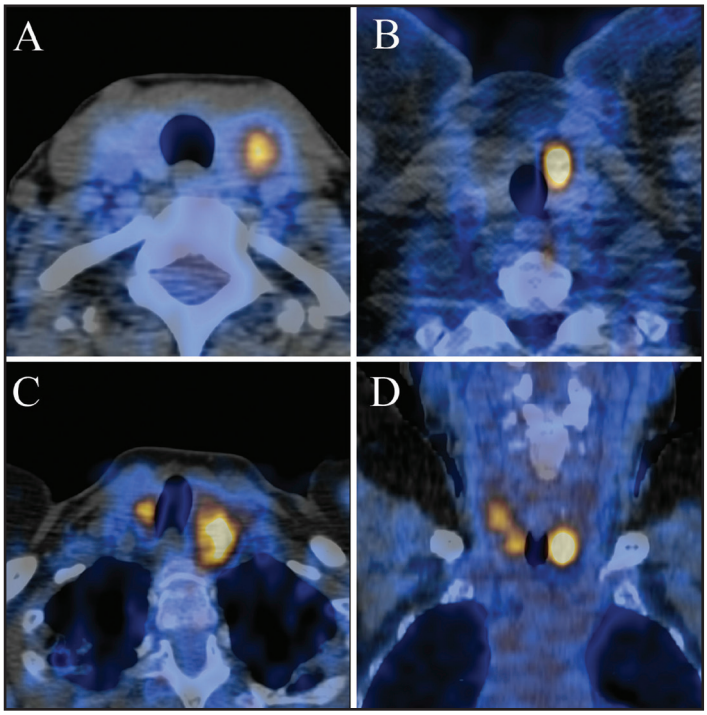

"Official Journal of the Turkish Society of Nuclear Medicine"

galenos yayinevi

TURKISH SOCIETY OF NUCLEAR MEDICINE 1975

MIRT

Molecular Imaging and Radionuclide Therapy

The Owner on Behalf of Turkish Society of Nuclear Medicine
Prof. Zehra Özcan, MD.
Ege University, Medical School, Department of Nuclear Medicine, İzmir, Turkey

Publishing Manager
Prof. Zehra Özcan, MD.
Ege University, Medical School, Department of Nuclear Medicine, İzmir, Turkey
E-mail: zehra.ozcan@yahoo.com

Editor in Chief
Prof. Zehra Özcan, MD.
Ege University, Medical School, Department of Nuclear Medicine, İzmir, Turkey
E-mail: zehra.ozcan@yahoo.com
ORCID ID: 0000-0002-6942-4704

Associate Editor
Associate Prof. Murat Fani Bozkurt, MD.
Hacettepe University, Medical School, Department of Nuclear Medicine, Ankara, Turkey
E-mail: fanibozkurt@gmail.com
ORCID ID: 0000-0003-2016-2624

Statistics Editors
Prof. Gül Ergör, MD.
Dokuz Eylül University, Medical School, Department of Public Health, İzmir, Turkey
E-mail: gulergor@deu.edu.tr

Prof. Sadettin Kılıçkap, MD.
Hacettepe University, Medical School, Department of Preventive Oncology, Ankara, Turkey
E-mail: skilickap@yahoo.com

English Language Editor
Didem Öncel Yakar, MD.
İstanbul, Turkey

Scientific Advisory Board

Ayşegül Akgün
Ege University, Medical School, Department of Nuclear Medicine, İzmir, Turkey
Esma Akın
The George Washington University, Medical School, Department of Diagnostic Radiology, Wahington DC, USA
Claudine Als
Hopitaux Robert Schuman Zitha Klinik, Médecine Nucléaire, Luxembourg
Vera Artiko
Clinical Center of Serbia, Center for Nuclear Medicine, Belgrade, Serbia
Nuri Arslan
Gülhane Training and Research Hospital, Clinic of Nuclear Medicine, Ankara, Turkey
Marika Bajc
Lund University Hospital, Clinic of Clinical Physiology, Lund, Sweden
Recep Bekiş
Dokuz Eylül University, Medical School, Department of Nuclear Medicine, İzmir, Turkey
Lorenzo Biassoni
Great Ormond Street Hospital for Children NHS Foundation Trust, Department of Radiology, London, United Kingdom
Hans Jürgen Biersack
University of Bonn, Department of Nuclear Medicine, Clinic of Radiology, Bonn, Germany
M. Donald Blaufox
Albert Einstein College of Medicine, Department of Radiology, Division of Nuclear Medicine, New York, USA
Patrick Bourguet
Centre Eugène Marquis, Department of Nuclear Medicine, Clinic of Radiology, Rennes, France
Adil Boz
Akdeniz University, Medical School, Department of Nuclear Medicine, Antalya, Turkey
Gülgün Büyükdereli
Çukurova University, Medical School, Department of Nuclear Medicine, Adana, Turkey
A. Cahid Civelek
NIH Clinical Center, Division of Nuclear Medicine, Bethesta, USA
Arturo Chiti
Humanitas University, Department of Biomedical Sciences; Humanitas Clinical and Research Center, Clinic of Nuclear Medicine, Milan, Italy
Josep Martin Comin
Hospital Universitari de Bellvitge, Department of Nuclear Medicine, Barcelona, Spain
Alberto Cuocolo
University of Naples Federico II, Department of Advanced Biomedical Sciences, Napoli, Italy
Tevfik Fikret Çermik
Health Sciences University, İstanbul Training and Research Hospital, Clinic of Nuclear Medicine, İstanbul, Turkey
Angelika Bischof Delaloye
University Hospital of Lausanne, Department of Radiology, Lausanne, Switzerland
Mustafa Demir
İstanbul University, Cerrahpaşa Medical School, Department of Nuclear Medicine, İstanbul, Turkey
Peter Josef Ell
University College Hospital, Institute of Nuclear Medicine, London, United Kingdom
Tanju Yusuf Erdil
Marmara University, Pendik Training and Research Hospital, Clinic of Nuclear Medicine, İstanbul, Turkey
Türkan Ertay
Dokuz Eylül University, Medical School, Department of Nuclear Medicine, İzmir, Turkey
Jure Fettich
University Medical Centre Ljubljana, Department for Nuclear Medicine, Ljubljana, Slovenia
Christiane Franzius
Klinikum Bremen Mitte Center, Center for Modern Diagnostics, Bremen, Germany
Lars Friberg
University of Copenhagen Bispebjerg Hospital, Department of Nuclear Medicine, Copenhagen, Denmark
Jørgen Frøkiær
Aarhus University Hospital, Clinic of Nuclear Medicine and PET, Aarhus, Denmark

MIRT

Molecular Imaging and Radionuclide Therapy

Maria Lyra Georgosopoulou
University of Athens, 1st Department of Radiology, Aretaieion Hospital, Radiation Physics Unit, Athens, Greece
Gevorg Gevorgyan
The National Academy of Sciences of Armenia, H. Buniatian Institute of Biochemistry, Yerevan, Armenia
Nedim Gülaldı
Dr. Sami Ulus Training and Research Hospital, Clinic of Nuclear Medicine, Ankara, Turkey
Seza Güleç
Florida International University Herbert Wertheim College of Medicine, Departments of Surgery and Nuclear Medicine, Miami, USA
Liselotte Højgaard
University of Copenhagen, Department of Clinical Physiology, Nuclear Medicine and PET, Rigshospitalet, Copenhagen, Denmark
Ora Israel
Tel Aviv University Sackler Medical School, Assaf Harofeh Medical Center, Clinic of Otolaryngology-Head and Neck Surgery, Haifa, Israel
Csaba Juhasz
Wayne State University, Medical School, Children's Hospital of Michigan, PET Center and Translational Imaging Laboratory, Detroit, USA
Metin Kır
Ankara University, Medical School, Department of Nuclear Medicine, Ankara, Turkey
Irena Dimitrova Kostadinova
Alexandrovska University Hospital, Clinic of Nuclear Medicine, Sofia, Bulgaria
Lale Kostakoğlu
The Mount Sinai Hospital, Clinic of Nuclear Medicine, New York, USA
Rakesh Kumar
All India Institute of Medical Sciences, Department of Nuclear Medicine, New Delhi, India
Georgios S. Limouris
Athens University, Medical School, Department of Nuclear Medicine, Athens, Greece
Luigi Mansi
Second University of Naples, Medical School, Department of Nuclear Medicine, Naples, Italy
Yusuf Menda
University of Iowa Health Care, Carver College of Medicine, Department of Radiology, Iowa City, USA
Vladimir Obradović
University of Belgrade, Faculty of Organizational Sciences, Department of Human Development Theory, Business Administration, Organizational Studies, Belgrade, Serbia
Özhan Özdoğan
Dokuz Eylül University, Medical School, Department of Nuclear Medicine, İzmir, Turkey
Asuman Yekta Özer
Hacettepe University, Faculty of Pharmacy, Department of Radiopharmaceutical, Ankara, Turkey
Elgin Özkan
Ankara University, Medical School, Department of Nuclear Medicine, Ankara, Turkey
Özlem Özmen
Atatürk Chest Diseases Hospital, Clinic of Nuclear Medicine, Ankara, Turkey
Berna Polack
Dokuz Eylül University, Medical School, Department of Nuclear Medicine, İzmir, Turkey
Francesca Pons
Hospital Clinic, Clinic of Nuclear Medicine, Barcelona, Spain
Monica Rossleigh
Sydney Children's Hospital, Clinic of Nuclear Medicine, Sydney, Australia
Haluk Burçak Sayman
İstanbul University, Cerrahpaşa Medical School, Department of Nuclear Medicine, İstanbul, Turkey
Dragana Sobic Saranovic
University of Belgrade, Medical School, Departments of Radiology, Oncology and Cardiology, Belgrade, Serbia
Mike Sathekge
University of Pretoria, Steve Biko Academic Hospital, Department of Nuclear Medicine, Pretoria, South Africa
Kerim Sönmezoğlu
İstanbul University, Cerrahpaşa Medical School, Department of Nuclear Medicine, İstanbul, Turkey
Zsolt Szabo
The Johns Hopkins Hospital, Divisions of Radiology and Radiological Science, Baltimore, USA
Istvan Szilvasi
Semmelweis University, Medical School, Department of Nuclear Medicine, Budapest, Hungary
Mathew L. Thakur
Thomas Jefferson University, Department of Radiology, Pennsylvania, USA
Bülent Turgut
Cumhuriyet University, Medical School, Department of Nuclear Medicine, Sivas, Turkey
Halil Turgut Turoğlu
Marmara University, Medical School, Department of Nuclear Medicine, İstanbul, Turkey
Gülin Uçmak
Health Sciences University, Ankara Oncology Training and Research Hospital, Clinic of Nuclear Medicine, Ankara, Turkey
Doğangün Yüksel
Pamukkale University, Medical School, Department of Nuclear Medicine, Denizli, Turkey

Turkish Society of Nuclear Medicine
Cinnah Caddesi Pilot Sokak No: 10/12 Çankaya 06650 Ankara, Turkey **Phone:** +90 312 441 00 45 **Fax:** +90 312 441 12 95 **Web:** www.tsnm.org **E-mail:** dernekmerkezi@tsnm.org
"Formerly Turkish Journal of Nuclear Medicine"

♾ The paper used to print this journal conforms to ISO 9706: 1994 standard (Requirements for Permanence). The National Library of Medicine suggests that biomedical publications be printed on acid-free paper (alkaline paper). Reviewing the articles' conformity to the publishing standards of the Journal, typesetting, reviewing and editing the manuscripts and abstracts in English, creating links to source data, and publishing process are realized by Galenos.

galenos yayınevi

Publisher
Erkan Mor

Publication Director
Nesrin Çolak

Web Coordinators
Eren Arsel
Soner Yıldırım
Turgay Akpınar

Graphics Department
Ayda Alaca
Çiğdem Birinci

Project Coordinators
Ebru Boz
Eda Kolukısa
Hatice Balta
Lütfiye Ayhan İrtem
Melis Kuru
Zeynep Altındağ

Finance Coordinator
Sevinç Çakmak

Publisher Contact
Address: Molla Gürani Mah. Kaçamak Sk. No: 21/1
34093 İstanbul, Turkey
Phone: +90 (212) 621 99 25 **Fax:** +90 (212) 621 99 27
E-mail: info@galenos.com.tr/yayin@galenos.com.tr
Web: www.galenos.com.tr

Printing at: Bizim Basım Limited Şirketi
Litros Yolu 2. Matbaacılar Sitesi ZD1 Topkapı, İstanbul, Turkey
Phone: +90 (212) 709 75 25
Printing Date: October 2017
ISSN: 2146-1414 **E-ISSN:** 2147-1959
International scientific journal published quarterly.

MIRT

Molecular Imaging and Radionuclide Therapy

ABOUT US

Molecular Imaging and Radionuclide Therapy (formerly Turkish Journal of Nuclear Medicine) is the official publication of Turkish Society of Nuclear Medicine.

Focus and Scope

Molecular Imaging and Radionuclide Therapy (Mol Imaging Radionucl Ther, MIRT) is a double-blind peer-review journal published in English language. It publishes original research articles, reviews, editorials, short communications, letters, consensus statements, guidelines and case reports with a literature review on the topic, interesting images in the field of molecular imaging, multimodality imaging, nuclear medicine, radionuclide therapy, radiopharmacy, medical physics, dosimetry and radiobiology. MIRT is published three times a year (February, June, October). Audience: Nuclear medicine physicians, medical physicists, radiopharmaceutical scientists, radiobiologists.

The editorial policies are based on the "Recommendations for the Conduct, Reporting, Editing, and Publication of Scholarly Work in Medical Journals (ICMJE Recommendations)" by the International Committee of Medical Journal Editors (2016, archived at http://www.icmje.org/) rules.

Open Access Policy

This journal provides immediate open access to its content on the principle that making research freely available to the public supports a greater global exchange of knowledge.

Open Access Policy is based on rules of Budapest Open Access Initiative (BOAI) (http://www.budapestopenaccessinitiative.org/). By "open access" to [peer-reviewed research literature], we mean its free availability on the public internet, permitting any users to read, download, copy, distribute, print, search, or link to the full texts of these articles, crawl them for indexing, pass them as data to software, or use them for any other lawful purpose, without financial, legal, or technical barriers other than those inseparable from gaining access to the internet itself. The only constraint on reproduction and distribution, and the only role for copyright in this domain, should be to give authors control over the integrity of their work and the right to be properly acknowledged and cited.

This journal is licensed under a Creative Commons 3.0 International License.

Permission Requests

Permission required for use any published under CC-BY-NC license with commercial purposes (selling, etc.) to protect copyright owner and author rights). Republication and reproduction of images or tables in any published material should be done with proper citation of source providing authors names; article title; journal title; year (volume) and page of publication; copyright year of the article.

Instructions for Authors

Instructions for authors are published in the journal and on the website http://mirt.tsnmjournals.org

Manuscripts can only be submitted electronically through the Journal Agent website (http://www.journalagent.com/mirt/?plng=eng) after creating an account. This system allows online submission and review.

All published volumes in full text can be reached free of charge through the website http://mirt.tsnmjournals.org

Material Disclaimer

Scientific and legal responsibilities pertaining to the papers belong to the authors. Contents of the manuscripts and accuracy of references are also the author's responsibility. The Turkish Society of Nuclear Medicine, the Editor, the Editorial Board or the publisher do not accept any responsibility for opinions expressed in articles.

Financial expenses of the journal are covered by Turkish Society of Nuclear Medicine.

Correspondence Address

Editor-in-Chief, Prof. Zehra Özcan, MD,

Ege University, Medical School, Department of Nuclear Medicine, İzmir, Turkey

Phone: +90 312 441 00 45

Fax: +90 312 441 12 97

E-mail: editor@tsnmjournals.org

Web page: http://mirt.tsnmjournals.org

Publisher Corresponding Address

Galenos Yayınevi Tic. Ltd. Şti.

Address: Molla Gürani Mah. Kaçamak Sk. No: 21/1 34093

Fındıkzade, İstanbul, Turkey

Phone: +90 212 621 99 25

Fax: +90 212 621 99 27

E-mail: info@galenos.com.tr

The journal is printed on an acid-free paper.

MIRT

Molecular Imaging and Radionuclide Therapy

INSTRUCTIONS TO AUTHORS

Molecular Imaging and Radionuclide Therapy (Mol Imaging Radionucl Ther, MIRT) publishes original research articles, short communications, reviews, editorials, case reports with a literature review on the topic, interesting images, consensus statements, guidelines, letters in the field of molecular imaging, multimodality imaging, nuclear medicine, radionuclide therapy, radiopharmacy, medical physics, dosimetry and radiobiology. MIRT is published by the Turkish Society of Nuclear Medicine three times a year (February, June, October). The journal is printed on an acid-free paper.

Molecular Imaging and Radionuclide Therapy does not charge any article submission or processing fees.

GENERAL INFORMATION

MIRT commits to rigorous peer review, and stipulates freedom from commercial influence, and promotion of the highest ethical and scientific standards in published articles. Neither the Editor(s) nor the publisher guarantees, warrants or endorses any product or service advertised in this publication. All articles are subject to review by the editors and peer reviewers. If the article is accepted for publication, it may be subjected to editorial revisions to aid clarity and understanding without changing the data presented.

Manuscripts must be written in English and must meet the requirements of the journal. The journal is in compliance with the uniform requirements for manuscripts submitted to biomedical journals published by the International Committee of Medical Journal Editors (NEJM 1997; 336:309-315, updated 2016). Manuscripts that do not meet these requirements will be returned to the author for necessary revision before the review. Authors of manuscripts requiring modifications have a maximum of two months to resubmit the revised text. Manuscripts returned after this deadline will be treated as new submissions.

It is the authors' responsibility to prepare a manuscript that meets ethical criteria. The Journal adheres to the principles set forth in the Helsinki Declaration October 2013 (https://www.wma.net/policies-post/wma-declaration-of-helsinki-ethical-principles-for-medical-research-involving-human-subjects/) and holds that all reported research involving "Human beings" conducted in accordance with such principles.

Reports describing data obtained from research conducted in human participants must contain a statement in the MATERIALS AND METHODS section indicating approval by the ethical review board (including the approval number) and affirmation that INFORMED CONSENT was obtained from each participant.

All manuscripts reporting experiments using animals must include a statement in the MATERIALS AND METHODS section giving assurance that all animals have received humane care in compliance with the Guide for the Care and Use of Laboratory Animals (www.nap.edu) and indicating approval by the ethical review board.

If the study should have ethical approval, authors asked to provide ethical approval in order to proceed the review process. If they provide approval, review of the manuscript will continue.

In case report(s) and interesting image(s) a statement regarding the informed consent of the patients should be included in the manuscript and the identity of the patient(s) should be hidden.

Subjects must be identified only by number or letter, not by initials or names. Photographs of patients' faces should be included only if scientifically relevant. Authors must obtain written consent from the patient for use of such photographs.

In cases of image media usage that potentially expose patients' identity requires obtaining permission for publication from the patients or their parents/guardians.

If the proposed publication concerns any commercial product, the author must include in the cover letter a statement indicating that the author(s) has (have) no financial or other interest with the product or explaining the nature of any relations (including consultancies) between the author(s) and editor the manufacturer or distributor of the product.

All submissions will be screened by Crossref Smilarity Check powered by "iThenticate". Manuscripts with an overall similarity index of greater than 25%, or duplication rate at or higher than 5% with a single source will be returned back to authors.

MANUSCRIPT CATEGORIES

1. Original Articles

2. Short Communications are short descriptions of focused studies with important, but very straightforward results.

3. Reviews address important topics in the field. Authors considering the submission of uninvited reviews should contact the editor in advance to determine if the topic that they propose is of current potential interest to the Journal. Reviews will be considered for publication only if they are written by authors who have at least three published manuscripts in the international peer reviewed journals and these studies should be cited in the review. Otherwise only invited reviews will be considered for peer review from qualified experts in the area.

4. Editorials are usually written by invitation of the editor by the editors on current topics or by the reviewers involved in the evaluation of a submitted manuscript and published concurrently with that manuscript.

5. Case Report and Literature Reviews are descriptions of a case or small number of cases revealing a previously undocumented disease process, a unique unreported manifestation or treatment of a known disease process, unique unreported complications of treatment regimens or novel and important insights into a condition's pathogenesis, presentation, and/or management. The journal's policy is to accept case reports only if it is accompanied by a review of the literature on the related topic. They should include an adequate number of images and figures.

6. Interesting Image

One of the regular parts of Molecular Imaging and Radionuclide Therapy is a section devoted to interesting images. Interesting image(s) should describe case(s) which are unique and include interesting findings adding insights into the interpretation of patient images, a condition's pathogenesis, presentation, and/or management.

7. Consensus Statements or Guidelines may be submitted by professional societies. All such submissions will be subjected to peer review, must be modifiable in response to criticisms, and will be published only if they meet the Journal's usual editorial standards.

8. Letters to the Editor may be submitted in response to work that has been published in the Journal. Letters should be short commentaries related to specific points of agreement or disagreement with the published work.

Note on Prior Publication

Articles are accepted for publication on the condition that they are original, are not under consideration by another journal, or have not been previously

MIRT
Molecular Imaging and Radionuclide Therapy

published. Direct quotations, tables, or illustrations that have appeared in copyrighted material must be accompanied by written permission for their use from the copyright owner and authors. Materials previously published in whole or in part shall not be considered for publication. At the time of submission, authors must report that the manuscript has not been published elsewhere. Abstracts or posters displayed at scientific meetings need not be reported.

MANUSCRIPT SUBMISSION PROCEDURES

MIRT only accepts electronic manuscript submission at the web site http://www.journalagent.com/mirt/. After logging on to the website Click the 'online manuscript submission' icon. All corresponding authors should be provided with a password and a username after entering the information required. If you already have an account from a previous submission, enter your username and password to submit a new or revised manuscript. If you have forgotten your username and/or password, please send an e-mail to the editorial office for assistance. After logging on to the article submission system please read carefully the directions of the system to give all needed information and attach the manuscript, tables and figures and additional documents.

All Submissions Must Include:

1. Completed Copyright Assignment & Disclosure of Potential Conflict of Interest Form; This form should be downloaded from the website (provided in the author section), filled in thoroughly and uploaded to the website during the submission.
2. All manuscripts describing data obtained from research conducted in human participants must be accompanied with an approval document by the ethical review board.
3. All manuscripts reporting experiments using animals must include approval document by the animal ethical review board.
4. All submissions must include the authorship contribution form which is signed by all authors.

Authors must complete all online submission forms. If you are unable to successfully upload the files please contact the editorial office by e-mail.

MANUSCRIPT PREPARATION

General Format

The Journal requires that all submissions be submitted according to these guidelines:

- Text should be double spaced with 2.5 cm margins on both sides using 12-point type in Times Roman font.
- All tables and figures must be placed after the text and must be labeled.
- Each section (abstract, text, references, tables, figures) should start on a separate page.
- Manuscripts should be prepared as a word document (*.doc) or rich text format (*.rtf).
- Please make the tables using the table function in Word.
- Abbreviations should be defined in parenthesis where the word is first mentioned and used consistently thereafter.
- Results should be expressed in metric units. Statistical analysis should be done accurately and with precision. Please consult a statistician if necessary.
- Authors' names and institutions should not be included in the manuscript text and should be written only in the title page.

Title Page

The title page should be a separate form from the main text and should include the following:

- Full title (in English and in Turkish). Turkish title will be provided by the editorial office for the authors who are not Turkish speakers.
- Authors' names and institutions.
- Short title of not more than 40 characters for page headings.
- At least three and maximum eight keywords. (in English and in Turkish). Do not use abbreviations in the keywords. Turkish keywords will be provided by the editorial office for the authors who are not Turkish speakers. If you are not a native Turkish speaker, please reenter your English keywords to the area provided for the Turkish keywords. English keywords should be provided from http://www.nlm.nih.gov/mesh (Medical Subject Headings) while Turkish keywords should be provided from http://www.bilimterimleri.com.
- Word count (excluding abstract, figure legends and references).
- Corresponding author's e-mail and address, telephone and fax numbers.
- Name and address of person to whom reprint requests should be addressed.

Original Articles

Authors are required to state in their manuscripts that ethical approval from an appropriate committee and informed consents of the patients were obtained.

Original Articles should be submitted with a structured abstract of no more than 250 words. All information reported in the abstract must appear in the manuscript. The abstract should not include references. Please use complete sentences for all sections of the abstract. Structured abstract should include background, objective, methods, results and conclusions. Turkish abstract will be provided by the editorial office for the authors who are not Turkish speakers. If you are not a native Turkish speaker, please reenter your English abstract to the area provided for the Turkish abstract.

- Introduction
- Materials and Methods
- Results
- Discussion
- Study Limitations
- Conclusion

May be given for contributors who are not listed as authors, or for grant support of the research.

References should be cited in numerical order (in parentheses) in the text and listed in the same numerical order at the end of the manuscript on a separate page or pages. The author is responsible for the accuracy of references. Examples of the reference style are given below. Further examples will be found in the articles describing the Uniform Requirements for Manuscripts Submitted to Biomedical Journals (Ann Intern Med.1988; 208:258-265, Br Med J. 1988; 296:401-405). The titles of journals should be abbreviated according to the style used in the Index Medicus. Journal Articles and Abstracts: Surnames and initials of author's name, title of the article, journal name, date, volume number, and pages. All authors should be listed regardless of number. The citation of unpublished papers, observations or personal communications is not permitted. Citing an abstract is

not recommended. Books: Surnames and initials of author's names, chapter title, editor's name, book title, edition, city, publisher, date and pages.

Sample References

Journal Article: Sayit E, Söylev M, Capa G, Durak I, Ada E, Yilmaz M. The role of technetium-99m-HMPAO-labeled WBC scintigraphy in the diagnosis of orbital cellulitis. Ann Nucl Med 2001;15:41-44.

Erselcan T, Hasbek Z, Tandogan I, Gumus C, Akkurt I. Modification of Diet in Renal Disease equation in the risk stratification of contrast induced acute kidney injury in hospital inpatients. Nefrologia 2009 doi: 10.3265/Nefrologia.2009.29.5.5449.en.full.

Article in a journal published ahead of print: Ludbrook J. Musculovenous pumps in the human lower limb. Am Heart J 2009;00:1-6. (accessed 20 February 2009).

Lang TF, Duryea J. Peripheral Bone Mineral Assessment of the Axial Skeleton: Technical Aspects. In: Orwoll ES, Bliziotes M (eds). Osteoporosis: Pathophsiology and Clinical Management. New Jersey, Humana Pres Inc, 2003;83-104.

Books: Greenspan A. Orthopaedic Radiology a Pratical Approach. 3th ed. Philadelphia, Lippincott Williams Wilkins 2000, 295-330.

Website: Smith JR. 'Choosing Your Reference Style', Online Referencing 2(3), http://orj.sagepub.com (2003, accessed October 2008).

- Tables

Tables must be constructed as simply as possible. Each table must have a concise heading and should be submitted on a separate page. Tables must not simply duplicate the text or figures. Number all tables in the order of their citation in the text. Include a title for each table (a brief phrase, preferably no longer than 10 to 15 words). Include all tables in a single file following the manuscript.

– Figure Legends

Figure legends should be submitted on a separate page and should be clear and informative.

– Figures

Number all figures (graphs, charts, photographs, and illustrations) in the order of their citation in the text. At submission, the following file formats are acceptable: AI, EMF, EPS, JPG, PDF, PPT, PSD, TIF. Figures may be embedded at the end of the manuscript text file or loaded as separate files for submission. All images MUST be at or above intended display size, with the following image resolutions: Line Art 800 dpi, Combination (Line Art + Halftone) 600 dpi, Halftone 300 dpi. Image files also must be cropped as close to the actual image as possible.

Short Communications:

Short communications should be submitted with a structured abstract of no more than 200 words. These manuscripts should be no longer than 2000 words, and include no more than two figures and tables and 20 references. Other rules which the authors are required to prepare and submit their manuscripts are the same as described above for the original articles.

Review Articles:

- Title page (see above)
- Abstract: Maximum 250 words; without structural divisions; in English and in Turkish . Turkish abstract will be provided by the editorial office for the authors who are not Turkish speakers. If you are not a native Turkish speaker, please reenter your English abstract to the area provided for the Turkish abstract.
- Text
- Conclusion
- Acknowledgements (if any)
- References

Editorial:

- Title page (see above)
- Abstract: Maximum 250 words; without structural divisions; in English and in Turkish. Turkish abstract will be provided by the editorial office for the authors who are not Turkish speakers. If you are not a native Turkish speaker, please re enter your English abstract to the area provided for the Turkish abstract.
- Text
- References

Case Report and Literature Review

- Title page (see above)
- Abstract: Approximately 100-150 words; without structural divisions; in English and in Turkish. Turkish abstract will be provided by the editorial office for the authors who are not Turkish speakers. If you are not a native Turkish speaker, please re-enter your English abstract to the area provided for the Turkish abstract.
- Introduction
- Case report
- Literature Review and Discussion
- References

Interesting Image:

No manuscript text is required. Interesting Image submissions must include the following:

Title Page: (see Original article section)

Abstract: Approximately 100-150 words; without structural divisions; in English and in Turkish. Turkish abstract will be provided by the editorial office for the authors who are not Turkish speakers. If you are not a native Turkish speaker, please re-enter your English abstract to the area provided for the Turkish abstract.

Image(s): The number of images is left to the discretion of the author. (See Original article section)

Figure Legend: Reference citations should appear in the legends, not in the abstract. Since there is no manuscript text, the legends for illustrations should be prepared in considerable detail but should be no more than 500 words total. The case should be presented and discussed in the Figure legend section.

References: Maximum eight references (see original article section).

Letters to the Editor:

- Title page (see above)
- Short comment to a published work, no longer than 500 words, no figures or tables.
- References no more than five.

Consensus Statements or Guidelines: These manuscripts should typically be no longer than 4000 words and include no more than six figures and tables and 120 references.

MIRT
Molecular Imaging and Radionuclide Therapy

INSTRUCTIONS TO AUTHORS

Proofs and Reprints

Proofs and a reprint orders are sent to the corresponding author. The author should designate by footnote on the title page of the manuscript the name and address of the person to whom reprint requests should be directed. The manuscript when published will become the property of the journal.

Archiving

The editorial office will retain all manuscripts and related documentation (correspondence, reviews, etc.) for 12 months following the date of publication or rejection.

Submission Preparation Checklist

As part of the submission process, authors are required to check off their submission's compliance with all of the following items, and submissions may be returned to authors that do not adhere to these guidelines.

1. The submission has not been previously published, nor is it before another journal for consideration (or an explanation has been provided in Comments to the Editor).
2. The submission file is in Microsoft Word, RTF, or WordPerfect document file format. The text is double-spaced; uses a 12-point font; employs italics, rather than underlining (except with URL addresses); and the location for all illustrations, figures, and tables should be marked within the text at the appropriate points.
3. Where available, URLs for the references will be provided.
4. All authors should be listed in the references, regardless of the number.
5. The text adheres to the stylistic and bibliographic requirements outlined in the Author Guidelines, which is found in About the Journal.
6. English keywords should be provided from http://www.nlm.nih.gov/mesh(Medical Subject Headings), while Turkish keywords should be provided fromhttp://www.bilimterimleri.com
7. The title page should be a separate document from the main text and should be uploaded separately.
8. The "Affirmation of Originality and Assignment of Copyright/The Disclosure Form for Potential Conflicts of Interest Form" and Authorship Contribution Form should be downloaded from the website, filled thoroughly and uploaded during the submission of the manuscript.

TO AUTHORS

Copyright Notice

The author(s) hereby affirms that the manuscript submitted is original, that all statement asserted as facts are based on author(s) careful investigation and research for accuracy, that the manuscript does not, in whole or part, infringe any copyright, that it has not been published in total or in part and is not being submitted or considered for publication in total or in part elsewhere. Completed Copyright Assignment & Affirmation of Originality Form will be uploaded during submission. By signing this form;

1. Each author acknowledges that he/she participated in the work in a substantive way and is prepared to take public responsibility for the work.
2. Each author further affirms that he or she has read and understands the "Ethical Guidelines for Publication of Research".
3. The author(s), in consideration of the acceptance of the manuscript for publication, does hereby assign and transfer to the Molecular Imaging and Radionuclide Therapy all of the rights and interest in and the copyright of the work in its current form and in any form subsequently revised for publication and/or electronic dissemination.

Privacy Statement

The names and email addresses entered in this journal site will be used exclusively for the stated purposes of this journal and will not be made available for any other purpose or to any other party.

Peer Review Process

1. The manuscript is assigned to an editor, who reviews the manuscript and makes an initial decision based on manuscript quality and editorial priorities.
2. For those manuscripts sent for external peer review, the editor assigns at least two reviewers to the manuscript.
3. The reviewers review the manuscript.
4. The editor makes a final decision based on editorial priorities, manuscript quality, and reviewer recommendations.
5. The decision letter is sent to the author.

Contact Address

All correspondence should be directed to the Editorial Office:
Cinnah Caddesi Pilot Sokak No:10/12 06650 Çankaya / Ankara, Turkey
Phone: +90 312 441 00 45
Fax: +90 312 441 12 97
E-mail: info@tsnmjournals.org

MIRT
Molecular Imaging and Radionuclide Therapy

CONTENTS

Original Articles

83 Uptake Patterns of Untreated Primary Gastrointestinal Extranodal Lymphomas on Initial Staging ^{18}F-FDG PET/CT and Metabolic Tumor Parameters

Primer Ekstranodal Gastrointestinal Sistem Lenfomalarında Primer Evreleme ^{18}F-FDG PET/BT'de Tutulum Paternleri ve Metabolik Tümör Parametreleri

Engin Alagöz, Kürşat Okuyucu, Semra İnce, Murat Kantarcıoğlu, Şükrü Özaydın, Cumhur Heper, Türker Türker, Nuri Arslan; Ankara, İstanbul, Turkey

93 Thyroid Incidentalomas on ^{18}F-FDG PET/CT: Clinical Significance and Controversies

^{18}F-FDG PET/BT'de Tiroid İnsidentalomalar: Klinik Önem ve Tartışmalar

William Makis, Anthony Ciarallo; Edmonton, Montreal, Canada

101 Bone Single Photon Emission/Computed Tomography in the Detection of Sacroiliitis in Seronegative Spondyloarthritis: A Comparison with Magnetic Resonance Imaging

Seronegatif Spondiloartritte Sakroiliit Tanısı için Kemik Sintigrafisi Pozitron Emisyon/Bilgisayarlı Tomografisi: Manyetik Rezonans Görüntüleme ile Karşılaştırma

Theodoros Pipikos, Dimitrios Kassimos, George Angelidis, John Koutsikos; Athens, Greece

110 A Comparison of Iterative Reconstruction and Prone Imaging in Reducing the Inferior Wall Attenuation in Tc-99m Sestamibi Myocardial Perfusion SPECT

Tc-99m Sestamibi Miyokard Perfüzyon SPECT Görüntülemede İnferior Duvar Attenüasyonunu Azaltmada İteratif Rekonstrüksiyon ile Pron Pozisyonun Karşılaştırması

Duygu Kuşlu, Emel Öztürk; Antalya, Ankara, Turkey

Interesting Images

116 Super Scan Caused by Parathyroid Carcinoma Observed Both in ^{18}F-FDG PET/CT Scan and Tc-99m MDP Bone Scintigraphy

^{18}F-FDG PET/BT ve Tc-99m MDP Kemik Sintigrafisinde Tespit Edilen Paratiroid Kanserinin Neden Olduğu Süper Görüntü

İsa Burak Güney, Semra Paydaş, Hüseyin Tuğsan Ballı; Adana, Turkey

120 Two Uncommon Sites of Metastasis: Breast and Hypophysis Metastases of Head and Neck Adenoid Cystic Carcinoma Detected by FDG PET/CT

Baş Boyun Adenoid Kistik Karsinomlu Olguda İki Olağan Dışı Metastaz Alanı: Hipofiz ve Meme

Evrim Sürer Budak, Şenay Yıldırım, Sevim Yıldız, Ali Ozan Öner, Şeyda Gündüz; Antalya, Afyon, Turkey

124 Cyclosporine and Vancomycin + Amikacin Induced Hot Kidney Appearance in a Young Adult and a Pediatric Patient

Genç Yetişkin ve Pediatrik Bir Hastada Siklosporin ve Vankomisin + Amikasin ile İndüklenen Hot Kidney Görünümü

Derya Çayır, Mine Araz, Mustafa Filik, Mehmet Erdoğan; Ankara, Turkey

MIRT
Molecular Imaging and Radionuclide Therapy

CONTENTS

128 Incidental Tc-99m Methylene Diphosphonate Uptake in an Active Thyroid Nodule
Aktif Tiroid Nodülünde İnsidental Tc-99m Metilen Difosfonat Tutulumu
Derya Çayır, Mine Araz, Şafak Akın, Melia Karaköse, Erman Çakal; Ankara, Turkey

131 False Positive Perfusion/Ventilation SPECT Study for Pulmonary Embolism in a Patient with Fontan Circulation
Fontan Dolaşımlı Bir Hastada Pulmoner Emboli için Yanlış Pozitif Perfüzyon/Ventilasyon SPECT İncelemesi
Emmanouil Panagiotidis; Liverpool, UK

Index

2017 Referee Index / *2017 Hakem Dizini*

2017 Subject Index / *2017 Konu Dizini*

2017 Author Index / *2017 Yazar Dizini*

Türkiye Nükleer Tıp Derneği

5. PET / MR KURSU

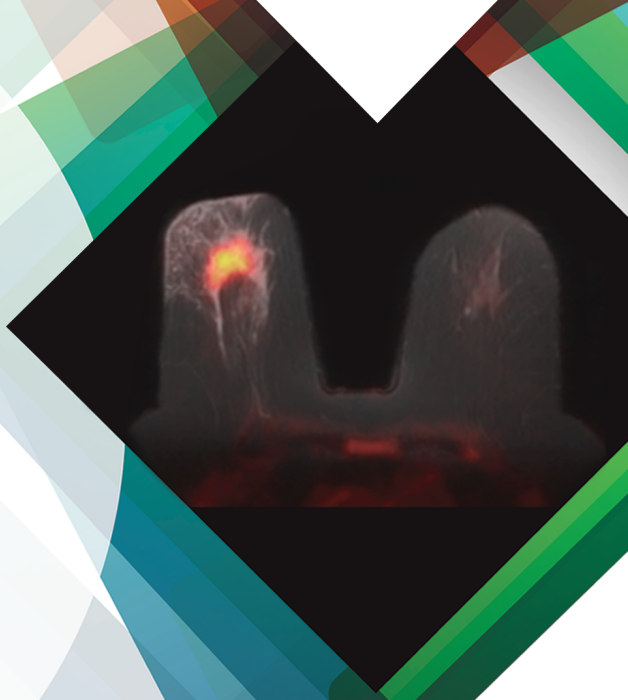

17 Kasım 2017

THE MARMARA OTEL, İSTANBUL

BİLİMSEL SEKRETERYA

TÜRKIYE NÜKLEER TIP DERNEĞİ

Cinnah Caddesi Pilot Sokak No:
10/12 – 06690, Çankaya ANKARA
Tel: +90 (0312) 441 00 45
Faks : +90 (0312) 441 12 97
E-posta: dernekmerkezi@tsnm.org
Web: www.tsnm.org

ORGANİZASYON SEKRETERYASI

SERENAS ULUSLARARASI TURİZM KONGRE ORGANİZASYON A.Ş.

Hilal Mh. Cezayir Cd.
No:13, 06550 Yıldız,
Çankaya - ANKARA
T: +90 (312) 440 50 11
F: +90 (312) 441 45 62
E-posta: yasemin.cekirdek@serenas.com.tr
Web: www.serenas.com.tr

Original Article
Mol Imaging Radionucl Ther 2017;26:83-92 DOI:10.4274/mirt.48658

Uptake Patterns of Untreated Primary Gastrointestinal Extranodal Lymphomas on Initial Staging ^{18}F-FDG PET/CT and Metabolic Tumor Parameters

Primer Ekstranodal Gastrointestinal Sistem Lenfomalarında Primer Evreleme ^{18}F-FDG PET/BT'de Tutulum Paternleri ve Metabolik Tümör Parametreleri

Engin Alagöz[1], Kürşat Okuyucu[1], Semra İnce[1], Murat Kantarcıoğlu[2], Şükrü Özaydın[3], Cumhur Heper[4], Türker Türker[5], Nuri Arslan[1]
[1]*Gülhane Training and Research Hospital, Clinic of Nuclear Medicine, Ankara, Turkey*
[2]*Gülhane Training and Research Hospital, Clinic of Gastroenterology, Ankara, Turkey*
[3]*Gülhane Training and Research Hospital, Clinic of Medical Oncology, Ankara, Turkey*
[4]*İstanbul University Institute of Cardiology, Clinic of Nuclear Medicine, İstanbul, Turkey*
[5]*Gülhane Training and Research Hospital, Clinic of Public Health, Ankara, Turkey*

Abstract

Objective: Non-Hodgkin's lymphomas arising from tissues other than primary lymphatic sites are classified as primary extranodal lymphomas (PEL). PELs of the gastrointestinal system (PGISL) originate from the lymphatic tissues within the gastrointestinal tract. The prognostic value of ^{18}F-FDG PET/CT in lymphomas is high in terms of both overall survival (OS) and disease-free survival (DFS). Our aim was to investigate the uptake patterns and properties of low-grade and high-grade PGISL on primary staging ^{18}F-FDG PET/CT, as well as the prognostic significance of metabolic tumor parameters in high grade PGISL.

Methods: Thirty-nine patients with PGISL were enrolled in this retrospective cohort study between 2004-2015. Primary staging ^{18}F-FDG PET/CT have been performed and quantitative parameters of SUV_{max}, SUV_{mean}, metabolic tumor volume (MTV), total lesion glycolysis (TLG) have been calculated for all patients prior to treatment. Low-grade and high-grade PGISL were compared in terms of metabolic tumor parameters. Cox regression models were performed to determine factors that correlate with DFS in high-grade PGISL.

Results: There were statistically significant differences between high-grade and low-grade PGISL in terms of SUV_{max}, SUV_{mean}, MTV, TLG, recurrence, mortality, DFS and OS. None of the potential risk factors (sex, age, site, SUV_{max}, SUV_{mean}, MTV, TLG) for recurrence and metastasis in high grade PGISL was identified as a risk factor on univariate and multivariate Cox regression analysis.

Conclusion: Metabolic tumor parameters are not predictive markers in high-grade PGISL, especially in diffuse large B cell variant and primary gastric lymphoma. The first implications suggest they will not play a role in patient management.

Keywords: ^{18}F-fluorodeoxyglucose positron emission tomography/computed tomography, metabolic tumor parameters, primary gastrointestinal lymphoma

Address for Correspondence: Engin Alagöz MD, Gülhane Training and Research Hospital, Clinic of Nuclear Medicine, Ankara, Turkey
Phone: +90 542 577 91 01 E-mail: enalamed@yahoo.com ORCID ID: orcid.org/0000-0002-4214-4016
Received: 28.03.2017 **Accepted:** 07.06.2017

©Copyright 2017 by Turkish Society of Nuclear Medicine
Molecular Imaging and Radionuclide Therapy published by Galenos Yayınevi.

Öz

Amaç: Primer lenfatik alanlar dışındaki dokulardan kaynaklanan Non-Hodgkin lenfomalara primer ekstranodal lenfoma (PEL) denmektedir. Gastrointestinal sistemin PEL'i (PGISL) buradaki lenfatik dokulardan köken alır. ^{18}F-FDG PET/BT lenfomalarda genel ve hastalıksız sağkalım açısından yüksek prognostik değere sahiptir. Amacımız düşük grad ve yüksek grad PGISL'de primer evreleme ^{18}F-FDG PET/BT'de tutulum şekillerini, özelliklerini, yüksek grad PGISL'de metabolik tümör parametrelerinin prognostik önemi ile birlikte araştırmaktır.

Yöntem: 2004-2015 yılları arasında PGISL (evre 1-2) tanısı konmuş 39 hasta bu retrospektif kohort çalışmaya dahil edildi. Hastalara tedaviden önce primer evreleme ^{18}F-FDG PET/BT çekilmiş ve maksimum standardize uptake değeri (SUV_{maks}), ortalama standardize uptake değeri ($SUV_{ortalama}$), metabolik tümör hacmi (MTV) ve total lezyon glikolizi (TLG) gibi metabolik tümör parametreleri hesaplanmıştı. Düşük grad ve yüksek grad PGISL metabolik tümör parametreleri açısından karşılaştırıldı. Yüksek grad PGISL'de Cox regresyon modelleri üzerinden hastalıksız sağkalım ile ilişkili faktörler tespit edildi.

Bulgular: Düşük grad ve yüksek grad PGISL arasında SUV_{maks}, $SUV_{ortalama}$, MTV, TLG, nüks, mortalite, genel ve hastalıksız sağkalım açısından istatistiksel olarak anlamlı fark saptanmıştır. Yüksek grad PGISL'de nüks ve metastaza etki eden tüm potansiyel risk faktörlerinin (cinsiyet, yaş, site, SUV_{maks}, $SUV_{ortalama}$, MTV, TLG) tek ve çok değişkenli Cox regresyon analizinden sonra metabolik tümör parametrelerinin bir risk faktörü olmadığı görülmüştür.

Sonuç: Metabolik tümör parametreleri özellikle diffüz büyük B hücreli varyant ve primer gastrik lenfoma başta olmak üzere yüksek grade PGISL'nin prognoz tahmininde faydalı değildir. İlk izlenimler hasta yönetiminde bir rolleri olamayacağı yönündedir.

Anahtar kelimeler: ^{18}F-fluorodeoksiglukoz pozitron emisyon tomografi/bilgisayarlı tomografi, metabolik tümör parametreleri, primer gastrointestinal lenfoma

Introduction

Non-Hodgkin's lymphomas (NHLs) arising from tissues other than primary lymphatic sites [lymph nodes (LNs), bone marrow, spleen, thymus and Waldeyer's ring of pharyngeal lymphatics] are classified as primary extranodal lymphoma (PEL) (1). Although PEL can be seen in almost any site, gastrointestinal system (GIS) is the most frequent site (2). Thus, PEL of the GIS (PGISL) is a NHL originating from lymphatic tissues of the gastrointestinal tract. The most commonly affected site is the stomach (50-60%) followed by the small intestine (approximately 30%), colon, very rarely pancreas and the liver (3). Approximately 1/2 to 2/3 of GIS NHLs are diffuse large B-cell (DLBC) lymphomas (1).

Primary gastric lymphoma (PGL) constitutes less than 5% of all gastric neoplasms (4). It is the most common site in all PEL patients with an incidence of 4-20%, and a preponderance in men over the age of 50 (5). Histologically, PGL is predominantly high-grade, DLBC or low-grade mucosa-associated lymphoid tissue (MALT), also defined as extranodal marginal zone B cell lymphoma (6). MALT lymphoma is the most common variety in PGL (7). A heterogeneous group of lymphomas including MALT, DLBC, mantle cell (MC), Burkitt and T-cell affect the small bowel (7). Primary colon lymphoma has features similar to small bowel disease with wall thickening without obstruction (8). 30-50% of patients with small bowel lymphoma initially present with an abdominal emergency (9).

The treatment of GIS lymphomas is controversial and depends on histologic type and disease stage (10). Although computed tomography (CT), 18-fluorodeoxyglucose positron emission tomography (^{18}F-FDG PET) and ^{18}F-FDG PET/CT are used to stage PEL, CT is the most commonly used imaging modality for the management of patients with lymphomas (2). Most patients present with residual masses after treatment (11). A decrease in the size of a lymphomatous mass after treatment is considered as treatment response. However, a decrease in size on CT does not occur in case of fibrosis, necrosis and inflammation (11). Therefore, CT cannot differentiate residual disease from fibrosis.

^{18}F-FDG PET is a superior imaging technique that proved its utility especially in Oncology. It can display functional alterations that precede anatomical changes. Several limitations of CT in lymphomas can be overcome with ^{18}F-FDG PET. Besides, integration of CT to ^{18}F-FDG PET creates a superior imaging modality combining anatomical detail with functional information, which results in excellent accuracy and detection capability. With all these advantages, ^{18}F-FDG PET/CT is being widely used in the primary staging, evaluation of treatment response, and restaging of PGISL just like other types of HL and many NHL lymphomas.

^{18}F-FDG PET/CT also has a high prognostic value with respect to overall survival (OS) and disease-free survival (DFS). The semi-quantitative measurement of standardized uptake value (SUV) is an easy-to-calculate and noninvasive index reflecting ^{18}F-FDG metabolic rate. Its assessment has additional prognostic value in early response to treatment and long-term outcome in lymphoma patients and improves the prognostic value of the test manifestly as compared to visual analysis (12). Many studies have proven the effectiveness of ^{18}F-FDG PET/CT for primary staging, restaging and evaluation of treatment response in lymphomas (13). Despite the high incidence of PEL of the GIS, only a few studies with limited number of

patients have been published in the literature on the use of ^{18}F-FDG PET/CT in the management of these patients (14). Moreover, to the best of our knowledge no prior studies have been published on metabolic tumor parameters in this selective subgroup of lymphoma. This study was conducted to investigate the usefulness of metabolic tumor indices on primary staging ^{18}F-FDG PET/CT for prognosis estimation in primary extranodal high-grade GIS lymphomas. We also studied the uptake patterns and properties of metabolic tumor parameters in different histological subtypes of PGISL.

Materials and Methods

Thirty-nine patients with PGISL (only stage 1-2 disease) from 2004 to 2015 were enrolled in this retrospective cohort study. The cases were histopathologically proven by excisional biopsy. The study was conducted at the Nuclear Medicine Department of a training and research hospital of a medical school. Primary staging ^{18}F-FDG PET or ^{18}F-FDG PET/CT have been performed for all patients prior to treatment. Disseminated nodal disease secondarily involving GIS and Hodgkin lymphoma (HL) with GIS involvement were excluded. Patients who didn't have primary staging ^{18}F-FDG PET/CT and inadequate follow-up were also not included. Involvement of GIS as the predominant site with a few minor draining LNs only were also categorized as PGISL and included in the study. These patients were treated and followed up by the Medical Oncology Department of our hospital. CD20 (+) cases were treated by R-CHOP protocol (rituximab, cyclophosphamide, doxorubicin, vincristine, prednisolone), while CD20 (-) cases received CHOP. The patients were followed by clinical history, physical examination, lactate dehydrogenase and sedimentation rate measurement, complete blood count, liver function tests, CT and/or ^{18}F-FDG PET/CT. Information and data were obtained from clinic follow-up files, radiation therapy records, physician records of other departments at our hospital or personal contact with the patients on telephone.

^{18}F-FDG PET/CT Imaging Protocol

Patients fasted for 6 hours and their blood glucose level had to be under 150 mg/dL before the injection of an activity of 370-555 MBq of ^{18}F-FDG according to patient's weight. Image acquisitions were performed 1 hour later with an integrated PET/CT scanner (Discovery 690-GE Healthcare). Unenhanced low dose CT and PET emission data were acquired from mid-thigh to the vertex of the skull in supine position with the arms raised over head. CT data was obtained by automated dose modulation of 120 kVp (maximal 100 mA), collimation of 64×0.625 mm, measured field of view (FOV) of 50 cm, noise index of 20% and reconstructed to images of 0.625 mm transverse pixel size and 3.75 mm slice thickness. PET data was acquired in 3D mode with scan duration of 2 min per bed position and an axial FOV of 153 mm. The emission data was corrected in a standardized way (random, scatter and attenuation) and iteratively reconstructed (matrix size 256×256, Fourier rebinning, VUE Point FX [3D] with 3 iterations, 18 subsets).

Visual and Quantitative Interpretation

Quantitative PET/CT parameters used in the study include maximum standardized uptake value (SUV_{max}), average standardized uptake value (SUV_{mean}), metabolic tumor volume (MTV) and total lesion glycolysis (TLG). They were calculated according to a standard protocol on a dedicated workstation (Volumetrix for PET/CT and AW volume share 4.5, GE Healthcare, Waukesha, WI, USA). SUV_{max} and SUV_{mean} corrected for body weight were computed by standard methods from the activity at the most intense voxel in three-dimensional tumor region from the transaxial whole body images on attenuation-corrected PET/CT images. MTV (cm^3) was measured with semiautomatic PET analysis software using an automatic isocontour threshold method based on a theory of being greater than 42% of the SUV_{max} value within the tumor. TLG values were calculated by multiplying MTV and SUV_{mean}. The corresponding CT scan of lesions were used as a guideline to demarcate them if their boundaries were difficult to define for the calculation of SUV_{max} (15).

We retrospectively examined demographic characteristics, clinical findings, histology, clinical stage, response to treatment and outcome of the patients. OS was defined as the interval between diagnosis and death of any cause including ones other than the disease itself or until last follow-up. DFS was defined as the interval between diagnosis to detection of relapse or until last follow-up. Informed consent was waived due to the retrospective design of the study using records, documents and data of patients referred to our clinic for the test. Ann-Arbor staging system and definitions were used in this study. The study was approved by The study was approved by a Gülhane Training and Research Hospital Local Ethics Committee (Date: 17.02.2016, Protocol number: 40).

Statistical Analysis

The data were analyzed by IBM Corp. Released 2013. IBM SPSS Statistics for Windows, Version 22.0. Armonk, NY:IBM Corp. Number and percentage values were used for description of categorical data; while mean, median, standard deviation, minimum (min) and maximum (max) values were used for description of continuous data. Fisher's exact test was used for comparison of high-grade and low-grade PGISL in terms of sex, recurrence and mortality; the chi-square test for site; the Student-t test for age and SUV_{max}; the Mann Whitney-U test for SUV_{mean}, MTV, TLG, OS and DFS. Univariate Cox regression analysis was used to determine factors that correlated with DFS and OS of high-grade PGISL DLBC variant. Univariate and multivariate analysis (Cox regression, Forward LR models)

were performed for the evaluation of factors impacting recurrence. The variables having a value of p<0.5 were further included into multivariate analysis. ROC curve was drawn to evaluate the diagnostic value of SUV_{max}, SUV_{mean}, MTV and TLG. They were dichotomized by splitting into two groups according to ROC curve. Kaplan-Meier method with log-rank test was used to compare DFS times of metabolic tumor parameters. The study was approved by our Institutional Review Board.

Results

There were 23 DLBC lymphomas (59%), 12 MALT lymphomas (31%), 2 T-cell lymphomas (5%), one MC lymphoma and one Burkitt lymphoma in the study. Totally, we had 26 high-grade PGISL (67%) and 13 low-grade PGISL (33%). Twenty-eight of the patients were male (72%) and 11 were female (28%). Mean age of the patients was 57±15 years (21-87 years). The site distribution amongst these 39 patients was as follows: 23 PGL (59%) (Figure 1), 7 small bowel (18%), 7 primary colon lymphoma (18%), one primary pancreas lymphoma, and one primary liver lymphoma. Thirty-four out of 39 (87%) cases had stage 1, while 5 (13%) had stage 2 disease. Patient characteristics and demographic findings, clinic-pathologic features and follow-up data of high-grade and low-grade PGISL are presented in Table 1 and Table 2. There were statistically significant differences between high-grade and low-grade PGISL in terms of SUV_{max}, SUV_{mean}, MTV, TLG, recurrence, mortality, DFS and OS. The comparison of high-grade and low-grade PGISL features is shown in Table 3.

Univariate Cox regression was performed for all potential risk factors (sex, age, site, SUV_{max}, SUV_{mean}, MTV, TLG) impacting recurrence and/or metastasis (met/rec). Site, SUV_{max}, SUV_{mean}, was determined as statistically significant on univariate analysis. The results of univariate Cox regression analysis are shown in Table 4. Factors with p<0.5 on univariate analysis (sex, age, SUV_{max}, SUV_{mean}, and site) were evaluated further with multivariate model. Only sex remained statistically significant on multivariate analysis (p=0.037).

Within the group of patients with high-grade PGISL, 8 patients (31%) died and 9 patients (34.5%) developed met/rec during follow-up. Four patients died of causes other than the disease (cardiovascular events, cerebrovascular diseases, aging, etc). Four patients died of disease related reasons (extensive metastasis and related complications). OS at the 5th year was 77%, and 73% at the 10th year. The average time to detection of met/rec was 12.6 months (4-22). DFS was 80.5% and 65% at the first and second years, respectively. ROC curve was drawn to evaluate the diagnostic value of SUV_{max}, SUV_{mean}, MTV and TLG in high-grade PGISL (Figure 2). Survival graphics of high-grade PGISL-DLBC variant obtained by univariate Cox regression analysis was plotted. Metabolic tumor parameters were

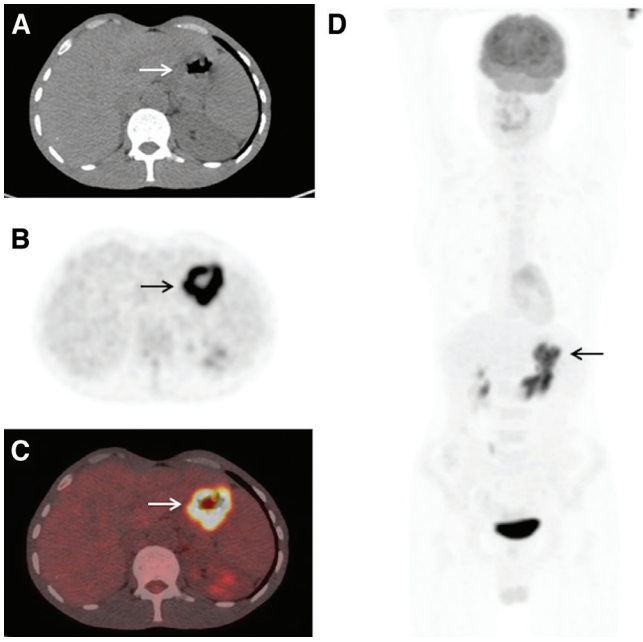

Figure 1. The SUV_{max}, SUV_{mean}, metabolic tumor volume and total lesion glycolysis values of a 58-year old male patient with primary gastric lymphoma diffuse large B-cell variant were 11.5, 5.2, 35 cm^3 and 176, respectively, on trans-axial computed tomography (A), positron emission tomography (B), fusion (C) and maximum intensity projection (D) images of baseline 18-fluorodeoxyglucose positron emission tomography (arrows). He responded to treatment and his disease-free survival and overall survival are 92 months

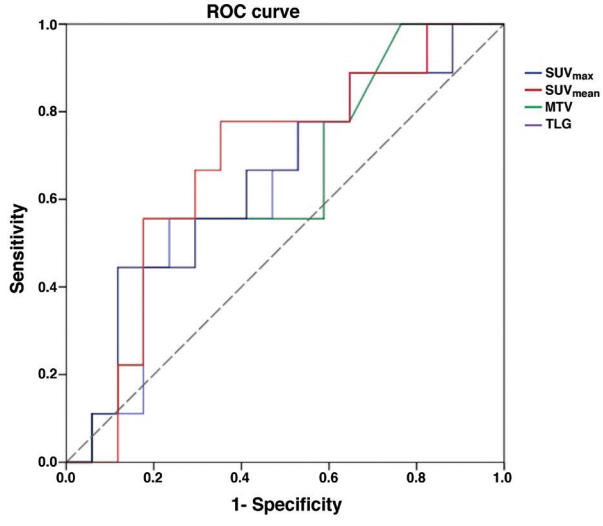

Figure 2. ROC curve of SUV_{max}, SUV_{mean}, metabolic tumor volume and total lesion glycolysis for high-grade primary extranodal lymphomas of the gastrointestinal system

MTV: Metabolic tumor volume, TLG: Total lesion glycolysis

dichotomized by splitting into two groups according to ROC curve. Kaplan-Meier method with log-rank test was used to compare DFS and SUV_{max}, SUV_{mean}, MTV and TLG. Kaplan-Meier curves of SUV_{max} (A), SUV_{mean}, (B), MTV (C), and TLG (D) with their cut-off values are illustrated in Figure 3. The sensitivity and specificity rates of SUV_{max} SUV_{mean}, MTV, and TLG according to cut-off values for high-grade PGISL are represented in Table 5.

Discussion

^{18}F-FDG PET/CT was performed in 447 patients with NHL during the study period in our department. The incidence of PGISL in our study group is 8.7% (39/447), evidently under the rates reported in the literature due to our selective population. The peak incidence is in the 6th-7th decades with a male predominance (16). The mean age of our group was 57 years with a male preponderance, in line with the literature. The risk of NHL is higher in men than in women, but there are certain types of NHL that are more common in women (16). However, there are no studies that have identified sex as a risk factor in the literature. We found that sex was the only factor affecting recurrence on multivariate analysis. Although female sex was the only risk factor for recurrence in our study, we attribute this finding to the insufficient sampling number,

Table 1. Demographic characteristics of patients with high-grade primary extranodal lymphomas of the gastrointestinal system, clinic-pathologic features and follow-up data

Patient no	Age	Gender	Variant	Organ	Rec/Met	Mortality	SUV_{max}	SUV_{mean}	MTV	TLG	DFS	OS
1	52	M	DLBC	Colon	-	-	7.5	4.4	12.4	56.5	43	43
2	75	M	DLBC	Stomach	-	-	26.8	15.1	1211	18286	39	39
3	45	M	DLBC	Pancreas	+	+	19.9	13	112	1456	9	17
4	65	M	DLBC	Jejunum	-	-	9.9	4.4	6.9	30.4	66	66
5	52	F	DLBC	Colon	+	-	8.5	5.7	37.2	212	22	142
6	72	F	DLBC	Stomach	+	+	27.3	18	29.8	536.4	7	25
7	69	M	DLBC	Stomach	-	+	10.1	5.3	70.2	372	34	34
8	52	F	DLBC	Rectum	+	-	14.7	7.1	13.8	98	4	39
9	82	M	DLBC	Stomach	-	+	15	8.8	90	792	47	47
10	50	M	DLBC	Ileum	-	-	6.2	4.5	35.2	158.4	27	27
11	47	M	DLBC	Stomach	-	-	9.9	5.7	96	547.2	110	110
12	35	M	DLBC	Stomach	-	-	39.8	21	144	3024	17	17
13	61	F	DLBC	Stomach	-	+	20.2	11.15	32.3	360.1	70	70
14	56	M	DLBC	Stomach	-	+	15.2	8.4	50.5	424.2	123	123
15	46	M	DLBC	Stomach	-	-	16.3	9	75	675	110	110
16	72	M	DLBC	Liver	+	+	14.4	7.1	79	560.9	13	21
17	51	F	DLBC	Stomach	+	-	24.4	14.8	98	1450	22	38
18	62	F	DLBC	Colon	-	-	16.5	10.4	23	239.2	21	21
19	73	M	DLBC	Stomach	-	-	11.8	6.7	23.7	158.8	43	43
20	50	M	DLBC	Stomach	-	-	27	17.7	82.6	1462	75	75
21	56	M	DLBC	Jejunum	+	-	22	13.4	59.5	797.3	11	35
22	58	M	DLBC	Stomach	-	-	11.5	5.2	35	176	92	92
23	61	F	DLBC	Stomach	+	+	25.7	15.3	107.2	1648	17	33
24	87	M	T-cell	Colon	-	-	7.3	4.1	14.4	59	6	6
25	64	M	T-cell	Ileum	-	-	13.9	8.6	23.5	202.1	43	43
26	21	M	Burkitt	Colon	+	-	10.7	5.3	468	2480	7	32

Rec: Recurrence, M: Male, F: Female, DLBC: Diffuse large B-cell, MTV: Metabolic tumor volume, TLG: Total lesion glycolysis, DFS: Disease-free survival, OS: Overall survival

and thus believe this finding might not be clinically important.

Gastrointestinal tract is the most common extranodal site of NHL (17). The stomach is the most frequently involved (60-74% of cases) site, followed by the duodenum and small bowel (10-20%), ileocecal region (7-10%), and colon (<10%) (18). Our results are consistent with these reports, except that the colon was affected in a greater percentage of patients (equal to small intestine involvement) than previous studies. The stomach is the most common site of primary GIS lymphoma, and gastric MALT lymphoma is the most common type (7). In our study, 39% of gastric

Table 2. Demographic characteristics of patients with low-grade primary extranodal lymphomas of the gastrointestinal system, clinic-pathologic features and follow-up data

Patient no	Age	Gender	Variant	Organ	Rec/Met	Ex	SUV_{max}	SUV_{mean}	MTV	TLG	DFS	OS
1	64	F	MALT	Stomach	-	-	5.2	2.7	57	153.9	62	62
2	25	M	MALT	Duodenum	-	-	6.5	4.1	30.8	126.3	121	121
3	65	F	MALT	Stomach	-	-	10.2	6.1	135.2	824.7	88	88
4	33	M	MALT	Stomach	-	-	3.3	2	17.9	36.5	33	33
5	57	M	MALT	Ileum	-	-	7.6	4	18.2	72.8	61	61
6	49	M	MALT	Stomach	-	-	3.65	2.8	8.6	24.1	57	57
7	77	M	MALT	Stomach	-	-	3	2.7	7.9	21.25	161	161
8	39	M	MALT	Stomach	-	-	5.4	2.8	27.8	77.8	119	119
9	57	F	MALT	Stomach	-	-	6	2.9	63.6	184.4	53	53
10	55	M	MALT	Stomach	-	-	7.5	4.3	16	68.8	70	70
11	80	F	MALT	Stomach	-	-	5.3	2.95	10	29.5	59	59
12	62	M	MALT	Jejunum	-	-	5.3	3.2	29	92.8	40	40
13	55	M	MC	Colon	-	-	4.6	2.2	18.3	40.3	60	60

Rec: Recurrence, M: Male, F: Female, MC: Mantle cell, MALT: Mucosa-associated lymphoid tissue, MTV: Metabolic tumor volume, TLG: Total lesion glycolysis, DFS: Disease-free survival, OS: Overall survival

Table 3. Comparison of high-grade and low-grade primary extranodal lymphomas of the gastrointestinal system in terms of patient characteristics, follow-up data and metabolic tumor parameters

Variables		Low-grade PGISL	High-grade PGISL	Significance (p value)
Sex	Male Female	9 (69%) 4 (31%)	19 (73%) 7 (27%)	0.542
Mean age (years)		55±16	58±14.5	0.730
Mean SUV_{max}		5.6±2	16.75±8	0.038
Mean SUV_{mean}		3.25±1	9.75±4.8	0.024
Mean MTV (cm^3)		34 (MD: 18)	117 (MD: 55.5)	<0.001
Mean TLG		135 (MD: 72.8)	1404 (MD: 487)	<0.001
Recurrence (+)		0	9 (34.5%)	0.018
Mortality (+)		0	8 (31%)	0.035
Mean DFS (months)		75.5±36.8	41.5±35.5	0.003
Organ	Colon Stomach Intestine	1 (8%) 9 (69%) 3 (23%)	6 (23%) 14 (54%) 4 (15%)	0.596
Mean OS (months)		75.5±36.8	52±36	0.002

MD: Median value, PGISL: Primary extranodal lymphomas of the gastrointestinal system, MTV: Metabolic tumor volume, TLG: Total lesion glycolysis, DFS: Disease-free survival, OS: Overall survival

Table 4. Univariate Cox regression analysis of high-grade primary extranodal lymphomas of the gastrointestinal system diffuse large B-cell variant

Factors	Significance (p value)	Hazard ratio	95% CI for Hazard ratio	
			Lower	Upper
Sex*	0.063	0.287	0.077	1.071
Age	0.460	0.982	0.938	1.030
SUV_{max}	0.026	1.073	1.009	1.141
SUV_{mean}	0.020	1.141	1.021	1.275
MTV	0.719	1,000	0.998	1.003
TLG	0.973	1.000	1.000	1.000
Organ**	0.034	Reference		
Stomach	0.040	0.186	0.037	0.929
Intestine	0.228	4.484	0.392	51.330

Reference groups: *Male sex,**Colon, MTV: Metabolic tumor volume, TLG: Total lesion glycolysis, CI: Confidence interval

lymphomas were MALT type while 61% were DLBC variant. Our incidence of gastric DLBC was markedly higher than gastric MALToma. This result is in contrast to the literature. MALT, DLBC, MC, Burkitt and T cell can all be seen in the small bowel and colon. The most common variant was DLBC (59%) in our patients followed by MALT (31%). These

Table 5. Cut-off value, sensitivity and specificity rates of SUV_{max}, SUV_{mean}, metabolic tumor volume and total lesion glycolysis in high-grade primary extranodal lymphomas of the gastrointestinal system

Factors	Cut-off value	Sensitivity (%)	Specificity (%)
SUV_{max}	18.2	89	62
SUV_{mean}	12.1	100	52
MTV (cm^3)	97	89	48
TLG	487	78	76

MTV: Metabolic tumor volume, TLG: Total lesion glycolysis

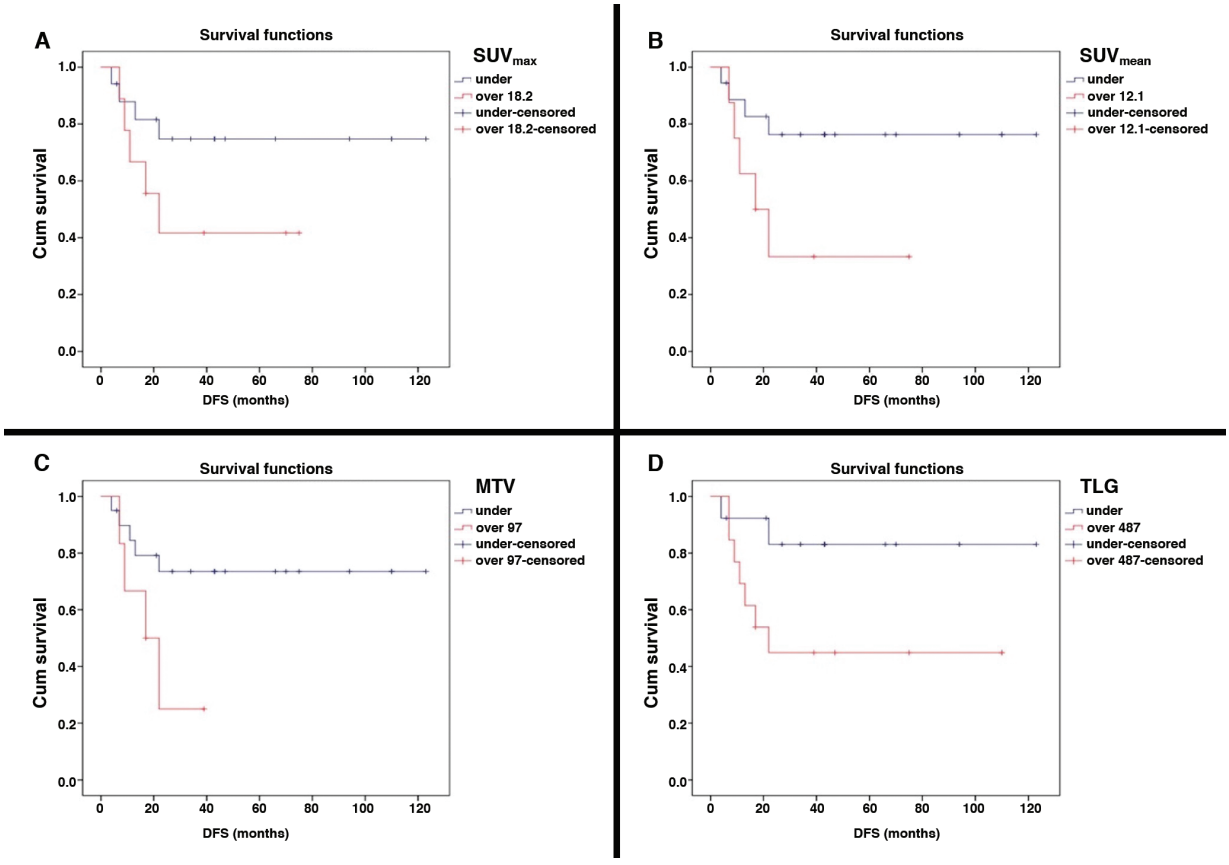

Figure 3. Survival graphic of high-grade primary extranodal lymphomas of the gastrointestinal system diffuse large B-cell variant obtained by univariate Cox regression test. Kaplan-Meier curves of SUV_{max} with a cut-off value of 18.2 (A), SUV_{mean} with a cut-off value of 12.1 (B), metabolic tumor volume with a cut-off value of 97 cm^3 (C), total lesion glycolysis with a cut-off value of 487 (D) for high-grade primary extranodal lymphomas of the gastrointestinal system

MTV: Metabolic tumor volume, TLG: Total lesion glycolysis, DFS: Disease-free survival

findings are also completely in agreement with previous reports.

Primary hepatic lymphoma (PHL) is very rare and up to date, only about 300 cases were published in the literature. Of all PELs, only 0.4% occurs in the liver (9). The most common variant in the liver is DLBC, accounting in one study for 71% of all cases (19). Our sole PHL patient was a DLBC subtype with poor prognosis (recurred at the 13th, died at the 21st month). Primary pancreatic lymphoma (PPL) is defined as an extranodal lymphoma arising in the pancreas with the bulk of the tumor localized to the pancreas. PPL is a very rare disease, accounting for less than 0.5% of pancreatic tumors (20). The only case with PPL in our study was a DLBC variant and his clinical course was fatal with high metabolic parameters (recurred at the 9th, died at the 17th month).

There is a correlation between ^{18}F-FDG uptake and histologic grade of lymphoma, since rapidly proliferating lymphoma cells have a high metabolic rate and aggressive subtypes of NHL take up high levels of ^{18}F-FDG (21). The ^{18}F-FDG PET imaging in our study showed that high-grade PGISL had high ^{18}F-FDG activity as confirmed with high metabolic tumor parameters. Particularly, DLBC variants exhibited usually high ^{18}F-FDG accumulation. Although low-grade PGISL lesions were identified with difficulty especially in MALT lymphoma, MALT types had variable (usually moderate) uptake in this study. Jerusalem et al. (22) reported that low-grade NHLs such as follicular lymphoma and MC lymphoma do not demonstrate ^{18}F-FDG-avidity to the same degree with high-grade lymphomas, but they are still ^{18}F-FDG-avid enough to be detected. There was a significant difference in terms of SUV_{max}, SUV_{mean}, MTV and TLG between high-grade and low-grade PGISL in our patients ($p=0.038$, $p=0.024$, $p<0.001$, $p<0.001$, respectively).

The majority of patients with MC present with advanced-stage disease and often have extranodal sites. These patients have a poor prognosis with a median survival of 3 to 4 years (23). One patient with MC lymphoma in this study accumulated mild ^{18}F-FDG and had a good prognosis, nevertheless, our patient had stage 1 disease. MALT lymphoma is the third most common NHL following DLBC and follicular lymphoma (24). Most studies report that MALT lymphomas demonstrate moderate to high ^{18}F-FDG accumulation while a few studies with limited number of patients claim that ^{18}F-FDG PET imaging is unreliable in case of primary extranodal MALT lymphoma (25). We detected usually moderate uptake and no recurrence or death in our cases with MALT lymphoma. Burkitt lymphoma is a highly aggressive B-cell NHL. There was only one patient with Burkitt type among our cases. The ^{18}F-FDG uptake was high in that patient with increased metabolic tumor parameters, and the tumor recurred at 7 months. T-cell lymphomas are generally aggressive neoplasms. Two of our cases with T-cell variant had a favorable prognosis with moderate ^{18}F-FDG uptake. Six gastric DLBC, one PHL and one PPL were responsible for deaths. We observed complete remission in 26 patients (13/26 in the high-grade group, all patients in the low-grade group). In our study group, DFS was identified as 77% and OS as 79.5% with a mean follow-up of 65 months (6-161). These results are in agreement with other studies in the literature.

Quantitative metabolic parameters (SUV_{max}, SUV_{mean}, MTV, TLG) obtained from initial staging PET/CT has been used in prognosis estimation and evaluation of treatment response for many cancers and lymphomas. Tumor cells utilize glucose at a higher metabolic rate as displayed by abnormal ^{18}F-FDG uptake. SUV measures this consumption rate that correlates with cellular metabolism (26). SUV_{max} is the first one of metabolic tumor parameters, which represents the highest ^{18}F-FDG uptake within the tumor volume. SUV_{mean} represents the average activity in a tumor burden. Recently, volume-based metabolic parameters (MTV and TLG) have been used to detect recurrent disease to the best of our knowledge, the literature lacks any study pertaining to the use of these metabolic factors for prognosis estimation in high-grade PGISL.

Although a study specifically on this subject has not been conducted, similar studies with SUV_{mean} has been previously reported. Most studies investigated metabolic tumor parameters for different sites or unique variants and aimed to evaluate them in treatment. Esfahani et al. (27) stated TLG as the most significant parameter for predicting detection of recurrence in DLBC on initial and interim PET. Gallicchio et al. (28) reported that quantitative parameters were helpful in the management of patients with DLBC. Recently, TLG emerged as a remarkable predictor in many cancers and lymphomas, since it contributes to patient management by assessing both tumor volume and metabolism. Ceriani et al. (29) suggested TLG as the most powerful predictor on baseline PET/CT in DLBC. However, there are no studies on these parameters in PGISL. To the best of our knowledge, our study is the first one in which the prognosis of high-grade PGISL was predicted by these metabolic indicators.

Previously reported studies on PGISL are usually focused on evaluating response to treatment by SUV_{max} alone. Phongkitkarun et al. (15) reported that SUV_{max} plays an important role in the evaluation of treatment response. Kumar et al. (2) identified high SUV_{max} as a strong predictor of recurrence after completion of therapy. We aimed to investigate the efficacy of all metabolic tumor parameters for predicting prognosis in high-grade PGISL. After evaluation of all potential risk factors effecting met/rec with univariate Cox regression analysis and multivariate model, none of the study parameters were detected to have a statistically significant correlation with DFS in our study. Analysis of the diagnostic value of these parameters by ROC curve determined high sensitivity rates for SUV_{max}, SUV_{mean}, MTV and a

high specificity rate for TLG with the selected cut-off values (487 for TLG). The results indicate that high-grade PGISL, especially DLBC subtype and PGL, tend to have high metabolic parameters indirectly reflecting high mitotic activity of tumor cells. This particularity is perhaps responsible for responding well to treatment. In other words, first results indicate that metabolic tumor parameters are not prognostic in high-grade PGISL despite their high values.

Conclusion

Metabolic tumor parameters are not predictive markers in primary high-grade gastrointestinal lymphomas, especially in DLBC variant and PGL. The findings suggest they will not play a role in patient management. Female sex was identified as the single risk factor for recurrence.

Ethics

Ethics Committee Approval: The study was approved by Gülhane Training and Research Hospital Local Ethics Committee (Date: 17.02.2016, Protocol number: 40).

Informed Consent: Consent form was filled out by all participants. Informed consent was waived due to the retrospective design of the study using records, documents and data of patients referred to our clinic for the test.

Peer-review: Externally peer-reviewed.

Authorship Contributions

Surgical and Medical Practices: E.A., K.O., S.İ., Concept: E.A., K.O., N.A., Design: E.A., K.O., M.K., Data Collection or Processing: E.A., K.O., S.İ., Analysis or Interpretation: E.A., C.H., T.T., Literature Search: E.A., K.O., S.İ., Ş.Ö., Writing: E.A., K.O., S.İ.

Conflict of Interest: The authors declared that there is no conflict of interest regarding the publication of this paper.

Financial Disclosure: The authors declared that this study received no financial support.

References

1. Kashyap R, Rai Mittal B, Manohar K, Balasubramanian Harisankar CN, Bhattacharya A, Singh B, Malhotra P, Varma S. Extranodal manifestations of lymphoma on [18F]FDG PET/CT: a pictorial essay. Cancer Imaging 2011;11:166-174.
2. Kumar R, Xiu Y, Potenta S, Mavi A, Zhuang H, Yu JQ, Dhurairaj T, Dadparvar S, Alavi A. 18F-FDG PET for evaluation of the treatment response in patients with gastrointestinal tract lymphomas. J Nucl Med 2004;45:1796-1803.
3. Koniaris LG, Drugas G, Katzman PJ, Salloum R. Management of gastrointestinal lymphoma. J Am Coll Surg 2003;197:127-141.
4. Al-Akwaa AM, Siddiqui N, Al-Mofleh IA. Primary gastric lymphoma. World J Gastroenterol 2004;10:5-11.
5. Radan L, Fischer D, Bar-Shalom R, Dann EJ, Epelbaum R, Haim N, Gaitini D, Israel O. FDG avidity and PET/CT patterns in primary gastric lymphoma. Eur J Nucl Med Mol Imaging 2008;35:1424-1430.
6. d'Amore F, Brincker H, Grønbaek K, Thorling K, Pedersen M, Jensen MK, Andersen E, Pedersen NT, Mortensen LS. Non-Hodgkin's lymphoma of the gastrointestinal tract: a population-based analysis of incidence, geographic distribution, clinicopathological presentation features and prognosis. Danish Lymphoma Study Group. J Clin Oncol 1994;12:1673-1684.
7. Dodd GD. Lymphoma of the hollow abdominal viscera. Radiol Clin North Am 1990;28:771-783.
8. Gollub MJ. Imaging of gastrointestinal lymphoma. Radiol Clin North Am 2008;46:287-312.
9. Freeman C, Berg JW, Cutler SJ. Occurrence and prognosis of extranodal lymphomas. Cancer 1972;29:252-260.
10. Zucca E, Cavalli F. Extranodal lymphomas. Ann Oncol. 2000;11(Suppl 3):219-222.
11. Weihrauch MR, Dietlein M, Schicha H, Diehl V, Tesch H. Prognostic significance of 18F-fluorodeoxyglucose positron emission tomography in lymphoma. Leuk Lymphoma 2003;44:15-22.
12. Schrepfer T, Haerle SK, Strobel K, Schaefer N, Hälg RA, Huber GF. The value of (18)F-fluorodeoxyglucose positron emission tomography/computed tomography for staging of primary extranodal head and neck lymphomas. Laryngoscope 2010;120:937-944.
13. Spaepen K, Stroobants S, Verhoef G, Mortelmans L. Positron emission tomography with [18F]FDG for therapy response monitoring in lymphoma patients. Eur J Nucl Med Mol Imaging 2003;30(Suppl 1):97-105.
14. Hoffmann M, Vogelsang H, Kletter K, Zettinig G, Chott A, Raderer M. 18F-fluoro-deoxy-glucose positron emission tomography (18F-FDG PET) for assessment of enteropathy-type T cell lymphoma. Gut 2003;52:347-351.
15. Phongkitkarun S, Varavithya V, Kazama T, Faria SC, Mar MV, Podoloff DA, Macapinlac HA. Lymphomatous involvement of gastrointestinal tract: evaluation by positron emission tomography with (18) F-fluorodeoxyglucose. World J Gastroenterol 2005;11:7284-7289.
16. Ezzat AA, Ibrahim EM, El Weshi AN, Khafaga YM, AlJurf M, Martin JM, Ajarim DS, Bazarbashi SN, Stuart RK, Zucca E Localized non-Hodgkin's lymphoma of Waldeyer's ring: clinical features, management, and prognosis of 130 adult patients. Head Neck 2001;23:547-558.
17. Amer MH, el-Akkad S. Gastrointestinal lymphoma in adults: clinical features and management of 300 cases. Gastroenterology 1994;106:846-858.
18. Kolve ME, Fischbach W, Wilhelm M. Primary gastric non-Hodgkin's lymphoma: requirements for diagnosis and staging. Recent Results Cancer Res 2000;156:63-68.
19. Bronowicki JP, Bineau C, Feugier P, Hermine O, Brousse N, Oberti F, Rousselet MC, Dharancy S, Gaulard P, Flejou JF, Cazals-Hatem D, Labouyrie E. Primary lymphoma of the liver: clinical-pathological features and relationship with HCV infection in French patients. Hepatology 2003;37:781-787.
20. Yoon WJ, Yoon YB, Kim YJ, Ryu JK, Kim YT. Primary pancreatic lymphoma in Korea–a single center experience. J Korean Med Sci 2010;25:536-540.
21. Yi JH, Kim SJ, Choi JY, Ko YH, Kim BT, Kim WS. 18F-FDG uptake and its clinical relevance in primary gastric lymphoma. Hematol Oncol 2010;28:57-61.
22. Jerusalem G, Beguin Y, Najjar F, Hustinx R, Fassotte MF, Rigo P, Fillet G. Positron emission tomography (PET) with 18F-fluorodeoxyglucose (18F-FDG) for the staging of low-grade non-Hodgkin's lymphoma (NHL). Ann Oncol 2001;12:825-830.
23. Alavi A, Shrikanthan S, Aydin A, Talanow R, Schuster S. Fluorodeoxyglucose positron-emission tomography findings in mantle cell lymphoma. Clin Lymphoma Myeloma Leuk 2011;11:261-266.
24. Cavalli F, Isaacson PG, Gascoyne RD, Zucca E. MALT Lymphomas. Hematology Am Soc Hematol Educ Program 2001:241-258.
25. Beal KP, Yeung HW, Yahalom J. FDG PET scanning for detection and staging of extranodal marginal zone lymphomas of the MALT type: a report of 42 cases. Ann Oncol 2005;16:473-480.

26. Song MK, Chung JS, Lee JJ, Jeong SY, Lee SM, Hong JS, Chong A, Moon JH, Kim JH, Lee SM, Kim SJ, Shin HJ. Metabolic tumor volume by positron emission tomography/computed tomography as a clinical parameter to determine therapeutic modality for early stage Hodgkin's lymphoma. Cancer Sci 2013;104:1656-1661.
27. Esfahani SA, Heidari P, Halpern EF, Hochberg EP, Palmer EL, Mahmood U. Baseline total lesion glycolysis measured with (18)F-FDG PET/CT as a predictor of progression-free survival in diffuse large B-cell lymphoma: a pilot study. Am J Nucl Med Mol Imaging 2013;3:272-281.
28. Gallicchio R, Mansueto G, Simeon V, Nardelli A, Guariglia R, Capacchione D, Soscia E, Pedicini P, Gattozzi D, Musto P, Storto G. F-18 FDG PET/CT quantization parameters as predictors of outcome in patients with diffuse large B-cell lymphoma. Eur J Haematol 2014;92:382-389.
29. Ceriani L, Martelli M, Zinzani PL, Ferreri AJ, Botto B, Stelitano C, Gotti M, Cabras MG, Rigacci L, Gargantini L, Merli F, Pinotti G, Mannina D, Luminari S, Stathis A, Russo E, Cavalli F, Giovanella L, Johnson PW, Zucca E. Utility of baseline 18FDG PET/CT functional parameters in defining prognosis of primary mediastinal (thymic) large B-cell lymphoma. Blood 2015;126:950-956.

Original Article
Mol Imaging Radionucl Ther 2017;26:93-100 DOI:10.4274/mirt.94695

Thyroid Incidentalomas on ^{18}F-FDG PET/CT: Clinical Significance and Controversies

^{18}F-FDG PET/BT'de Tiroid İnsidentalomalar: Klinik Önem ve Tartışmalar

William Makis[1], Anthony Ciarallo[2]
[1]*Cross Cancer Institute, Department of Diagnostic Imaging, Edmonton, Canada*
[2]*MUHC Glen Site, Department of Nuclear Medicine, Montreal, Canada*

Abstract

Objective: The purpose of the current study is to examine the incidence and clinical significance of unexpected focal uptake of ^{18}F-fluorodeoxyglucose (^{18}F-FDG) on positron emission tomography/computed tomography (PET/CT) in the thyroid gland of oncology patients, the maximum standardized uptake value (SUV_{max}) of benign and malignant thyroid incidentalomas in these patients, and review the literature.

Methods: Seven thousand two hundred fifty-two ^{18}F-FDG PET/CT studies performed over four years, were retrospectively reviewed. Studies with incidental focal ^{18}F-FDG uptake in the thyroid gland were further analyzed.

Results: Incidental focal thyroid ^{18}F-FDG uptake was identified in 157 of 7252 patients (2.2%). Sufficient follow-up data (≥12 months) were available in 128 patients, of whom 57 (45%) had a biopsy performed and 71 had clinical follow-up. Malignancy was diagnosed in 14 of 128 patients (10.9%). There was a statistically significant difference between the median SUV_{max} of benign thyroid incidentalomas (SUV_{max} 4.8) vs malignant (SUV_{max} 6.3), but the wide range of overlap between the two groups yielded no clinically useful SUV_{max} threshold value to determine malignancy.

Conclusion: ^{18}F-FDG positive focal thyroid incidentalomas occurred in 2.2% of oncologic PET/CT scans, and were malignant in 10.9% of 128 patients. This is the lowest reported malignancy rate in a North American study to date, and significantly lower than the average malignancy rate (35%) reported in the literature. Invasive biopsy of all ^{18}F-FDG positive thyroid incidentalomas, as recommended by some studies, is unwarranted and further research to determine optimal management is needed. There was no clinically useful SUV_{max} cut-off value to determine malignancy and PET/CT may not be a useful imaging modality to follow these patients conservatively.

Keywords: Thyroid incidentaloma, thyroid carcinoma, ^{18}F-fluorodeoxyglucose, ^{18}F-FDG, positron emission tomography, PET, PET/CT

Öz

Amaç: Bu çalışmanın amacı onkoloji hastalarının ^{18}F-florodeoksiglukoz (^{18}F-FDG) pozitron emisyon tomografisi/bilgisayarlı tomografisinde (PET/BT) tesadüfen saptanan tiroid bezi fokal tutulumunun insidansını ve klinik önemini ve bu hastalarda benign ve malign tiroid insidentalomalarının maksimum standardize tutulum değerini (SUV_{maks}) değerlendirmek ve literatürü gözden geçirmektir.

Yöntem: Dört yıl boyunca yapılmış 7252 ^{18}F-FDG PET/BT incelemesi retrospektif olarak değerlendirildi. Tiroid bezinde insidental fokal ^{18}F-FDG tutulumu olanlar incelemeye dahil edildi.

Address for Correspondence: William Makis MD, Cross Cancer Institute, Department of Diagnostic Imaging, Edmonton, Canada
Phone: 7804328760 E-mail: makisw79@yahoo.com ORCID ID: orcid.org/0000-0003-0241-3426
Received: 13.01.2017 **Accepted:** 22.06.2017

©Copyright 2017 by Turkish Society of Nuclear Medicine
Molecular Imaging and Radionuclide Therapy published by Galenos Yayınevi.

Öz

Bulgular: 7252 hastanın 157'sinde insidental fokal tiroid ^{18}F-FDG tutulumu saptandı (%2,2). Yüz yirmi sekiz hastada yeterli takip verisi mevcuttu (≥12 ay), bunların 57'sine (%45) biyopsi uygulanmış ve 71'i klinik olarak takip edilmişti. Yüz yirmi sekiz hastanın 14'ünde malignite saptanmıştı (%10,9). Benign tiroid insidentalomalarının ortanca maksimum standardize tutulum değeri (SUV_{maks} 4,8) ile malign tiroid insidentalomalarının değerleri (SUV_{maks} 6,3) arasında istatistiki olarak anlamlı fark saptandı, ancak her iki grup arasındaki geniş aralıklı örtüşme olduğundan malignite saptamada klinik olarak yararlı olabilecek bir SUV_{maks} eşik değeri saptanmadı.

Sonuç: ^{18}F-FDG pozitif fokal tiroid insidentaloması onkolojik PET/BT taramalarının %2,2'sinde görüldü ve 128 hastanın %10,9'unda malignite mevcuttu. Bu oran günümüze kadar Kuzey Amerika çalışmalarında bildirilen en düşük düzeydir ve literatürde bildirilen ortalama malignite oranından (%35) ciddi şekilde azdır. Bazı çalışmalarda önerildiği gibi tüm ^{18}F-FDG pozitif tiroid insidentalomalarının invazif biyopsisi sağlam bir temele dayanmamaktadır, optimal yaklaşımı belirlemek için ileri çalışmalara ihtiyaç vardır. Malignite saptamak için klinikte kullanılabilecek bir SUV_{maks} eşik değeri bulunmamıştır, bu hastaları konservatif olarak takip etmek için PET/BT yararlı bir modalite olmayabilir.

Anahtar kelimeler: Tiroid insidentaloma, tiroid karsinoma, ^{18}F-florodeoksiglukoz, ^{18}F-FDG, pozitron emisyon tomografisi, PET, PET/BT

Introduction

One of the main challenges that face positron emission tomography/computed tomography (PET/CT) readers is the interpretation of foci of abnormal ^{18}F-FDG uptake in unexpected anatomic locations (1,2,3,4,5,6,7,8,9,10). The thyroid gland is the best studied anatomic location of incidental ^{18}F-FDG uptake, with well over 30 studies examining the clinical significance of thyroid incidentaloma (11-22), including 3 systematic reviews (11-13). However, thyroid incidentalomas still remain a source of controversy in the literature.

The malignancy rates in thyroid incidentalomas range in the literature from 10% up to 64%. Three systematic reviews have reported a pooled malignancy rate of 33-35%. One major point of contention with most of these studies is that only a small subset of patients is biopsied (usually patients with a high clinical suspicion of malignancy), and most thyroid incidentaloma patients are not investigated or followed further. The largest systematic review of thyroid incidentaloma studies (27 studies) revealed a biopsy rate of only 35%. Many papers in the literature recommend that all thyroid incidentaloma patients be invasively biopsied, however this recommendation is based on a malignancy rate derived from a subset of non-randomly selected thyroid incidentaloma patients.

There is also controversy over the utilization of SUV_{max} to differentiate benign from malignant thyroid incidentalomas. Many studies have made attempts to determine an optimal cut-off SUV_{max} value for differentiating benign from malignant lesions. Only half of these studies have managed to detect a statistically significant difference. Three meta-analyses reflect these conflicting results.

The purpose of this retrospective review was to determine the incidence of unexpected focal uptake of ^{18}F-FDG in the thyroid gland of oncology patients (with no prior history of thyroid cancer) and what proportion of these cases were malignant. We also evaluated the feasibility of using SUV_{max} to identify malignant causes of incidental focal thyroid ^{18}F-FDG uptake and investigated whether a clinically useful cut-off value of SUV_{max} could be determined.

Materials and Methods

A retrospective review of 7252 oncologic ^{18}F-FDG PET/CT studies performed over the course of 48 months (January 1, 2006-December 31, 2009) was done. PET/CT studies with incidental focal ^{18}F-FDG thyroid gland uptake, regardless of corresponding CT findings, formed the basis for this review.

One hundred fifty-seven (n=157) patients out of 7252 (2.2%) had unexpected focal ^{18}F-FDG thyroid uptake and comprised the study group. We excluded patients who had a history of a previous thyroid malignancy or predisposing condition (e.g. Cowden syndrome) (n=6), and patients who had insufficient follow-up data (less than 12 months) (n=23). The remaining 128 patients comprised the study group that was evaluated further to determine the clinical significance of unexpected focal ^{18}F-FDG thyroid gland uptake. The primary malignant diagnoses of these 128 patients are listed in Table 1.

PET/CT Examination and Interpretation

The PET scanner used in this study was the Discovery ST with a 16-slice CT (GE Healthcare, WI, USA). ^{18}F-FDG PET/CT exams were performed according to routine institutional protocol. After a minimum of 4 to 6 hours of fasting, patients waited in a quiet and dark room just prior to their exam. Serum glucose levels were tested and 0.22 mCi (8.14 MBq)/kg dose of ^{18}F-FDG was injected (to a maximum dose of 20 mCi, or 740 MBq). Approximately 60 minutes after injection of ^{18}F-FDG, PET portion of the study was acquired in 2D from the base of the skull to the proximal thighs. Data were acquired

for 4-5 min per bed position (depending on patient body weight). CT portion of the study was acquired (140 kVp, 90-110 mA) with a rotation time of 0.8 s, pitch 1.75:1 and detector row configuration of 16x0.625 mm. The patient was breathing normally during both PET and CT acquisitions.

The PET data were reconstructed iteratively with ordered-subsets expectation maximization algorithm (21 subsets, 2 iterations). PET emission data were corrected for photon attenuation effects using CT images. PET/CT exams were interpreted by two nuclear medicine board certified physicians independently on a dedicated Xeleris 2.0 workstation (GE Healthcare, Waukesha, WI, USA). Any unexpected focal ^{18}F-FDG thyroid gland uptake was noted and maximum standardized uptake value (SUV_{max} corrected for body weight) was measured using a spherical region of interest (ROI) at the site of most intense ^{18}F-FDG accumulation.

Table 1. Study population (n=128)

Primary malignancy	n (%)	Malignant incidentaloma
Lymphoma	24 (18.8)	2
Rectal	14 (10.9)	1
Unknown origin	14 (10.9)	1
Lung	12 (9.4)	1
Sarcoma	10 (7.8)	
Cervical	8 (6.3)	
Colon	8 (6.3)	2
Breast	7 (5.5)	1
Melanoma	6 (4.7)	2
Uterine	4 (3.1)	
Gastric	3 (2.3)	1
GIST	3 (2.3)	1
Dermatomyositis	2 (1.6)	
Neuroendocrine	2 (1.6)	
Vulvar	2 (1.6)	
Brain	1 (0.8)	
Desmoid	1 (0.8)	1
Esophageal	1 (0.8)	
Hepatocellular	1 (0.8)	
Ovarian	1 (0.8)	
Pancreatic	1 (0.8)	
Prostate	1 (0.8)	
Pseudomyxoma p.	1 (0.8)	
Renal	1 (0.8)	1

GIST: Gastrointestinal stromal tumor

Diagnosis

Histopathologic evaluation or clinical follow-up (with or without serial PET/CT examinations) over a time period of at least 12 months determined the final diagnosis of either benign thyroid incidentaloma or malignant thyroid incidentaloma. Histological sampling was available in 57 of 128 patients and the other 71 patients were assessed clinically over a minimum period of 12 months or more, with a mean clinical follow-up time of 28 months (range: 12-70 months). Global clinical assessment comprised a physical examination and evaluation of all available biochemical and diagnostic imaging studies.

Statistical Analysis

The Wilcoxon-Mann-Whitney test was used to compare the ^{18}F-FDG PET/CT SUV between benign and malignant thyroid lesions. Numeric data were expressed as median ± interquartile range (IQR). P values of less than 0.05 were considered to indicate a statistically significant difference.

Ethical statement: The study was approved by an institutional review board or equivalent and has been performed in accordance with the ethical standards laid down in the 1964 Declaration of Helsinki and its later amendments. All subjects in the study gave written informed consent or the institutional review board waived the need to obtain informed consent.

Results

Out of 128 patients included in the study, there were 31 men and 97 women. One hundred fourteen (89.1%) were diagnosed with a benign thyroid process and 14 (10.9%) were diagnosed with a thyroid malignancy. The mean age of patients with benign thyroid lesions was 62.8 years, compared to 57.1 years for patients with malignant thyroid lesions. A total of 154 individual ^{18}F-FDG positive thyroid lesions were identified in these 128 patients. The locations of the thyroid lesions are given in Table 2.

Histological evaluation was available in 57 of 128 patients. Fourteen of 57 were malignant (11 papillary, 1 follicular, 1 lymphoma and 1 metastasis) and 43 of 57 were benign (23 Hurthle cell metaplasia, 11 nodular goiter, 5 benign epithelium, 2 thyroiditis, 2 follicular adenoma) (Table 3). The mean SUV_{max} of each lesion type is given in Table 3.

The remaining 71 patients were followed clinically. In addition to global clinical assessment, PET/CT follow-up

Table 2. Location of thyroid incidentalomas

Total ^{18}F-FDG (+) lesions	n=154	%
Left	73	47.4
Right	77	50.0
Isthmus	4	2.6
Bilateral	26	16.9

studies were available in 29 of 71 patients, and the results of follow-up PET/CT SUV_{max} of incidental focal thyroid uptake are summarized in Table 4.

There was a statistically significant difference between the median SUV_{max} values in benign thyroid incidentalomas (median SUV_{max} 4.8) versus malignant lesions (median SUV_{max} 6.3), p value=0.03, Wilcoxon Mann Whitney-U test (Table 5). However, there was a significant overlap between the ranges of benign and malignant thyroid incidentalomas with benign SUV_{max} values ranging from 2.1-30.5, and malignant SUV_{max} values ranging from 3.4 to 28.1.

Table 3. Biopsied thyroid incidentalomas (n=57)

Malignant (n=14)	**n**	**Mean SUV_{max}**
Papillary carcinoma	11	9.3
Follicular carcinoma	1	8.3
Lymphoma	1	9.9
Metastasis (renal cell)	1	4.2
Benign (n=43)	**n**	**Mean SUV_{max}**
Hurthle cell metaplasia	23	5.6
Nodular goiter	11	5.3
Benign epithelium	5	4.3
Thyroiditis	2	6.8
Follicular adenoma	2	3.8

Table 4. Clinical follow-up

Type of follow-up	**(n=71)**
Clinical follow-up only	42
Clinical and PET/CT follow-up	29
Increased SUV_{max} on follow-up	8
Same SUV_{max} on follow-up	2
Decreased SUV_{max} on follow-up	15
Resolved ^{18}F-FDG uptake	4

PET/CT: Positron emission tomography/computed tomography

A few potential SUV_{max} cut-offs were examined and a kappa statistic was calculated for each value to see which would maximize sensitivity and specificity. The SUV_{max} cut-off with the highest kappa coefficient is provided (Table 6). These calculations were performed to determine if there was a satisfactory SUV_{max} cut-off to differentiate benign thyroid lesions from malignant ones.

A receiver-operating-characteristic (ROC) curve analysis of sensitivities and specificities was performed to determine a clinically useful SUV_{max} cut-off value to aid in differentiating between benign and malignant lesions (Figure 1). PET/CT image examples of four patients with incidental thyroid uptake and their biopsy results, are provided in Figure 2.

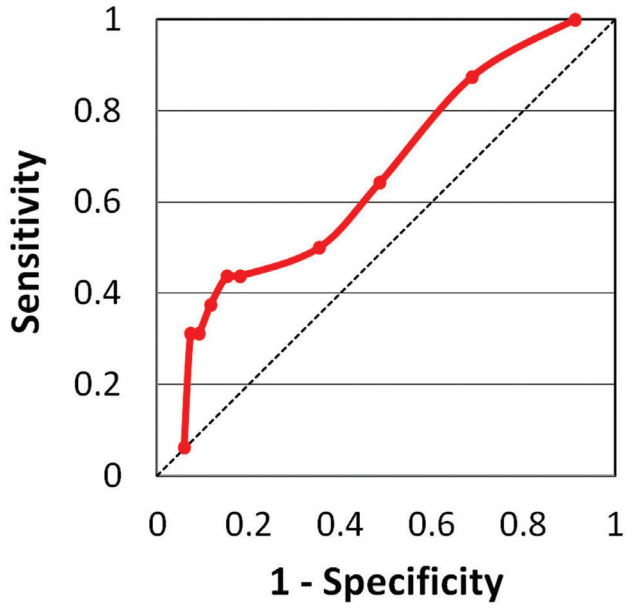

Figure 1. Receiver-operating-characteristic curve with sensitivity (y-axis) versus 1-Specificity (x-axis) shows no satisfactory value for SUV_{max} to differentiate benign from malignant thyroid incidentalomas

Table 5. Thyroid lesion analysis

	Benign (n=138)	**Malignant (n=16)**	**p value**
Mean age [y] (SD)	62.8 (13.6)	57.1 (14.2)	0.14
Median age [y] (IQR)	63.5 (53.0; 72.0)	56.5 (49.0; 69.0)	0.19
SUV_{max}			
Mean (SD)	5.9 (3.6)	8.6 (6.1)	0.10
Median (IQR)	4.8 (3.6; 6.9)	6.3 (4.6; 11.7)	**0.03**
Range (min.; max.)	(2.1; 30.5)	(3.4; 28.1)	
Follow-up			
Months (min.; max.)	28 (12; 70)	n/a	–

SD: Standard deviation, IQR: Interquartile range, min.: Minimum, max.: Maximum

Discussion

Incidental and unexpected focal uptake of ^{18}F-FDG in oncologic PET/CT studies has been well studied in anatomic locations such as the breast, adrenal, gastrointestinal, parotid, prostate and thyroid glands (1,2,3,4,5,6,7,8,9,10). The thyroid gland is probably the best studied location of incidental ^{18}F-FDG uptake on PET/CT, however, it remains a source of significant controversy. In recent years, three systematic reviews have been published, examining thyroid incidentaloma literature over the past 15 years, including an analysis of 18 papers by Shie et al. (11), 22 papers by Soelberg et al. (12), and 27 papers by Bertagna et al. (13). Although these three meta-analyses showed similar conclusions, the issue of the clinical significance of ^{18}F-FDG positive thyroid incidentalomas has not been settled.

In our review of 7252 consecutive oncologic PET/CT studies, incidental focal thyroid ^{18}F-FDG uptake was identified in 2.2% (n=157) of patients. This is within the range reported in the literature, with reports ranging from 0.2 to 8.9%. Shie et al. (11) reported 1% in 55,160 PET studies, Soelberg et al. (12) reported 1.6% in 125,754 PET studies and Bertagna et al. (13) reported a pooled incidence of 2.5% in 147,505 PET studies.

The rate of malignancy of thyroid incidentalomas varies tremendously in the literature from 10% to 64% (14,15) and remains a source of controversy. The rate of malignancy for our cohort was 10.9%. The mean malignancy rate was reported as 33.2% in the Shie et al. (11) review, as 34.8% by Soelberg et al. (12), and as 34.6% by Bertagna et al. (13). The concordance of these meta-analysis results is not surprising as many of the same thyroid incidentaloma papers were examined by all three reviews. However, these meta-analyses did not examine possible reasons why thyroid incidentaloma malignancy rates varied so much in the literature (10 to 64%).

Most published studies included in the three meta-analyses did not have histopathologic correlation or clinical follow-up on the majority of thyroid incidentaloma patients. In fact, the reported malignancy rates were usually calculated from a subset of biopsied patients who were biopsied most likely due to a high clinical suspicion of malignancy, which yielded, unsurprisingly, high malignancy rates. Soelberg et al. (12) reported a pooled biopsy rate of 46% (923/1994), and Shie et al. (11) reported a biopsy + follow-up rate of 56% (322/571). The largest meta-analysis by Bertagna et al. (13) reported a biopsy rate of only 35% (1308/3727) and noted that in the majority of the studies, the proportion of ^{18}F-FDG positive thyroid incidentalomas that had further investigations was "inferior". Shie et al. (11) expressed that the malignancy rate in the 44% of thyroid incidentalomas that were not investigated would be similar to the malignancy rate of those who were biopsied because of similar demographic characteristics in the two groups. This assumption is flawed. If the patients chosen for biopsy had been chosen randomly, then the assumption may have had merit, but biopsied patients were not chosen randomly. Studies generally do not provide any explanations of how

Table 6. Malignancy vs. SUV_{max} cut-off (Receiver-operating-characteristic)

SUV cut-off	Sens (95% CI)	Spec (95% CI)	PPV (95% CI)	NPV (95% CI)
5.0	69 (42-88)	51 (43-60)	14 (8-24)	93 (85-98)
6.0	50 (26-75)	65 (56-73)	14 (7-26)	92 (85-96)
8.3*	44 (21-69)	85 (78-90)	25 (11-45)	93 (87-97)

*Kappa=0.74, NPV: Negative predictive value, PPV: Positive predictive value, CI: Confidence interval

Table 7. Thyroid incidentaloma studies with biopsy rates >80%

Ref	Year	Author	Country	Incidentaloma	Malignant/ biopsied	Reported malignancy rate	Biopsied rate	Issues/problems
(14)	2003	Hsieh	Taiwan	12/477	1/10	**10%**	83% (10/12)	
(16)	2005	Chen	Taiwan	60/4803	7/50	**14%**	83% (50/60)	Healthy volunteers only
(17)	2007	King	USA	22/15711	3/21	**14%**	95% (21/22)	
(19)	2010	Zhai	China	115/3580	48/96	**50%**	83% (96/115)	Unknown type of patient
(20)	2010	Kim	Korea	159/11623	37/140	**23% 37/159**	88% (140/159)	
(21)	2010	Ohba	Japan	20/1501	11/20	**55%**	100% (20/20)	Healthy volunteers only
(22)	2012	Bonabi	Swiss	53/3062	10/42	**24%**	80% (42/53)	

Note: Study by Kwak et al. (18) in the Bertagna et al. (13) meta-analysis cannot be considered in this analysis of thyroid incidentaloma studies as patients in that study were selected based on ultrasound positivity for a nodule in the thyroid, and only then checked for any positron emission tomography/computed tomography imaging and positivity. Thus only a small subset of positron emission tomography/computed tomography thyroid incidentalomas were included by the authors

or why certain patients were chosen for biopsy, but it is reasonable to assume that those selected for biopsy had a high clinical or imaging suspicion for malignancy. Soelberg et al. (12) admitted in their meta-analysis: "One cannot exclude that surgical confirmation was most likely obtained in those patients with the highest likelihood of malignancy and therefore the malignancy risk of focal uptake is overestimated". We suspect that the reported average malignancy rate of 35% in the literature is overestimated and that the actual value is significantly lower.

An overview of the largest meta-analysis done by Bertagna et al. (13) (27 studies) reveals that the lowest malignancy rates are reported by studies with the highest biopsy rates. This pattern has not been noted either by Bertagna et al. (13) or the other two meta-analyses. We examined all papers with a biopsy rate of over 80% and further analyzed the available data (Table 7). Studies by Chen et al. (16) and Ohba et al. (21) were excluded as they were done on healthy volunteers only, and the study by Zhai et al. (19) was excluded as the patient population was unspecified. This leaves only four studies of oncologic patients with thyroid incidentalomas with high biopsy rates of more than 80%. These studies showed malignancy rates of 10% (14), 14% (17), 23% (20) and 24% (22). It is worth noting that the only North American study published in the literature with a high biopsy rate showed a malignancy rate of 14% (17), very close to our rate of 11%.

In our cohort of 128 thyroid incidentaloma patients, there was a statistically significant difference between the SUV_{max} values of benign thyroid incidentalomas (median SUV_{max} 4.8) and malignant incidentalomas (median SUV_{max} 6.3), however, there was a wide overlap of SUV_{max} values between the two groups. An ROC curve was generated, however no suitable SUV_{max} cut-off value was

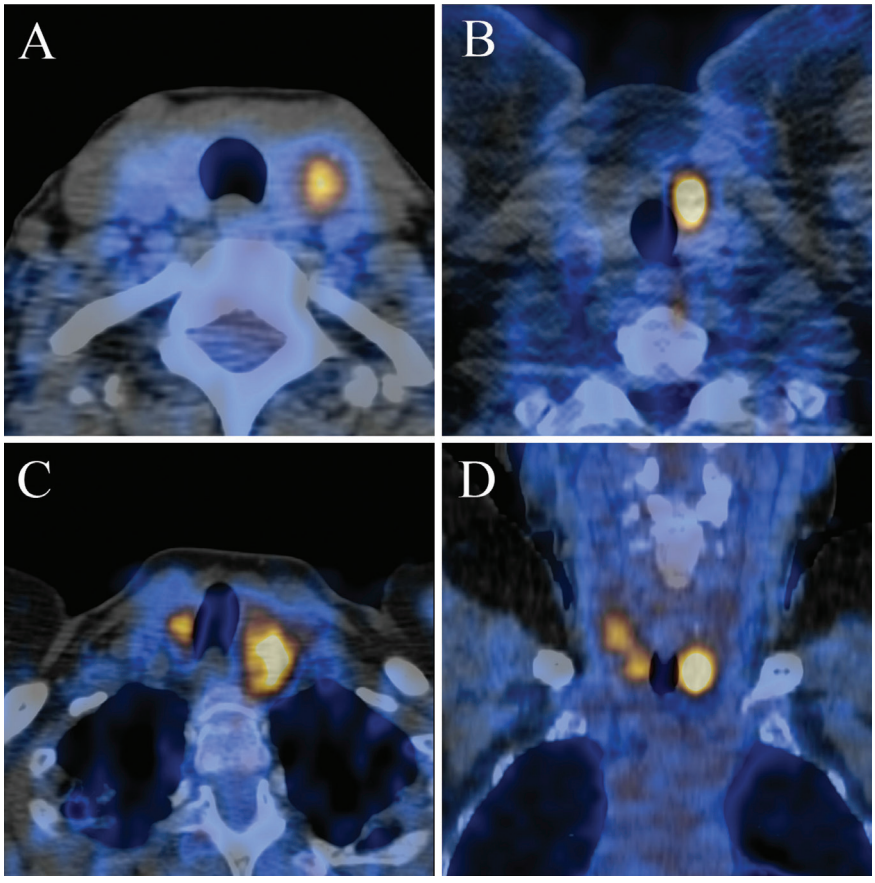

Figure 2. Four cases of incidental focal ^{18}F-FDG uptake in the thyroid. Transaxial PET/CT fusion image of a benign left thyroid incidentaloma in a 52-year-old woman with a prior history of cervical cancer, with SUV_{max} 4.4, biopsied to reveal a benign follicular lesion (A), transaxial PET/CT fusion image of a malignant left thyroid incidentaloma in a 40-year-old man with a prior history of melanoma, with SUV_{max} 11.8, biopsied to reveal a papillary carcinoma follicular variant (B). Transaxial PET/CT fusion image of a bilateral focal benign thyroid incidentaloma in a 65-year-old woman with a prior history of lymphoma, with SUV_{max} 7.8 of left lesion and SUV_{max} 6.4 of right lesion, biopsied to reveal benign nodular hyperplasia (C), coronal PET/CT fusion image of a bilateral malignant thyroid incidentaloma in a 70-year-old woman with a prior history of colorectal carcinoma, with SUV_{max} 8.1 in the left lesion and SUV_{max} 4.5 in the right lesion, biopsied to reveal a multifocal papillary carcinoma, classical variant on a background of Hashimoto's thyroiditis (D)

found to be useful in differentiating benign from malignant thyroid incidentalomas (Figure 1). This is in agreement with all three meta-analyses, all of which found a statistically significant difference between SUV_{max} of benign lesions vs malignant lesions, with a wide overlap and no clear SUV_{max} cut-off value, or role for the use of SUV_{max} to differentiate benign from malignant thyroid incidentalomas.

In our clinically followed group (71 of 128 patients), 29 of 71 (41%) patients also had a follow-up PET/CT and incidental thyroid uptake was re-evaluated on the follow-up PET/CT. Interestingly, although all 29 patients were determined to have benign thyroid incidentalomas on long term clinical follow-up, 8 of 29 (28%) follow-up PET/CTs showed increased SUV_{max} in the thyroid incidentaloma (defined as any increase over the previous SUV_{max} value), with the rest showing equal or lower SUV_{max}, suggesting that increasing SUV_{max} on a follow-up PET/CT may not be helpful in assessing whether a thyroid incidentaloma was benign or malignant, and therefore a follow-up PET/CT is unlikely to be a useful imaging modality to monitor and follow thyroid incidentaloma patients. Further research in this area is needed to determine the optimal management of thyroid incidentaloma patients.

Study Limitations

A limitation of our study was that only 57 of 128 thyroid incidentaloma patients (45%) were biopsied. Ideally, a thyroid incidentaloma study would be prospective and all ^{18}F-FDG positive focal thyroid incidentalomas would have biopsy results available. However, unlike most studies that had not evaluated or followed thyroid incidentaloma patients who were not biopsied, our 71 patients who were not biopsied were followed for at least 12 months.

Conclusion

^{18}F-FDG positive focal thyroid incidentalomas occurred in 2.2% of oncologic PET/CT scans, and of these, 10.9% were malignant. This is the lowest malignancy rate reported in a North American study and second lowest in the world to date, and is much lower than the average 33-35% malignancy rate reported in recent systematic reviews. Higher reported malignancy rates in the literature may be the result of selection bias. The decision to biopsy a thyroid incidentaloma should be deferred in the absence of a high clinical or imaging suspicion of malignancy. Recommendations to biopsy all ^{18}F-FDG positive focal thyroid incidentalomas should not be followed until further research is available. We suspect that the true malignancy rates of thyroid incidentalomas are in the 10-20% range, rather than 35% (or higher) range which is often quoted in the literature. SUV_{max} values cannot be used to differentiate benign from malignant thyroid incidentalomas, and follow-up PET/CT may not be useful in monitoring these patients. Future studies should be prospective and biopsy rates should be as high as possible, to avoid selection bias that may significantly impact reported malignancy rates.

Acknowledgements

The authors would like to thank Dr. Robert Battat, Dr. James Curtis and Dr. Han Zeng for their assistance in data collection and processing.

Ethics

Ethics Committee Approval: Retrospective study.

Informed Consent: Retrospective study.

Peer-review: Internally peer-reviewed.

Authorship Contributions

Concept: W.M., Design: W.M., A.C., Data Collection and Processing: A.C., Analysis and interpretation: W.M., A.C., Literature Search: W.M., A.C., Writing: W.M., A.C.

Conflict of Interest: No conflict of interest was declared by the authors.

Financial Disclosure: The authors declared that this study received no financial support.

References

1. Cook GJ, Fogelman I, Maisey MN. Normal physiological and benign pathological variants of 18-fluoro-2-deoxyglucose positron emission tomography scanning: potential for error in interpretation. Semin Nucl Med 1996;26:308-314.
2. Bakheet SM, Powe J. Benign causes of 18-FDG uptake on whole body imaging. Semin Nucl Med 1998;28:352-358.
3. Kostakoglu L, Hardoff R, Mirtcheva R, Goldsmith SJ. PET-CT fusion imaging in differentiating physiologic from pathologic FDG uptake. Radiographics 2004;24:1411-1431.
4. Israel O, Yefremov N, Bar-Shalom R, Kagana O, Frenkel A, Keidar Z, Fischer D. PET/CT detection of unexpected gastrointestinal foci of 18F-FDG uptake: incidence, localization patterns, and clinical significance. J Nucl Med 2005;46:758-762.
5. Tatlidil R, Jadvar H, Bading JR, Conti PS. Incidental colonic fluorodeoxyglucose uptake: correlation with colonoscopic and histopathologic findings. Radiology 2002;224:783-787.
6. Litmanovich D, Gourevich K, Israel O, Gallimidi Z. Unexpected foci of 18F-FDG uptake in the breast detected by PET/CT: incidence and clinical significance. Eur J Nucl Med Mol Imaging 2009;36:1558-1564.
7. Choi JY, Lee KS, Kim HJ, Shim YM, Kwon OJ, Park K, Baek CH, Chung JH, Lee KH, Kim BT. Focal thyroid lesions incidentally identified by integrated 18F-FDG PET/CT: clinical significance and improved characterization. J Nucl Med 2006;47:609-615.
8. Han EJ, HOJ, Choi WH, Yoo IR, Chung SK. Significance of incidental focal uptake in prostate on 18-fluoro-2-deoxyglucose positron emission tomography CT images. Br J Radiol 2010;83:915-920.
9. Metser U, Miller E, Lerman H, Lievshitz G, Avital S, Even-Sapir E. 18F-FDG PET/CT in the evaluation of adrenal masses. J Nucl Med 2006;47:32-37.
10. Basu S, Houseni M, Alavi A. Significance of incidental fluorodeoxyglucose uptake in the parotid glands and its impact on patient management. Nucl Med Commun 2008;29:367-373.
11. Shie P, Cardarelli R, Sprawls K, Fulda KG, Taur A. Systematic review: prevalence of malignant incidental thyroid nodules identified on fluorine-18 fluorodeoxyglucose positron emission tomography. Nuc Med Comm 2009;30:742-748.

12. Soelberg KK, Bonnema SJ, Brix TH, Hegedüs L. Risk of malignancy in thyroid incidentalomas detected by 18F-fluorodeoxyglucose positron emission tomography: a systematic review. Thyroid 2012;22:918-925.
13. Bertagna F, Treglia G, Piccardo A, Giubbini R. Diagnostic and clinical significance of F-18-FDG PET/CT thyroid incidentalomas. J Clin Endocrinol Metab 2012;97:3866-3875.
14. Hsieh HJ, Lin SH, Yang BH, Chu YK, Chang CP, Liu RS. The clinical relevance of thyroid incidentalomas detected by 18F-fluorodeoxyglucose positron emission tomography. Ann Nucl Med Sci 2003;16:53-58.
15. Chen W, Parsons M, Torigian DA, Zhuang H, Alavi A. Evaluation of thyroid FDG uptake incidentally identified on FDG PET/CT imaging. Nucl Med Commun 2009;30:240-244.
16. Chen YK, Ding HJ, Chen KT, Chen YL, Liao AC, Shen YY, Su CT, Kao CH. Prevalence and risk of cancer of focal thyroid incidentaloma identified by 18F-fluorodeoxyglucose positron emission tomography for cancer screening in healthy subjects. Anticancer Res 2005;25:1421-1426.
17. King DL, Stack BC Jr, Spring PM, Walker R, Bodenner DL. Incidence of thyroid carcinoma in fluorodeoxyglucose positron emission tomography-positive thyroid incidentalomas. Otolaryngol Head Neck Surg 2007;137:400-404.
18. Kwak JY, Kim EK, Yun M, Cho A, Kim MJ, Son EJ, Oh KK. Thyroid incidentalomas identified by 18F-FDG PET: sonographic correlation. AJR Am J Roentgenol 2008;191:598-603.
19. Zhai G, Zhang M, Xu H, Zhu C, Li B. The role of 18F-fluorodeoxyglucose positron emission tomography/computed tomography whole body imaging in the evaluation of focal thyroid incidentaloma. J Endocrinol Invest 2010;33:151-155.
20. Kim BH, Na MA, Kim IJ, Kim SJ, Kim YK. Risk stratification and prediction of cancer of focal thyroid fluorodeoxyglucose uptake during cancer evaluation. Ann Nucl Med 2010;24:721-728.
21. Ohba K, Nishizawa S, Matsushita A, Inubushi M, Nagayama K, Iwaki H, Matsunaga H, Suzuki S, Sasaki S, Oki Y, Okada H, Nakamura H. High incidence of thyroid cancer in focal thyroid incidentaloma detected by 18F-fluorodeoxyglucose [corrected] positron emission tomography in relatively young healthy subjects: results of 3-year follow-up. Endocr J 2010;57:395-401.
22. Bonabi S, Schmidt F, Broglie MA, Haile SR, Stoeckli SJ. Thyroid incidentalomas in FDG PET/CT: prevalence and clinical impact. Eur Arch Otorhinolaryngol 2012;269:2555-2560.

Original Article
Mol Imaging Radionucl Ther 2017;26:101-109 DOI:10.4274/mirt.50570

Bone Single Photon Emission/Computed Tomography in the Detection of Sacroiliitis in Seronegative Spondyloarthritis: A Comparison with Magnetic Resonance Imaging

Seronegatif Spondiloartritte Sakroiliit Tanısı için Kemik Sintigrafisi Pozitron Emisyon/Bilgisayarlı Tomografisi: Manyetik Rezonans Görüntüleme ile Karşılaştırma

Theodoros Pipikos[1], Dimitrios Kassimos[2], George Angelidis[3], John Koutsikos[3]
[1]*401 General Military Hospital, Clinic of Nuclear Medicine, Athens, Greece*
[2]*401 General Military Hospital, Clinic of Rheumatology, Athens, Greece*
[3]*Army Share Fund Hospital (417 NIMTS), Clinic of Nuclear Medicine, Athens, Greece*

Abstract

Objective: Seronegative spondyloarthritis (SpA) is characterized by chronic inflammation affecting the axial skeleton, entheses and occasionally peripheral joints. The involvement of the sacroiliac joints, sacroiliitis, is considered as a pathognomonic radiographic finding. Magnetic resonance imaging (MRI) is the method of choice for its early detection. Bone scintigraphy (BS) is characterized by high sensitivity in the diagnosis of bone and articular diseases. Limited value of BS in the diagnosis of sacroiliitis may be attributed to the use of planar imaging. In the present study, we aimed to investigate the role of SPECT in SpA, compared to MRI.

Methods: Forty-three patients suffering from inflammatory back pain underwent MRI evaluation of the sacroiliac joints and BS, combined with SPECT in the same region, for the assessment of sacroiliitis.

Results: Bone SPECT revealed no findings of sacroiliitis in 11 patients, with total agreement with MRI. Findings of chronic lesions were demonstrated from both modalities in 2 patients. Bone SPECT and MRI findings were in concordance regarding the investigation of active sacroiliitis, with the exception of one patient with mild SPECT findings and negative MRI examination; the diagnosis of AS however, was established one year later, after a positive follow-up MRI. The evaluation of the planar imaging of the whole skeleton and SPECT imaging, revealed additional lesions.

Conclusion: Bone SPECT is a reliable imaging method in the diagnosis of active sacroiliitis. Its application on planar BS, an economic and widely available diagnostic technique, appears to be a valuable aid for the clinician.

Keywords: Bone scintigraphy, SPECT, sacroiliitis, spondyloarthritis, magnetic resonance imaging

Öz

Amaç: Seronegatif spondiloartrit (SpA) aksiyal iskelet, entezler ve nadiren perifer eklemlerin kronik enflamasyonu ile karakterizedir. Sakroiliak eklem tutulumu, sakroiliit, patognomonik bir radyografik bulgu olarak kabul edilir. Manyetik rezonans görüntüleme (MRG) erken tanı için tercih edilen yöntemdir. Kemik sintigrafisi (KS) kemik ve eklem hastalığının tanısında yüksek duyarlılığa sahiptir. KS'nin sakroiliit tanısındaki kısıtlı değeri planar görüntüleme kullanılmasına bağlı olabilir. Bu çalışmada SpA'da SPECT'in rolünün MRG ile karşılaştırılması amaçlandı.

Address for Correspondence: George Angelidis MD, 401 General Military Hospital, Clinic of Nuclear Medicine, Athens, Greece
Phone: +302107288380 E-mail: angelidis@protonmail.ch ORCID ID: orcid.org/0000-0003-1059-0502
Received: 22.05.2017 **Accepted:** 10.07.2017

©Copyright 2017 by Turkish Society of Nuclear Medicine
Molecular Imaging and Radionuclide Therapy published by Galenos Yayınevi.

Öz

Yöntem: Enflamatuvar sırt ağrısı olan 43 hastaya sakroiliak değerlendirme için MRG ve KS uygulandı, sakroiliit tanısı için aynı bölgenin SPECT değerlendirilmesi ile kombine edildi.

Bulgular: Kemik SPECT, MRG ile tam tutarlılıkla, 11 hastada herhangi bir sakroiliit bulgusu ortaya koymadı. İki hastada kronik lezyonlara ait bulgular her iki modalitede de görüldü. Kemik SPECT ve MRG bulguları aktif sakroiliit değerlendirmesi açısından hafif SPECT bulguları ve negatif MRG değerlendirmesi olan ancak bir yıl sonra pozitif takip MRG'si ile AS tanısı konulan bir hasta haricinde, tamamen uyumlu idi. Tüm iskelet sistemi planar görüntülemesi ve SPECT ile değerlendirme ek lezyonlar ortaya koydu.

Sonuç: Kemik SPECT aktif sakroiliit tanısı için güvenilir bir görüntüleme yöntemidir. Ekonomik ve yaygın olarak erişilebilen bir tanı yöntemi olan planar KS ile kullanımı klinisyene yardımcı olabilecek değerli bir yöntem olarak gözükmektedir.

Anahtar kelimeler: Kemik sintigrafisi, SPECT, sakroiliit, spondiloartrit, manyetik rezonans görüntüleme

Introduction

Ankylosing spondylitis (AS) is the most common form of seronegative spondyloarthritis (SpA). It is characterized by chronic inflammation affecting the axial skeleton, entheses and occasionally peripheral joints. The involvement of the sacroiliac joints, sacroiliitis, is considered as a pathognomonic radiographic finding, and is required for the diagnosis of AS based on the 1984 modified New York criteria (1). A broader term, axial spondyloarthritis (ax-SpA), has been introduced in order to describe all SpA types affecting the axial joints, including those without radiographic findings (2).

Magnetic resonance imaging (MRI) is the method of choice for the early detection of sacroiliitis (3). MRI can detect acute (and chronic) inflammation, even before the radiographic depiction of structural changes (erosions, sclerosis, ankylosis). In general, the interpretation of radiographic images regarding sacroiliitis is quite difficult, and the corresponding findings are present only after significant disease progression (4).

The role of single photon emission tomography (SPECT) imaging, as a sensitive and specific test for the detection of sacroiliitis and spinal inflammation, has been investigated previously (5). However, studies comparing SPECT and MRI are limited. In the present study, we aimed to investigate the role of SPECT in ax-SpA. Sacroiliac joints are formed by the articular surfaces of the sacrum and ilium; the upper third is a syndesmosis, whereas the other two thirds are lined by articular cartilage and only the lower third is lined by synovium. We proposed a scintigraphic classification based on the presence (or not) of intense focal radiopharmaceutical uptake at the synovial part, as a sign of active sacroiliitis. Then, we evaluated SPECT results in comparison to MRI findings.

Materials and Methods

The present study was conducted by the Department of Nuclear Medicine of the 401 General Military Hospital in Athens, Greece. Forty-three patients (38 males, 5 females, mean age 28.2 years) suffering from inflammatory back pain (IBP) with disease duration >6 months underwent MRI evaluation of the sacroiliac joints, and bone scintigraphy (whole body scan, combined with SPECT in the same region) for the assessment of sacroiliitis. Ten patients had IBP without established diagnosis of SpA, whereas 33 patients were diagnosed with SpA (22 patients with AS, 8 patients with undifferentiated SpA, 3 patients with psoriatic arthritis). Before testing, all subjects gave informed consent for their complete participation, in compliance with the Hospital Ethics Committee guidelines and the ethical guidelines of the 1964 Declaration of Helsinki. The study was approved by the Local Ethics Committee of the 401 General Military Hospital of Athens, Greece (Protocol number: 2009/5).

Radiographic stage was recorded in all patients according to the 1984 modified New York criteria (1). Absence of radiographic findings was apparent in 11 patients. Suspicious changes (stage 1) were observed in 11 patients, whereas 10 patients had minimal abnormalities (such as erosions or sclerosis) without alteration of joint width (stage 2). Eight patients were classified as stage 3 (unequivocal abnormalities with 1 or more of the following findings: erosions, sclerosis, widening, narrowing, or partial ankylosis), and total ankylosis was demonstrated in two patients (stage 4). In MRI studies, the presence of clear bone marrow edema on STIR images or osteitis on T1 post-gadolinium images was indicative of active sacroiliitis (new Assessment of Spondyloarthritis-ASAS-classification criteria) (2,6,7). Structural abnormalities (i.e. fat deposition, erosions, sclerosis, ankylosis) were associated with chronic disease in the absence of the aforementioned ASAS criteria.

Bone SPECT imaging was performed with the patient in prone position using a single head camera (Sophy ds7, France). Acquisition included 64 projections (45 sec/frame, 64x64 matrix) in an 180^0 contour. Raw data was processed on a Mirage-Segami workstation based on iterative reconstruction methodology (RESPECT).

All participants underwent laboratory investigations that included measurements of erythrocyte sedimentation rate (ESR) and C-reactive protein (CRP), and the presence of human leukocyte antigen (HLA). The 2-tailed Mann-Whitney U nonparametric test was used to evaluate differences. Kruskal-Wallis test was used to assess differences in HLA. P values 0.05 were considered statistically significant.

Both imaging techniques, whole body scan and MRI, were performed within a seven day period, and datasets were evaluated by two blinded reviewers; a radiologist and a nuclear medicine physician with expertise in the imaging of the musculoskeletal system.

Results

Bone SPECT Findings

Bone SPECT images were classified as positive for active sacroiliitis (Figure 1) in patients with intense focal radiopharmaceutical uptake at the base of the sacroiliac joints (synovial part). Findings of active sacroiliitis were recorded in 30 patients; 23 patients with definite findings of active sacroiliitis (Table 1) and seven patients with mildly increased radiotracer uptake at the sacroiliac joints indicating low-grade sacroiliitis (Table 2). On the other hand, no uptake at the synovial part was indicative of a negative study (Figure 2). Bone SPECT revealed no findings of sacroiliitis in eleven patients. Finally, a diffused uptake at the sacroiliac joints was considered as a sign of chronic inflammation (Figure 3). Chronic sacroiliitis was found in two patients.

Comparison with MRI and Radiographic Staging

In patients with no scintigraphic findings of sacroiliitis (stage 0: 9 patients, stage 1: 1 patient, stage 2: 1 patient), MRI was also negative. Moreover, concordant magnetic resonance imaging results were obtained in patients with

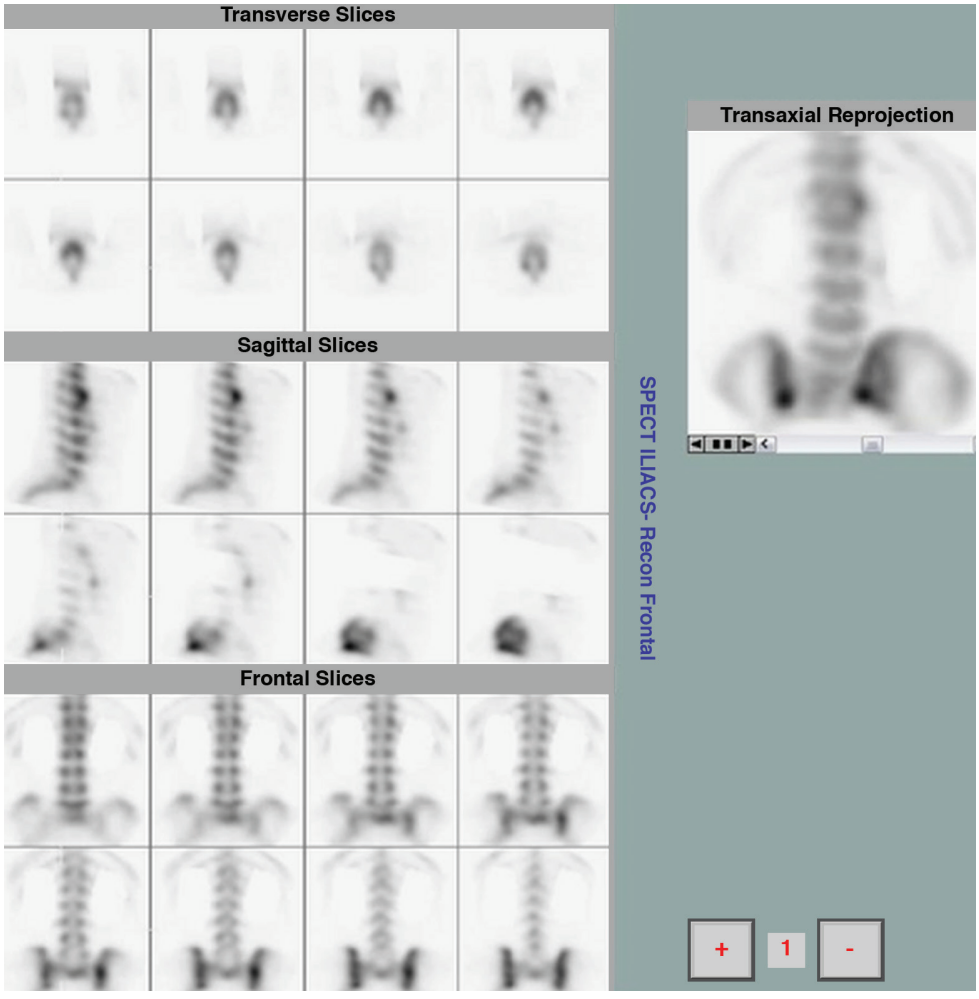

Figure 1. Intense focal uptake of the radiotracer at the base of the sacroiliac joints (synovial part), indicating the presence of active sacroiliitis (positive study). Also, enthesopathy of the T12-L1 vertebrae is noted (syndesmophytosis)

scintigraphic findings of chronic sacroiliitis (stage 2: 1 patient, stage 4: 1 patient).

Among patients with definite scintigraphic findings of active sacroiliitis (stage 0: 1 patient, stage 1: 5 patients, stage 2: 8 patients, stage 3: 7 patients, stage 4: 2 patients), chronic inflammation co-existed with SPECT findings of active disease in 11 patients. MRI chronic structural changes were evident in three more patients. Two patients showed definite evidence of the disease in one sacroiliac joint, according to both imaging modalities.

Among patients with mildly increased radiotracer uptake at the sacroiliac joints (stage 0: 1 patient, stage 1: 5 patients, stage 2: 1 patient), six patients had mild findings of bone marrow edema in MRI without corresponding osteitis. However, no structural MRI abnormalities were found in one patient (stage 1) suffering from persistent symptoms. Interestingly, the presence of sacroiliitis was evident in the MRI study performed after one year, and the diagnosis of AS was eventually established.

Whole Body Imaging

After evaluating planar images of the whole skeleton and SPECT findings of the lumbar spine-pelvis region, additional lesions were recorded (Table 3).

Laboratory Variables

The mean values [± standard deviation (SD)] of ESR were 28.8±26.9 mm/hr in patients with active sacroiliitis (according to SPECT and MRI findings), 20.3±16.4 mm/hr in patients with findings of low-grade sacroiliitis, and 19.8±17.6 mm/hr in the remaining patients (P=NS). The mean values (± SD) of CRP were 20.2±16.7 mg/L, 15±14.1 mg/L and 36±37 mg/L, respectively (P=NS).

No correlations were found between HLA results and imaging findings according to bone SPECT and MRI.

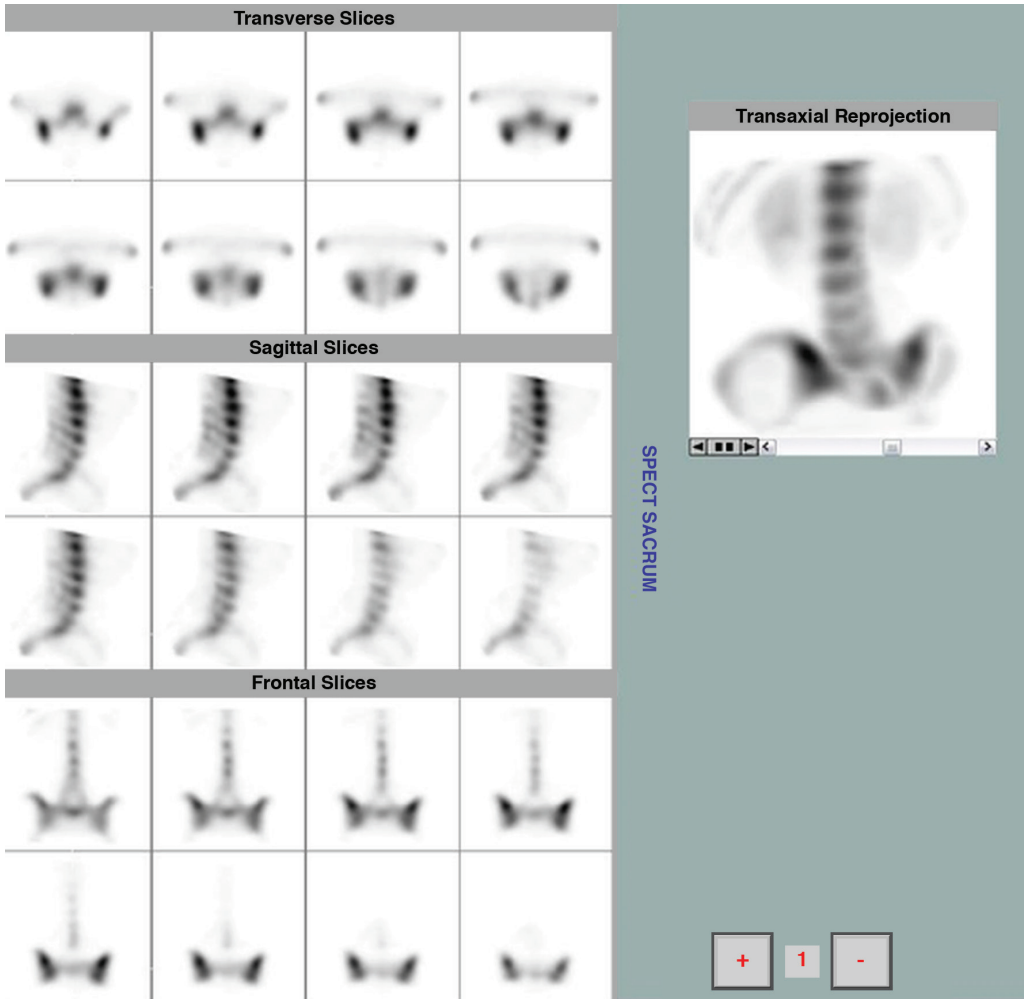

Figure 2. Absence of focal radiopharmaceutical uptake at the lower part of the sacroiliac joints (synovial part), excluding the presence of active sacroiliitis in a patient with negative magnetic resonance imaging findings

Discussion

To the best of our knowledge, this is one of limited studies investigating the role of SPECT imaging in SpA. Our study population consisted of 43 subjects with a relatively low mean age (28.2 years). Also, we enrolled more males than females (38 vs. 5). These particularities of our study population are associated with the special role of our institution providing care mainly to men and women serving at the Hellenic Armed Forces. We showed that SPECT findings are reliable; eleven negative SPECT and MRI studies, positive SPECT findings with concordant MRI results in 31 patients, while in one patient with SPECT evidence of sacroiliitis and negative MRI, the diagnosis of AS was established in a later follow-up MRI study.

Traditionally, the diagnostic investigation and classification of SpA were based on plain radiograms of the sacroiliac joints. MRI was added to the diagnostic algorithm with the introduction of ASAS criteria (2,6,7,8). MRI findings of active sacroiliitis include bone marrow edema, capsulitis, synovitis and inflammation in tendons and ligaments. Particularly, bone marrow edema may be present in a number of pathological states; therefore, it is not a specific finding. On the other hand, synovitis and capsulitis are more specific. Furthermore, sclerosis, erosions, bony bridges and bone marrow transformation are considered as signs of chronic lesions. The inter-observer agreement in the assessment of inflammation in patients with IBP has been investigated in previous MRI studies showing adequate levels of agreement, but not exceeding 85% (9,10,11).

Nuclear medicine techniques, particularly bone scintigraphy, are characterized by high sensitivity in the diagnosis of bone and articular diseases, as well as enthesopathies (12). Initial trials investigating the role of bone scintigraphy in sacroiliitis assessment included planar imaging and a semi-quantitative approach. Regions of interest were drawn over

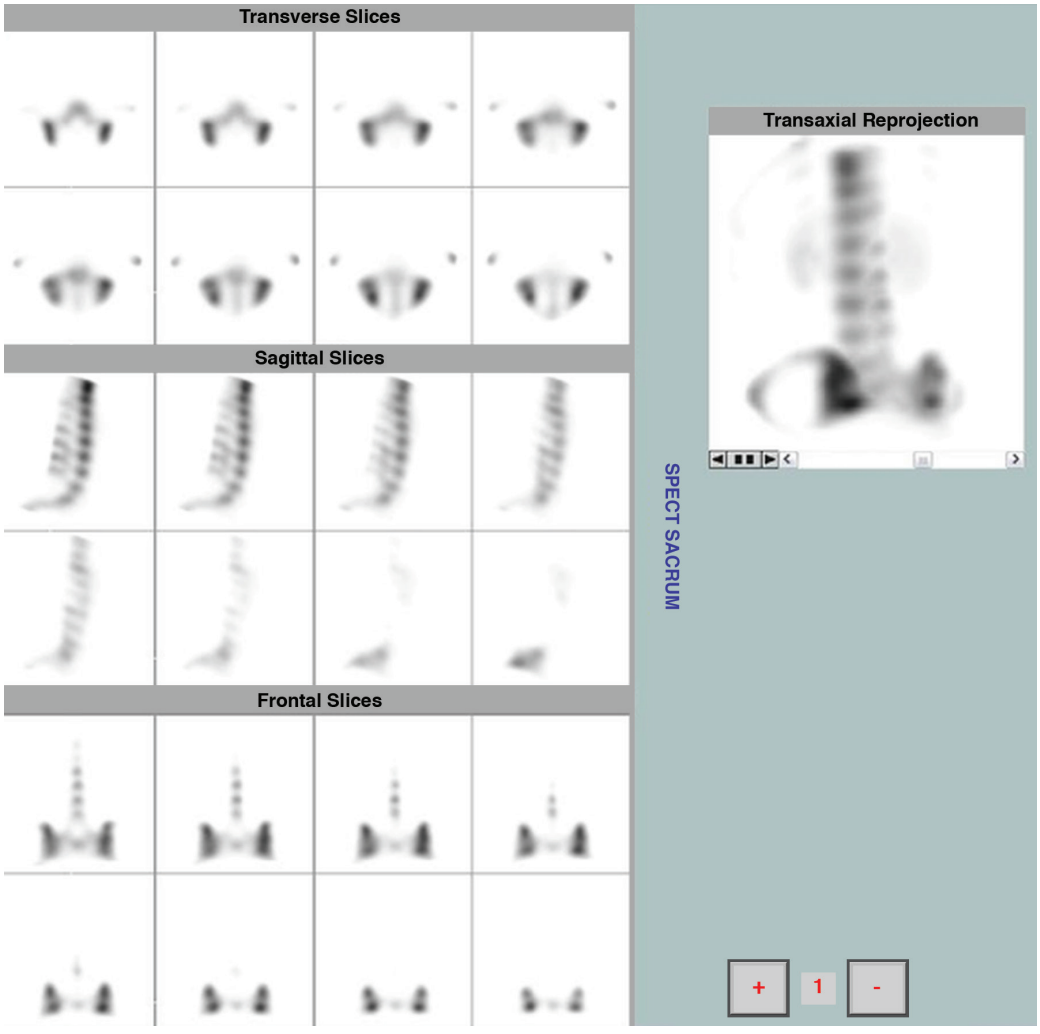

Figure 3. Diffuse increase in radiopharmaceutical uptake at the sacroiliac joints as a sign of chronic inflammation, co-existing with active disease

the sacroiliac joints and reference structures, such as the sacrum and lumbar vertebrae (13). Although the results were promising, the diagnostic performance was inferior to MRI (14). On the other hand, preliminary bone SPECT studies confirmed the ability of the method for detecting sacroiliitis, indicating its potential role in the diagnostic investigation of these patients (15). The sensitivity and specificity of bone SPECT were demonstrated in a study that enrolled age-matched controls; the authors reported sensitivity of 85% and specificity of 90% in the detection

Table 1. Patients with definite findings of active sacroiliitis

Sex	ESR	CRP	HLA-B27	Stage	SPECT	MRI
F	133	77	+	0	Bilateral	Bilateral
F	47	6	+	1	Bilateral	Bilateral&chronic
M	15	<3.2	-	1	Unilateral*	Unilateral*
M	8	<3.2	+	1	Unilateral**	Unilateral**
M	22	14	-	1	Bilateral	Bilateral
F	34	24	+	1	Bilateral	Bilateral
M	5	<3.2	+	2	Bilateral&chronic	Bilateral&chronic
M	16	9	-	2	Bilateral	Bilateral
M	27	20	+	2	Bilateral&chronic	Bilateral&chronic
M	12	5	+	2	Bilateral&chronic	Bilateral&chronic
M	19	24	+	2	Bilateral&chronic	Bilateral&chronic
M	16	9	+	2	Bilateral&chronic	Bilateral&chronic
M	16	<3.2	+	2	Bilateral	Bilateral&chronic
M	8	<3.2	+	2	Bilateral	Bilateral&chronic
M	35	20	+	3	Bilateral&chronic	Bilateral&chronic
M	38	15	n/a	3	Bilateral	Bilateral
M	25	16	+	3	Bilateral	Bilateral
M	8	9	+	3	Bilateral&chronic	Bilateral&chronic
M	45	29	+	3	Bilateral&chronic	Bilateral&chronic
M	3	10.5	+	3	Bilateral&chronic	Bilateral&chronic
F	42	19	+	3	Bilateral&chronic	Bilateral&chronic
M	46	14	+	4	Bilateral&chronic	Bilateral&chronic
M	43	34	+	4	Bilateral	Bilateral

F: Female, M: Male, CRP: C-reactive protein, ESR: Erythrocyte sedimentation rate, HLA-B27: Human leukocyte antigen-B27, MRI: Magnetic resonance imaging, *Active sacroiliitis at the right sacroiliac joint, **Active sacroiliitis at the left sacroiliac joint

Table 2. Patients with mildly increased radiotracer uptake at the sacroiliac joints, indicating low-grade sacroiliitis

Sex	ESR	CRP	HLA-B27	Stage	SPECT	MRI
M	9	<3.2	+	0	Bilateral	Bilateral
M	3	<3.2	+	1	Bilateral	Bilateral
M	40	48.5	-	1	Unilateral*	Negative
M	13	5	-	1	Unilateral*	Unilateral*
M	33	<3.2	+	1	Bilateral	Bilateral
M	5	<3.2	-	1	Unilateral**	Unilateral**
M	39	25	-	2	Unilateral**	Unilateral**

M: Male, CRP: C-reactive protein, ESR: Erythrocyte sedimentation rate, HLA-B27: Human leukocyte antigen-B27, MRI: Magnetic resonance imaging, *Active sacroiliitis at the left sacroiliac joint, **Active sacroiliitis at the right sacroiliac joint

of sacroiliitis (5). Ryan et al. (16) noted that SPECT abnormalities in the lower thoracic and lumbar spine are often observed in patients with AS, particularly in chronic cases. However, Çevik et al. (17) concluded that MRI provides the strongest evidence of the disease in cases showing clinical features of inflammatory lesions in the spine. More recently, Zilber et al. (18) suggested that bone SPECT combined with calculation of indices or low-dose computed tomography (CT) can be used in the diagnostic investigation of axial SpA, with favourable sensitivity and specificity. Interestingly, Cui et al. (19) reported that the diagnostic value of SPECT and MRI is comparable to that of plain radiograms and CT, and can be performed for the (quantification of the inflammatory process. Moreover, sacroiliac index measurements confirming positive findings may increase the specificity of bone scintigraphy (20). In our study population, bone SPECT and MRI findings were in concordance regarding the investigation of active sacroiliitis, with the exception of one patient with mild SPECT findings and negative MRI examination. However, the diagnosis of AS was established for this patient one year later, after a positive follow-up MRI. Further, MRI demonstrated chronic inflammation in more patients compared to bone SPECT, as expected based on the superior diagnostic performance of MRI in depicting chronic structural lesions.

In general, the previously observed limited value of bone scintigraphy in the diagnosis of sacroiliitis may be attributed to the use of planar imaging. Based on a systematic literature research that resulted in the analysis of 25 published studies, bone scintigraphy demonstrated overall sensitivity of approximately 50% in detecting sacroiliitis, either in patients with established AS or in patients with probable sacroiliitis (21). The interpretation of planar imaging findings in areas with complex anatomical features, such as the sacroiliac joints, could be quite challenging due to the overlying and underlying structures that may lead to false positive or false negative results. The limited diagnostic value of planar imaging (combined with semi-quantitative measurements) was also confirmed in a previous study performed in our institution. MRI detected features of active sacroiliitis in 34/36 patients, bone SPECT was in total agreement with MRI findings, whereas planar sacroiliac scintigraphy was positive in only 19/36 patients (22).

Significant advances in the field of SPECT imaging have been achieved during the previous decade. Particularly, the introduction of iterative reconstruction algorithms offered images of superior quality compared to those produced from other processing methods. Moreover, reconstructed 3D images permitted a more accurate evaluation of the synovial part of sacroiliac joints. Previously, due to the small dimensions of the synovial part with respect to the spatial resolution of SPECT technique, uptake in the sacrum or other parts of the sacroiliac joints could be falsely diagnosed as sacroiliitis. Given the current availability of 3D images, the clear discrimination of the lower synovial part facilitates the evaluation of the sacroiliac region, increasing intra-observer agreement regarding the diagnosis of the disease. However, at the time that the aforementioned studies investigated the role of SPECT imaging in the detection of sacroiliitis, these advances were not available.

Further, it is unclear if the diagnosis of sacroiliitis, in previous SPECT studies, was only linked to increased uptake at the synovial part (chronic changes associated with SpA can result in faint uptake at the whole joint mimicking active sacroiliitis). We suggest that active sacroiliitis should be reported only in cases with focal uptake at the synovial part; other types of uptake seem to be associated with chronic changes or enthesopathy. According to the results of the present study, focal uptake at the synovial part was demonstrated in 23/42 patients; therefore, SPECT findings were in accordance with the diagnosis of acute sacroiliitis based on MRI criteria. Moreover, the level of uptake in SPECT imaging was positively related to MRI features. Patients with higher uptake in bone scintigraphy showed more intense MRI findings. Among the 23 patients with active sacroiliitis based on MRI results, fourteen had also findings of chronic structural changes. 11/14 patients showed faint linear uptake at the sacroiliac joints which was associated with the co-existing chronic changes. However, 3D images permitted the depiction of focal uptake at the synovial part, enhancing the diagnostic performance of the technique. In 12 patients with no signs of the disease according to

Table 3. Additional lesions revealed based on the evaluation of the whole skeleton

Skeletal lesions	Anatomical localization	Number of patients
Arthritis	Lumbar spine	2
	Radiocarpal joints	4
	Metacarpophalangeal joints	1
	Knee joints	5
	Talocrural joints	3
Enthesopathy	Pelvis	9
	Lumbar spine	5
	Medial collateral ligament	1
	Lateral collateral ligament/tibial tubercle	1
	Achilles tendon	2
	Plantar fascia	2

MRI technique, normal uptake of radiopharmaceutical was observed in the lower part of the sacroiliac joints in eleven patients. In two of these patients, low back pain was linked to the presence of facet arthritis located at the lumbar spine. Diffuse pattern of uptake (without focal uptake in the lower part of the sacroiliac joints) was demonstrated in two patients with MRI findings indicating chronic changes. Additional lesions, including spinal lesions, peripheral arthritis and enthesitis, were revealed after the evaluation of the whole skeleton, while we suggest that if a SPECT study of thoracic spine, or a three phase scan were added, further findings could be demonstrated.

SPECT imaging was performed with a 180-degree rotation of the gantry, a procedure that increased the counts collected from the spine in a reasonable time frame with no further radiation for the patients compared to the whole body scintigraphy. Notably, the radiation burden of the whole procedure is not too high, with a total effective dose of approximately 5 mSv (for example, a plain x-ray of the lumbar spine is associated with an effective dose of 1.5 mSv). Obviously, it is linked to the limitations related to radiation exposure (e.g. pregnant women, patients who underwent multiple radiological examinations in a short time period). Therefore, the diagnostic evaluation, as described above, can be performed as a one-stop examination, providing valuable evidence concerning both the axial and the appendicular skeleton. Further studies could also investigate the use of bone SPECT as an imaging tool for the assessment of treatment outcomes in patients with SpA. In the same field, Zilber et al. (18) have proposed a potential role of ^{18}F positron emission tomography and immunoscintigraphy with labelled monoclonal anti-cytokine antibodies in the evaluation of patients with suspected sacroiliitis.

Conclusions

In conclusion, our study, based on imaging findings in patients with SpA, demonstrated the potential role of bone SPECT in the diagnostic investigation of SpA. According to our results, bone SPECT is a reliable imaging method in the diagnosis of active sacroiliitis and enthesitis. In comparison to MRI, whole body scan combined with SPECT imaging is a less expensive diagnostic approach per patient, while it is more widely available. Nevertheless, the implementation of this procedure in the clinical setting will require proper adjustment of the diagnostic investigation in patients with suspected sacroiliitis. Moreover, larger multi-centre studies are needed to confirm these encouraging findings regarding the role of bone SPECT in the detection of sacroiliitis in patients with SpA.

Acknowledgements

The authors would like to acknowledge P. Patouras, MD, who was the interpreting physician of MRI studies, and K. Athanasiou, nuclear medicine technologist, for his contribution regarding the proper performance of scintigraphic studies.

Ethics

Ethics Committee Approval: The study was approved by the Local Ethics Committee of the 401 General Military Hospital of Athens, Greece (Protocol number: 2009/5).

Informed Consent: Consent form was filled out by all participants.

Peer-review: Internally peer-reviewed.

Authorship Contributions

Surgical and Medical Practices: T.P., D.K., G.A., J.K., Concept: T.P., D.K., J.K., Design: T.P., D.K., J.K., Data Collection or Processing: T.P., D.K., G.A., J.K., Analysis or Interpretation: T.P., D.K., G.A., J.K., Literature Search: T.P., D.K., G.A., J.K., Writing: T.P., D.K., G.A., J.K.

Conflict of Interest: No potential conflicts of interest were disclosed.

Financial Disclosure: The authors declared that this study received no financial support.

References

1. van der Linden S, Valkenburg HA, Cats A. Evaluation of diagnostic criteria for ankylosing spondylitis. A proposal for modification of the New York criteria. Arthritis Rheum 1984;27:361-368.
2. Rudwaleit M, van der Heijde D, Landewé R, Listing J, Akkoc N, Brandt J, Braun J, Chou CT, Collantes-Estevez E, Dougados M, Huang F, Gu J, Khan MA, Kirazli Y, Maksymowych WP, Mielants H, Sørensen IJ, Ozgocmen S, Roussou E, Valle-Oñate R, Weber U, Wei J, Sieper J. The development of assessment of Spondyloarthritis International Society classification criteria for axial spondylarthritis (part II) validation and final selection. Ann Rheum Dis 2009;68:777-783.
3. Rudwaleit M, van der Heijde, Khan MA, Braun J, Sieper J. How to diagnose axial spondyloarthritis early. Ann Rheum Dis 2004;63:535-543.
4. van Tubergen A, Heuft-Dorenbosch L, Schulpen G, Landewé R, Wijers R, van der Heijde D, van Engelshoven J, van der Linden S. Radiographic assessment of sacroiliitis by radiologists and rheumatologists: does training improve quality? Ann Rheum Dis 2003;62:519-525.
5. Hanly JG, Barnes DC, Mitchell MJ, MacMillan L, Docherty P. Single photon emission computed tomography in the diagnosis of inflammatory spondyloarthropathies. J Rheumatol 1993;20:2062-2068.
6. Reveille JD. Epidemiology of spondyloarthritis in North America. Am J Med Sci 2011;341:284-286.
7. Sieper J, Rudwaleit M, Baraliakos X, Brandt J, Braun J, Burgos-Vargas R, Dougados M, Hermann KG, Landewé R, Maksymowych W, van der Heijde D. The Assessment of SpondyloArtritis international Society (ASAS) handbook: a guide to assess spondyloarthritis. Ann Rheum Dis 2009;689(Suppl 2):1-44.
8. Tuite MJ. Sacroiliac joint imaging. Semin Musculoskelet Radiol 2008;12:72-82.
9. Heuft-Dorenbosch L, Weijers R, Landewé R, van der Linden S, van der Heijde D. Magnetic resonance imaging changes of sacroiliac joints in patients with recent onset inflammatory back pain: inter reader reliability and prevalence of abnormalities. Arthritis Res Ther 2006;8:11.
10. Bigot J, Loeuille D, Chary-Valckenaere I, Pourel J, Cao MM, Blum A. Determination of the best diagnostic criteria of sacroiliitis with MRI. J Radiol 1999;80:1649-1657.

11. Puhakka KB, Jurik AG, Egund N, Schiottz-Christensen B, Stengaard-Pedersen K, van Overeem Hansen G, Christiansen JV. Imaging of sacroiliitis in early seronegative spondylarthropathy. Assessment of abnormalities by MR in comparison with radiography and CT. Acta Radiol 2003;44:218-229.
12. Frater C, Vu D, Van der Wall H, Perera C, Halasz P, Emmett L, Fogelman I. Bone scintigraphy predicts outcome of steroid injection for plantar fasciitis. J Nucl Med 2006;47:1577-1580.
13. Zafeirakis A, Kasimos D, Sioka C, Aravanis I, Zoumboulidis A. Evaluation of a quantitative diagnostic sacroiliac bone scan index in cases of chronic low back pain in young male adults. Hell J Nucl Med 2005;8:19-26.
14. Battafarano DF, West SG, Rak KM, Fortenbery EJ, Chantelois AE. Comparison of bone scan, computed tomography, and magnetic resonance imaging in the diagnosis of active sacroiliitis. Semin Arthritis Rheum 1993;23:161-176.
15. Hanly JG, Mitchell MJ, Barnes DC, MacMillan L. Early recognition of sacroiliitis by magnetic resonance imaging and single photon emission computed tomography. J Rheumatol 1994;21:2088-2095.
16. Ryan PJ, Gibson T, Fogelman I. Spinal bone SPECT in chronic symptomatic ankylosing spondylitis. Clin Nucl Med 1997;22:821-824.
17. Çevik R, Nas K, Gür A, Özateş M, Ataoğlu S, Erdoğan F, Saraç AJ, Satıcı Ö. Comparison of imaging techniques in the early diagnosis of sacroiliitis. Romatizma 2000;15:99-104.
18. Zilber K, Gorenberg M, Rimar D, Boulman N, Kaly L, Rozenbaum M, Rosner I, Slobodin G. Radionuclide methods in the diagnosis of sacroiliitis in patients with spondyloarthritis: An update. Rambam Maimonides Med J 2016:7.
19. Cui Y, Zhang X, Zhao Z, Liu Y, Zheng J. The relationship between histopathological and imaging features of sacroiliitis. Int J Clin Exp Med 2015;8:5904-5910.
20. Koç ZP, Kin Cengiz A, Aydın F, Samancı N, Yazısız V, Koca SS, Karayalçın B. Sacroiliac indicis increase the specificity of bone scintigraphy in the diagnosis of sacroiliitis. Mol Imaging Radionucl Ther 2015;24:8-14.
21. Song IH, Carrasco-Fernández J, Rudwaleit M, Sieper J. The diagnostic value of scintigraphy in assessing sacroiliitis in ankylosing spondylitis: a systematic literature research. Ann Rheum Dis 2008;67:1535-1540.
22. Pipikos T, Zafeirakis A, Episkopopoulou S, Koniaris G, Kassimos D, Koutsikos J. Should planar sacroiliac scintigraphy be abandoned in the investigation of active sacroilitis in ankylosing spondylitis patients? Eur J Nucl Med Mol Imaging 2014;41:278.

Original Article
Mol Imaging Radionucl Ther 2017;26:110-115 DOI:10.4274/mirt.83007

A Comparison of Iterative Reconstruction and Prone Imaging in Reducing the Inferior Wall Attenuation in Tc-99m Sestamibi Myocardial Perfusion SPECT

Tc-99m Sestamibi Miyokard Perfüzyon SPECT Görüntülemede İnferior Duvar Attenüasyonunu Azaltmada İteratif Rekonstrüksiyon ile Pron Pozisyonun Karşılaştırması

Duygu Kuşlu[1], Emel Öztürk[2]
[1]*Antalya Training and Research Hospital, Clinic of Nuclear Medicine, Antalya, Turkey*
[2]*Memorial Hospital, Clinic of Nuclear Medicine, Ankara, Turkey*

Abstract

Objective: Prone positioning, iterative reconstruction (IR-OSEM) and electrocardiography (ECG) gating have been demonstrated to improve the specificity of myocardial perfusion SPECT (MPS) in the diagnosis of coronary artery disease.

Methods: The gated supine and prone MPS images of 45 patients were reconstructed with both IR-OSEM [supine (SIR) and prone (PIR)] FBPs [supine (SFBP), prone (PFBP)] for comparison. Perfusion, wall motion (WM) and wall thickening were also interpreted semi-quantitatively. Two groups were generated as those with normal or abnormal findings. Segmental myocardial tracer uptake values were noted from four of the reconstructed images from 17 segment model of bullseye.

Results: The difference between mean values and the standard deviations of the % tracer uptakes of inferior wall segments were statistically significant in all images. The normalcy rates were highest in PIR images, followed by PFBP and SIR images. The number of patients with any perfusion abnormality were 42, 12, 32, and 6, in SFBP, PFBP, SIR and PIR images, respectively. The six patients with perfusion abnormality in PIR images were re-evaluated with rest images and were diagnosed with a fixed perfusion defect. There was positive correlation between WM and either PFBP or PIR images. Sixteen patients' WM were evaluated as abnormal while only 6 patients' perfusions were abnormal in PIR.

Conclusion: Prone imaging in addition to a supine perfusion SPECT improves imaging quality of the inferior wall, especially when reconstructed with iterative methods. If prone imaging can not be performed, ECG-gating can also be used as a beneficial method.

Keywords: Myocardial perfusion SPECT, attenuation correction, prone positioning, iterative reconstruction

Öz

Amaç: Koroner arter hastalığı tanısında miyokard perfüzyon SPECT (MPS) görüntüleme spesifitesini artırmak için pron pozisyonlama, iteratif rekonstrüksiyon (IR-OSEM) ve elektrokardiyogram (EKG) tetikleme gibi yöntemler geliştirilmiştir.

Yöntem: Bu yöntemleri birbirleriyle karşılaştırmak amacıyla, kombine gated supin ve pron Tc-99m MIBI MPS görüntülemesi yapılan 45 hastanın görüntüleri retrospektif olarak yeniden değerlendirildi. Her iki görüntüleme de IR-OSEM ile rekonstrükte edilerek [supin (SIR), prone (PIR)], rutin filtered-back projeksiyon (FBP) ile rekonstrükte edilmiş görüntülerle [supin (SFBP), prone (PFBP)] karşılaştırıldı. Perfüzyon, duvar hareketi (WM) ve kalınlaşması görsel olarak

Address for Correspondence: Duygu Kuşlu MD, Antalya Training and Research Hospital, Clinic of Nuclear Medicine, Antalya, Turkey
Phone: +90 505 869 54 41 E-mail: duygutokbay@gmail.com ORCID ID: orcid.org/0000-0002-0542-254X
Received: 12.07.2016 **Accepted:** 24.07.2017

©Copyright 2017 by Turkish Society of Nuclear Medicine
Molecular Imaging and Radionuclide Therapy published by Galenos Yayınevi.

Öz

değerlendirilerek normal veya anormal olarak gruplandırıldı. Miyokardiyal segmental aktivite tutulum oranları 17 segment modeline göre değerlendirildi.

Bulgular: İnferior duvar % aktivite tutulum oranlarında dört yöntemde anlamlı farklılık bulundu. Normallik oranı en yüksek PIR görüntülerde ve takiben sırasıyla PFBP ile SIR görüntülerdeydi. Perfüzyonu anormal hasta sayısı SFBP, PFBP, SIR ve PIR görüntülerde sırasıyla 42, 12, 32 ve 6 olarak değerlendirildi. Bu altı hasta istirahat görüntüleriyle birlikte tekrar değerlendirildiğinde sabit perfüzyon defekti tespit edildi. WM ile PFBP perfüzyon ve PIR perfüzyonu arasında korelasyon tespit edildi. WM anormal olan hasta sayısı 16 iken, PIR görüntülerde perfüzyonu anormal olan hasta sayısı 6 idi.

Sonuç: Egzersiz sonrası MPS'ye eklenen pron görüntüleme, özellikle IR-OSEM ile rekonstrükte edildiğinde, inferior duvarda atenüasyonu belirgin azaltmaktadır. Pron görüntüleme uygulanamadığında EKG-tetikleme de yardımcı bir yöntemdir.

Anahtar kelimeler: Miyokard perfüzyon SPECT, atenüasyon düzeltme, pron pozisyon, iteratif rekonstrüksiyon

Introduction

Although myocardial perfusion SPECT (MPS) imaging is accepted as the method of choice to evaluate coronary artery disease (CAD), tissue attenuation and reconstruction artifacts reduce the test's specificity. Tissue attenuation artifacts are mostly located in the inferior wall in men and the anterior wall in women. Intense sub-diaphragmatic activity in the neighborhood of the heart also may produce artifacts (1,2). It can either mask a true perfusion defect (1,3), or cause false perfusion defects (3,4) due to filtered back projection (FBP) reconstruction that suppresses inferior wall counts adjacent to intense sub-diaphragmatic activity (5).

Various methods have been used to reduce artifacts in MPS, such as gated imaging and prone imaging. Prone imaging has been demonstrated to decrease inferior wall attenuation as well as improving the specificity rate (6,7). However, since prone imaging can cause false positive anteroseptal wall defects it needs to be combined with supine acquisitions (8,9,10). Our primary aim in this study was to compare the effectiveness of the methods performed to increase the specificity of the exam [gated-prone scans and iterative reconstruction (IR)] especially on artifact correction.

Materials and Methods

Study Population

The supine and prone MPS images of 45 patients [42 male, 3 female, mean age: 58.76±11.84 years, mean body mass index (BMI): 28.5±4.2 kg/m^2] were re-examined. Images with suboptimal image and gating quality were excluded.

Stress Testing and Radiopharmaceutical Administrations

Patients underwent a 2-day protocol using Tc-99m MIBI for each study. When achievable, a symptom limited treadmill exercise test with Bruce protocol was applied, acquisition was started approximately 30 minutes after radiopharmaceutical administration. Adenosine stress was performed in 3 patients and infused at 40 mcg/kg/min for 4 minutes. Acquisition was started approximately 40 minutes after radiopharmaceutical administration.

All patients drank 200 mL milk or ate 100 mg chocolate 10 minutes after radiopharmaceutical injection to accelerate hepatobiliary excretion. All patients also drank 200 mL soda prior to imaging in order to decrease infra-diaphragmatic activity.

Data Acquisition and Processing

Gated SPECT was performed with a dual-head camera (Millenium MG, GE Medical Systems, Milwaukee, WI, USA) equipped with high resolution collimators, with the following parameters for supine acquisition: 180 rotation arc, 64 projections, 25 s/projection, 8 frames/heart cycle, no arrhythmia rejection and 64x64 matrix. Prone imaging was performed immediately after supine image acquisition with 15 s/projection and with the same parameters without gating. Attenuation or scatter correction was not applied. Supine and prone images were reconstructed with both FBP (butterworth, frequency: 0.52, power: 5) [supine (SFBP), prone (PFBP)] and IR-OSEM [supine (SIR), prone (PIR)] by Cedars-Sinai QGS/QPS (Los Angeles, California) software in multiple color scales. MPS scans were viewed on a dedicated workstation (Xeleris; GE Healthcare) by using default reconstruction parameters in the standard format for display of tomographic cardiac studies.

Image Interpretation

Semi-quantitative visual interpretation was performed from short-axis and vertical long-axis slices using a 17-segment model (11). Only the segments representing the inferior wall (segment number 4, 10, 15) and the apex (segment number 17) were scored by an experienced observer using a 5-point scoring system (0-normal, 1-equivocal, 2-moderate, 3-severe reduction of isotope uptake, and 4-absence of detectable tracer uptake). Scores 0 and 1 were accepted as normal. Since we did not aim to make a clinical diagnosis, the normality scores were accepted with this narrow range to be able to recognize any possible changes.

Quantitative myocardial isotope uptake percentages of all myocardial segments were obtained from the 17 segment bullseye model.

Visual wall motion (WM) [6-point scoring system (0-normal, 1-mild hypokinesia, 2-moderate hypokinesia, 3-severe hypokinesia, 4-akinesia, 5-dyskinesia)], and wall thickening (WT) [4-point scoring system (0-normal, 1-mild, 2-moderate to severe, 3-absent)] scoring of the inferior wall and apical segments was made only in supine images that allowed electrocardiography (ECG) gating (11).

Statistical Analysis

All continuous variables were expressed as mean±SD. Repeated measures variant analysis was used to compare semi-quantitative interpretations ($p<0.05$), McNemar analysis was used to compare normalcy rates ($p<0.05$). Friedmann tests and correlation analysis was used to compare differences (SPSS Software, Version 20.0; SPSS Inc., Chicago, Illinois).

Results

Patient Demographic Characteristics

There was a heterogeneous patient population regarding the likelihood of CAD; however mostly low likelihood of disease.

The differences of % tracer uptakes of all myocardial segments: In the inferior wall segments the difference (between % tracer uptakes) were significant in terms of all variables ($p<0.01$). In the apical segment (Seg. No. 17), the difference between SFBP, SIR and PIR in terms of % tracer uptakes were also significant ($p=0.000$), but not significant in PFBP and SIR images ($p=0.314$) (Table 1). In the anterior and septal wall segments the difference between PFBP and SIR in terms of % tracer uptakes was not significant similar to the apex, except segment 14 that indicates the septum in the short axis image of the apical section. Hereby PFBP and PIR counts were similar ($p=0.405$). Within the lateral wall segments, there were no differences between SFBP and SIR, PFB and PIR in terms of % tracer uptakes, except segment 16 that indicates the lateral wall in the short axis image of the apical section and in segment 17 that indicates the apex in only SFBP and SIR ($p=0.404$).

Table 1. Mean ± standard deviations and comparisons of the % tracer activities of the inferior wall and apical segments

Mean ± SD	Seg. No. 4	Seg. No. 10	Seg. No. 15	Seg. No. 17
SFBP	34.0±5.68	57.71±5.55	67.31±7.08	71.57±9.47
SIR	38.17±6.9	61.71±6.22*	70.31±7.25	76.33±9.75**
PFBP	43.44±7.2	67.76±7.78*	74.33±7.81	74.07±10.42**
PIR	48.04±7.1	73.76±7.72	76.89±7.38	78.13±10.15

*p=0.001, **p=0.314, SD: Standard deviation

The results of the semi-quantitative perfusion interpretations of the inferior wall and apical segments: There were 42, 32, 12 and 6 patients who were evaluated as abnormal in SFBP, SIR, PFBP, and PIR images, respectively. Thus, the highest normalcy rate was in PIR images with 86.7%, followed by PFBP images with 73.3%, and SIR images with 28.9% (Figure 1, Table 2). The differences between the groups in terms of normalcy rates were significant ($p<0.05$). The rest images of the 6 patients who have been evaluated as abnormal in stress PIR images were re-evaluated and the summed difference scores were calculated to be '0', which indicates a fixed perfusion defect.

There were 29 (64.4%) and 11 patients (24.4%) that normal regional WM and WT, respectively, as the WM and WT interpretations were made semi-quantitatively only in inferior and apical segments (Figure 1). In daily practice, we evaluate myocardial functions often while interpreting a patient's images. To compare the differences and consider the similarities of the methods, we performed a correlation analysis between functional data, prone FBP and IR-OSEM. There was a significant but weak correlation between WM and PFBP ($p=0.008$, $r=0.392$), and a significant and moderate correlation between WM and PIR images ($p=0.000$, $r=0.528$) (Table 3). Although there were 16 patients with abnormal WM, perfusion was considered as abnormal in only 6 patients in PIR. There was also a significant but weak correlation between WT and SIR images ($p=0.031$, $r=0.322$) (Table 3). When we compared WM and WT scores with the related perfusion scores in the segment base; the most powerful correlations were detected between WT and PFBP Seg. No. 17 ($p=0.000$, $r=0.863$), SIR Seg. No. 15 ($p=0.000$, $r=0.744$), SFBP Seg. No. 15 ($p=0.000$, $r=0.706$), as well as between WM and

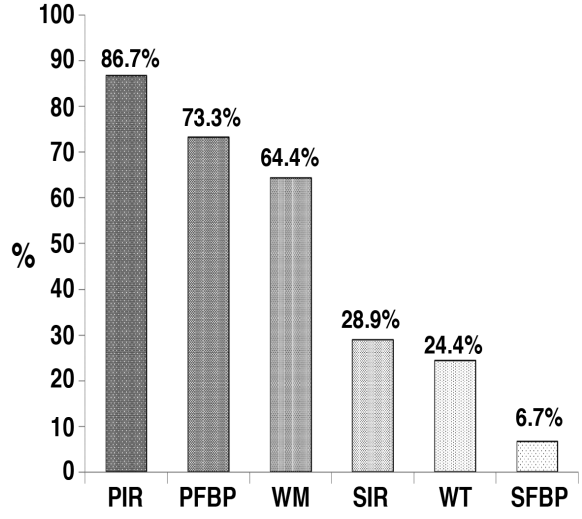

Figure 1. Normalcy rates of the groups

SFBP Seg. No. 17 (p=0.000, r=0.626), and PIR Seg. No.15 (p=0.000, r=0.588) (Table 4).

Discussion

Our study is thought to be unique in comparing different methods being used to detect attenuation artifacts of the inferior wall (supine vs. prone positioning, IR-OSEM vs FBP and ECG gating methods) in MPS. Images included in this study were the patients' with supine gated MPS which have inferior wall perfusion abnormality, requiring prone imaging. The primary aim of this study was to compare the supine images with prone images in two different projection methods (FBP and IR-OSEM) with a secondary aim to correlate this data with functional scores.

In this study, the percentage of inferior wall segments tracer activities were significantly high in PIR, followed by PFBP (p<0.01). Normalcy rates were also the highest in PIR (86.7%) followed by PFBP images (73.3%). Among regional WM and thickening assessments of the inferior wall and apex, the performance of the WM scores was better than the thickening scores (normalcy rates 64.4%

Table 2. Comparison of the normalcy rates between groups (McNemar, p<0.05)

		SIR		p
		N	A	
	N	2	1	
SFBP	A	11	31	**0.006**
	PIR			
	N	3	0	
SFBP	A	36	6	**0.000**
	SIR			
	N	12	21	
PFBP	A	1	11	**0.000**
	PIR			
	N	33	0	
PFBP	A	6	6	**0.031**
	PFBP			
	N	3	0	
SFBP	A	30	12	**0.000**
	PIR			
	N	13	0	
SIR	A	26	6	**0.000**

N: Normal, A: Abnormal, p: p value

Table 4. Correlation analysis of wall motion and wall thickening scores according to segments (p<0.05 Spearman)

p<0.05, Spearman		WM		WT	
		r	p	r	p
SFBP	Seg. No. 4	0.072	0.271	0.000	0.558
	Seg. No. 10	0.000	0.496	0.000	0.654
	Seg. No. 15	0.000	0.504	**0.000**	**0.706**
	Seg. No. 17	**0.000**	**0.626**	0.066	0.276
PFBP	Seg. No. 4	0.005	0.424	0.008	0.391
	Seg. No. 10	0.062	0.281	0.112	0.240
	Seg. No. 15	0.000	0.500	0.002	0.440
	Seg. No. 17	0.005	0.415	**0.000**	**0.863**
SIR	Seg. No. 4	0.013	0.368	0.000	0.553
	Seg. No. 10	0.009	0.385	0.001	0.497
	Seg. No. 15	0.000	0.588	**0.000**	**0.744**
	Seg. No. 17	0.000	0.526	0.013	0.367
PIR	Seg. No. 4	0.021	0.344	0.018	0.350
	Seg. No. 10	0.010	0.378	0.041	0.306
	Seg. No. 15	**0.000**	**0.716**	0.000	0.584
	Seg. No. 17	0.001	0.478	0.000	0.646

WM: Wall motion, WT: Wall thickening, Seg: Segment

Table 3. Distribution of the number of patients according to wall motion and wall thickening scores considered as normal/abnormal and their statistical comparisons (χ^2, p<0.05)

		WM				WT			
		N	A	p (χ^2)	Corr. (Pearson)	N	A	p (χ^2)	Corr. (Pearson)
SFBP Perfusion	N	3	0	0.183	p=0.191 r=0.199	1	2	0.711	p=0.718 r=0.055
	A	26	16			10	32		
PFBP Perfusion	N	25	8	**0.009**	**p=0.008 r=0.392**	10	13	0.129	p=0.135 r=0.226
	A	4	8			1	11		
SIR Perfusion	N	10	3	0.265	p=0.275 r=0.166	6	7	**0.031**	**p=0.031 r=0.322**
	A	19	13			5	27		
PIR Perfusion	N	29	10	**0.000**	**p=0.000 r=0.528**	10	29	0.634	p=0.643 r=0.071
	A	0	6			1	5		

WM: Wall motion, WT: Wall thickening, N: Normal, A: Abnormal, Corr.: Correlation

vs 24.4%, respectively). The correlation was significant but poor between WM and PFBP (p=0.008, r=0.392), while there was a significant and moderate correlation between WM and PIR images (p=0.000, r=0.528). The results indicate that prone imaging and IR-OSEM reconstruction have similar impacts on the % tracer uptake by the anterior and septal walls, prone imaging with statistically insignificant higher count rates. However, prone imaging significantly increases the counts of the lateral wall. Count rates of the segments were higher in IR-OSEM as compared to FBP, and in prone images as compared to supine images. Nevertheless, the highest counts were obtained from PIR images in all segments except in segment No. 16.

One of the most common problems with perfusion SPECT is the decrease in the radiotracer uptake due to several artifacts, thus reducing its specificity rate in detecting CAD. Various methods have been suggested to overcome this obstacle.

Katayama et al. (12) reported the sensitivity rate of the supine stress-rest Tl-201 images to be higher than stress-combined supine-prone images (77% vs 55%). However, prone imaging has been shown to improve the accuracy of diagnosing CAD of the inferior wall (71% vs 83%). Some authors have suggested that prone imaging improved the accuracy for diagnosing CAD without decreasing the sensitivity rate (7,10,12).

Reconstruction with IR-OSEM enabled reduction in attenuation correction (AC), thus provided modest improvement in the diagnostic accuracy. When AC (IR + AC) was added, a good correlation with PET in diagnostic accuracy was obtained as well as in stress perfusion scores (13). Qutub et al. (13) evaluated a new RR reconstruction algorithm for equivocal SPECT MPS. IR showed better results than FBP with the frequency of ''perceived'' non-equivocal studies. Bai et al. (14) have shown that OSEM significantly decreased the count-loss artifact in both the inferior and posterior walls.

Evaluation of left ventricular functional parameters from gated scans with cinematic display mode increases the diagnostic accuracy, hereby, true perfusion defects can be separated from the artifactual defects (15). Our findings were in accordance with these results, the normalcy rate increased to 64.4% with WM analysis in this study. However, it should be taken into account that in case of sub-endocardial infarction, a true myocardial perfusion defect can be false-negatively interpreted as soft-tissue attenuation since there may not be any functional abnormalities (16).

Another technique that has been shown to reduce this problem is nonuniform AC, unfortunately requires specialized hardware and software and, in some implementations, may overcorrect the inferior wall, leading to lower sensitivity for detection of a true perfusion defect (17,18).

In their study on comparing computed tomography-based AC vs. prone scanning, Malkerneker et al. (19) reported that prone imaging added to a supine imaging with and without AC did not significantly reduce the equivocal evaluation numbers. Prone imaging and AC were more helpful in men as compared to women. However, they used FBP for supine and OSEM for AC images.

Although prone imaging requires additional acquisition time, it is easy to perform since it does not require any dedicated system/software. The prone posture itself displaces the diaphragm downward, thus reducing diaphragmatic attenuation. In addition, it enables the heart to come closer to the imaging table, indirectly limiting patient movement during acquisition (6,7,20,21). Patients with inferior wall perfusion abnormality on normal prone images have been shown to have an excellent and comparable prognosis to patients with normal supine alone myocardial perfusion (10). Supine imaging is advised as the ''standard'' imaging protocol for MPS by ASNC. In case of suspicion, combined protocols followed by post-stress prone imaging can be a useful ''option'' to differentiate perfusion abnormalities caused by artifacts (22).

Several studies reported that prone imaging increased false positive anteroseptal and lateral wall defects (7,23). Slomka et al. (9) reported no difference in normalcy rates between prone and supine acquisitions in women. Our study findings also did not support aforementioned studies. In our study, the count rates were higher in IR-OSEM than FBP, and in prone images than supine images. However, the highest counts were obtained from PIR images in all segments except segment No. 16. To the best of our knowledge, there are no studies evaluating the effect of IR-OSEM methods on myocardial perfusion. This study needs to be improved by including coronary angiography (CAG) results to evaluate the sensitivity, specificity, negative and positive predictive values of these methods.

Study Limitations

We did not compare the diagnostic accuracy of SPECT MPS with CAG. This is a small, single center study. Though few patients had subsequent invasive CAG and therefore anatomical data does not exist to compare.

Due to the low number of female patients, gender difference could not be evaluated.

We didn't compare the effect of mean BMI, since we think obese patients were more likely to be interpreted as equivocal. Nevertheless, it has been shown that BMI does not significantly effect equivocal interpretation numbers (19).

Semi-quantitatively, we focused on inferior defects. However, it has been shown that most perfusion defects are located in the inferior wall in men, and to a lesser extent in the anterior wall in women (19).

Another limitation of this study is the heterogeneous patient population including those with a relatively low likelihood of CAD, those with known CAD, and those who underwent coronary bypass grafting and percutaneous coronary interventions.

Conclusion

Prone imaging added to a stress MPS significantly improves the inferior wall attenuation artifact, especially when reconstructed with IR-OSEM. Since prone imaging and WM is well correlated, WM analysis can be used as a helpful method if prone imaging cannot be performed.

Ethics

Ethics Committee Approval: No ethics committee approval required since the study was retrospective.

Informed Consent: Retrospective study

Peer-review: Externally peer-reviewed.

Authorship Contributions

Surgical and Medical Practices: D.K., E.Ö., Concept: D.K., E.Ö., Design: D.K., E.Ö., Data Collection or Processing: D.K., Analysis or Interpretation: D.K., Literature Search: D.K., Writing: D.K.

Conflict of Interest: No conflict of interest was declared by the authors.

Financial Disclosure: The authors declared that this study received no financial support.

References

1. Samady H, Wackers FJ, Joska TM, Zaret BL, Jain D. Pharmacologic stress perfusion imaging with adenosine: role of simultaneous low-level treadmill exercise. J Nucl Cardiol 2002;9:188-196.
2. Funahashi M, Shimonagata T, Mihara K, Kashiyama K, Shimizu R, Machida S, Izumi K, Kusuoka H, Nishimura T, Hoki N, Kawamoto S. Application of pixel truncation to reduce intensity artifacts in myocardial SPECT imaging with Tc-99m tetrofosmin. J Nucl Cardiol 2002;9:622-631.
3. Thompson RC. The problem of radiotracer abdominal activity in myocardial perfusion imaging studies. J Nucl Cardiol 2008;15:159-161.
4. Ibrahim DY, DiFilippo FP, Steed JE, Cerqueira MD. Optimal SPECT processing and display: making bad studies look good to get the right answer. J Nucl Cardiol 2006;13:855-866.
5. DePuey EG. Advances in SPECT camera software and hardware: currently available and new on the horizon. J Nucl Cardiol 2012;19:551-585.
6. Segall GM, Davis MJ, Goris ML. Improved specificity of prone versus supine thallium SPECT imaging. Clin Nucl Med 1988;13:915-916.
7. Kiat H, Van Train KF, Friedman JD, Germano G, Silagan G, Wang FP, Maddahi J, Prigent F, Berman DS. Quantitative stress-redistribution thallium-201 SPECT using prone imaging: methodologic development and validation. J Nucl Med 1992;33:1509-1515.
8. Nishina H, Slomka PJ, Abidov A, Yoda S, Akincioglu C, Kang X, Cohen I, Hayes SW, Friedman JD, Germano G, Berman DS. Combined supine and prone quantitative myocardial perfusion SPECT: method development and clinical validation in patients with no known coronary artery disease. J Nucl Med 2006;47:51-58.
9. Slomka PJ, Nishina H, Abidov A, Hayes SW, Friedman JD, Berman DS, Germano G. Combined quantitative supine-prone myocardial perfusion SPECT improves detection of coronary artery disease and normalcy rates in women. J Nucl Cardiol 2007;14:44-52.
10. Hayes SW, De Lorenzo A, Hachamovitch R, Dhar SC, Hsu P, Cohen I, Friedman JD, Kang X, Berman DS. Prognostic implications of combined prone and supine acquisitions in patients with equivocal or abnormal supine myocardial perfusion SPECT. J Nucl Med 2003;44:1633-1640.
11. Berman DS, Hachamovitch R, Kiat H, Cohen I, Cabico JA, Wang FP, Friedman JD, Germano G, Van Train K, Diamond GA. Incremental value of prognostic testing in patients with known or suspected ischemic heart disease: a basis for optimal utilization of exercise technetium-99m sestamibi myocardial perfusion single-photon emission computed tomography. J Am Coll Cardiol 1995;26:639-647.
12. Katayama T, Ogata N, Tsuruya Y. Diagnostic accuracy of supine and prone thallium-201 stress myocardial perfusion single-photon emission computed tomography to detect coronary artery disease in inferior wall of left ventricle Ann Nucl Med 2008;22:317-321.
13. Qutub MA, Dowsley T, Ali I, Wells RG, Chen L, Ruddy TD, Chow BJ. Incremental diagnostic benefit of resolution recovery software in patients with equivocal myocardial perfusion single-photon emission computed tomography (SPECT) J Nucl Cardiol 2013;20:545-552.
14. Bai J, Hashimoto J, Suzuki T, Nakahara T, Kubo A, Iwanaga S, Mitamura H, Ogawa S. Comparison of image reconstruction algorithms in myocardial perfusion scintigraphy. Ann Nucl Med 2001;15:79-83.
15. DePuey EG, Rozanski A. Using gated technetium-99m-sestamibi SPECT to characterize fixed myocardial defects as infarct or artifact. J Nucl Med 1995;36:952-955.
16. Choi JY, Lee KH, Kim SJ, Kim SE, Kim BT, Lee SH, Lee WR. Gating provides improved accuracy for differentiating artifacts from true lesions in equivocal fixed defects on technetium 99m tetrofosmin perfusion SPECT. J Nucl Cardiol 1998;5:395-401.
17. Hendel RC, Corbett JR, Cullom SJ, DePuey EG, Garcia EV, Bateman TM. The value and practice of attenuation correction for myocardial perfusion SPECT imaging: a joint position statement from the American Society of Nuclear Cardiology and the Society of Nuclear Medicine. J Nucl Cardiol 2002;9:135-143.
18. Shotwell M, Singh BM, Fortman C, Bauman BD, Lukes J, Gerson MC. Improved coronary disease detection with quantitative attenuation-corrected Tl-201 images. J Nucl Cardiol 2002;9:52-62.
19. Malkerneker D, Brenner R, Martin WH, Sampson UK, Feurer ID, Kronenberg MW, Delbeke D. CT-based attenuation correction versus prone imaging to decrease equivocal interpretations of rest/stress Tc-99m tetrofosmin SPECT MPI. J Nucl Cardiol 2007;14:314-323.
20. Esquerré JP, Coca FJ, Martinez SJ, Guiraud RF. Prone decubitus: a solution to inferior wall attenuation in thallium-201 myocardial tomography. J Nucl Med 1989;30:398-401.
21. Segall GM, Davis MJ. Prone versus supine thallium myocardial SPECT: a method to decrease artifactual inferior wall defects. J Nucl Med 1989;30:548-555.
22. Hansen CL, Goldstein RA, Akinboboye OO, Berman DS, Botvinick EH, Churchwell KB, Cooke CD, Corbett JR, Cullom SJ, Dahlberg ST, Druz RS, Ficaro EP, Galt JR, Garg RK, Germano G, Heller GV, Henzlova MJ, Hyun MC, Johnson LL, Mann A, McCallister BD Jr, Quaife RA, Ruddy TD, Sundaram SN, Taillefer R, Ward RP, Mahmarian JJ; American Society of Nuclear Cardiology. Myocardial perfusion and function: single photon emission computed tomography. J Nucl Cardiol 2007;14:39-60.
23. Perault C, Loboguerrero A, Liehn JC, Wampach H, Gibold C, Ouzan J, Pron T, Fortier A, Bouchard A. Quantitative comparison of prone and supine myocardial SPECT MIBI images. Clin Nucl Med 1995;20:678-684.

Interesting Image
Mol Imaging Radionucl Ther 2017;26:116-119 DOI:10.4274/mirt.70188

Super Scan Caused by Parathyroid Carcinoma Observed Both in ^{18}F-FDG PET/CT Scan and Tc-99m MDP Bone Scintigraphy

^{18}F-FDG PET/BT ve Tc-99m MDP Kemik Sintigrafisinde Tespit Edilen Paratiroid Kanserinin Neden Olduğu Süper Görüntü

İsa Burak Güney[1], Semra Paydaş[2], Hüseyin Tuğsan Ballı[3]
[1]*Çukurova University Faculty of Medicine, Department of Nuclear Medicine, Adana, Turkey*
[2]*Çukurova University Faculty of Medicine, Department of Medical Oncology, Adana, Turkey*
[3]*Çukurova University Faculty of Medicine, Department of Radiology, Adana, Turkey*

Abstract

Super scan is a well-known finding described in skeletal scintigraphy characterized by uniform symmetrically increased radiopharmaceutical uptake by bones and consequently diminished renal parenchymal activity. Sy et al. hypothesized that the faint visualization of renal cortex in bone scintigraphy might be the result of increased uptake of radiopharmaceutical by pathologic bones and reduced phosphate excretion. The super scan on ^{18}F-fluorodeoxyglucose positron emission tomography/computed tomography (^{18}F-FDG PET/CT) has been observed in various conditions such as prostate cancer, lung cancer, renal adenocarcinoma, gastric cancer and primitive neuroectodermal tumor of the kidney. Herein we report the first case of super scan in a 68-year-old-woman with parathyroid carcinoma observed both in ^{18}F-FDG PET/CT and Tc-99m methylene diphosphonate bone scintigraphy. There were extensive hypermetabolic lesions throughout the skeleton in ^{18}F-FDG PET/CT. In contrast to the intense hypermetabolism of the skeleton; the liver, skeletal muscles of the limbs, mediastinum, bowel and especially the brain showed very low FDG uptake. Additionally, there was increased skeletal radiotracer uptake relative to soft tissue, and faint genitourinary tract activity in bone scintigraphy.

Keywords: Super scan, ^{18}F-fluorodeoxyglucose positron emission tomography/computed tomography, parathyroid carcinoma

Öz

Süper görüntü kemik sintigrafisinde iyi bilinen bir bulgu olup simetrik olarak artmış kemik tutulumu ve böbreklerin görüntülenmemesi ile karakterizedir. Sy ve ark. hastalıklı kemik tarafından artan radyofarmasötik alımının azalmış fosfat atılımına ve kemik sintigrafisinde böbreklerin çok düşük düzeyde görüntülenmesine neden olduğunu ileri sürmüşlerdir. ^{18}F-florodeoksiglukoz pozitron emisyon tomografisi/bilgisayarlı tomografide (^{18}F-FDG PET/BT) süper görüntü, prostat kanseri, akciğer kanseri, böbrek adenokarsinomu, gastrik kanser ve böbreğin ilkel nöroektodermal tümörü gibi çeşitli kanserlerde rapor edilmiştir. Burada ilk kez paratiroid karsinoması olan 68 yaşındaki bir kadında hem ^{18}F-FDG PET/BT, hem de Tc-99m metilen difosfonat kemik sintigrafisinde süper görüntü bulgularını sunduk. ^{18}F-FDG PET/BT'de tüm iskelet sisteminde geniş hipermetabolik lezyonlar vardı. İskelet sistemindeki hipermetabolizmanın aksine, karaciğerde, interkostal kaslarda, mediastinumda, barsaklarda ve özellikle beyinde FDG tutulumu çok düşük seviyedeydi. Ek olarak, kemik sintigrafisinde yumuşak dokuya nazaran iskelet sisteminde artmış radyofarmasötik tutulumu ve zayıf genitoüriner sistem aktivitesi vardı.

Anahtar kelimeler: Süper görüntü, ^{18}F-florodeoksiglukoz pozitron emisyon tomografi/bilgisayarlı tomografi, paratiroid kanseri

Address for Correspondence: İsa Burak Güney MD, Çukurova University Faculty of Medicine, Department of Nuclear Medicine, Adana, Turkey
Phone: +90 532 377 70 03 E-mail: isaburak@gmail.com ORCID ID: orcid.org/0000-0002-7642-9546
Received: 18.04.2017 **Accepted:** 23.06.2017

©Copyright 2017 by Turkish Society of Nuclear Medicine
Molecular Imaging and Radionuclide Therapy published by Galenos Yayınevi.

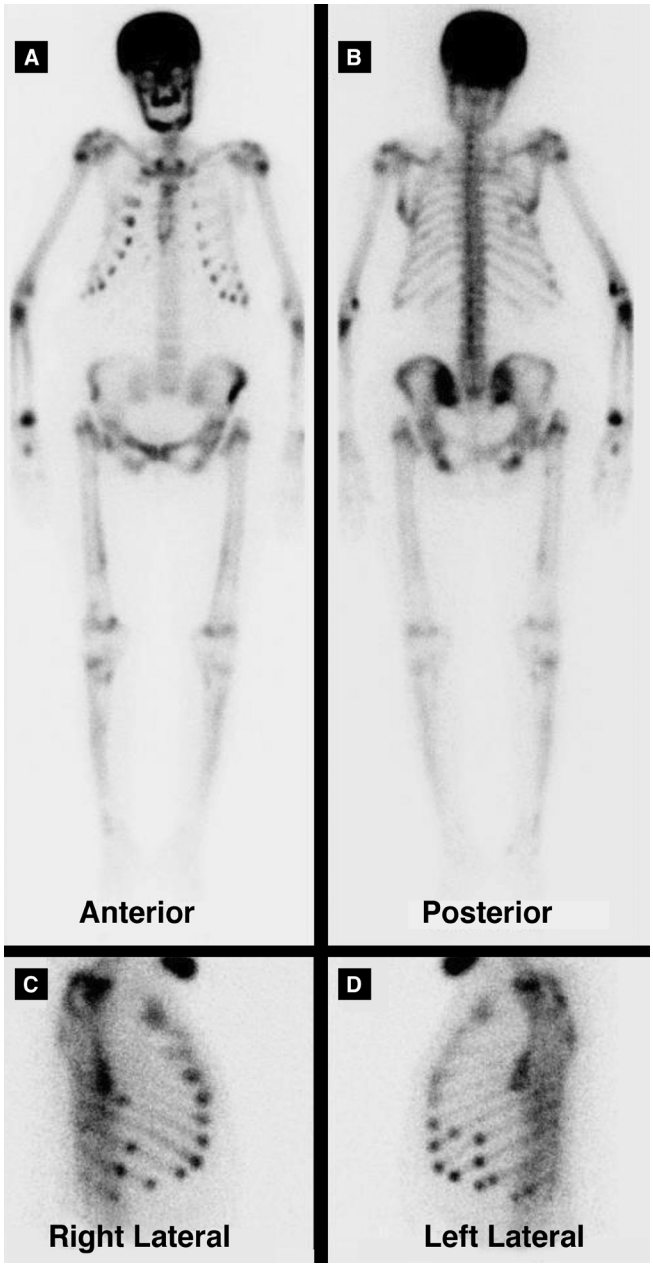

Figure 1. Tc-99m MDP bone scintigraphy. A 68-year-old women was admitted to the hospital on October 2013 with a mass on the cervical region. An excisional biopsy revealed parathyroid cancer. PET/CT showed multiple hypermetabolic lesions in the skeleton. The patient was treated by combination chemotherapy (including cisplatin and etoposide) plus zoledronic acid with good clinical response. Two years later, she presented with fatigue. Her laboratory results showed severe hypercalcemia and renal failure (serum calcium level 16.6 mg/dL, blood urea nitrogen/creatinine: 32/2.3 mg/dL). The parathormone level was 1859.6 pg/mL. Hydration was performed, calcitonin was prescribed but the hypercalcemia could not be controlled. Tc-99m MDP bone scintigraphy revealed intense radiotracer uptake involving almost the entire skeleton with high bone to soft tissue uptake (A and B). Bilateral kidneys were almost invisible (A and B). These findings are suggestive of 'metabolic superscan'. There was focal radiotracer uptake in several ribs considered as Brown tumors according to CT findings (C and D). Brown tumors represent a reparative cellular process rather than a neoplastic process (1). The increased uptake of radiopharmaceutical by pathologic bone results in reduced phosphate excretion, thereby producing faint renal images on bone scintigraphy. Wiegemann et al. (2) reported that bone resorption, alkaline phosphatase level, and parathyroid hormone activity were not correlated with Tc-99m pyrophosphate uptake by the bone. Malignancies with known super scan in bone scintigraphy include prostate cancer, breast cancer, lung cancer, lymphoma, urinary tract transitional cell carcinoma, nasopharyngeal carcinoma and carcinoma of the colon (3,4,5). Hematologic conditions like leukemia, lymphoma, myelofibrosis, Waldenstrom's macroglobulinemia have also been reported to be associated with super scan. This feature can also be detected in metabolic bone diseases like renal osteodystrophy, Paget's disease and hyperparathyroidism (2)

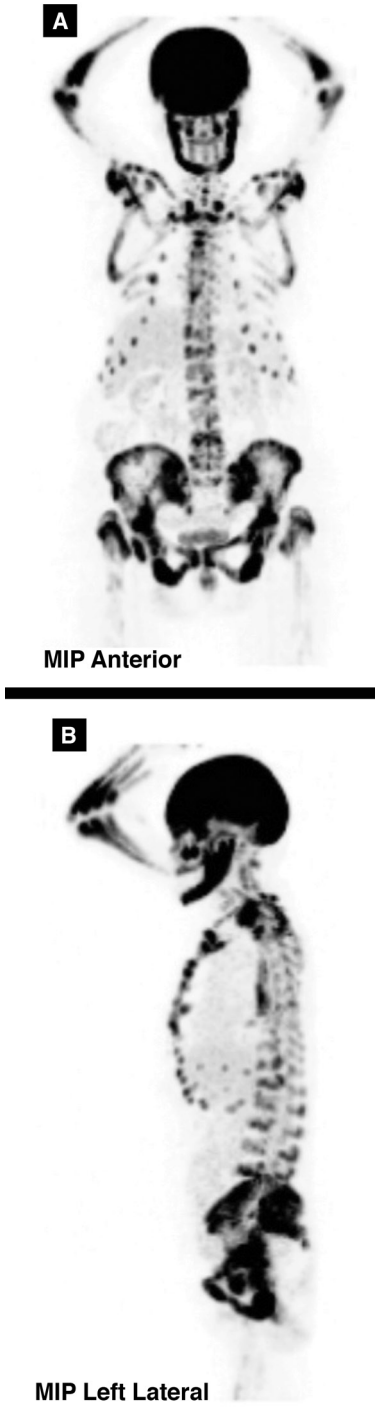

Figure 2. ^{18}F-FDG PET/CT demonstrated diffuse and intense hypermetabolism throughout the skeleton (A and B). In FDG PET scan, the faint visualization of the brain, renal cortex, and soft tissue might be the result of extraordinarily high uptake of FDG by skeletal lesions. The presented patient was not on any medications that could have disturbed cerebral glucose metabolism, such as corticosteroids or sedatives

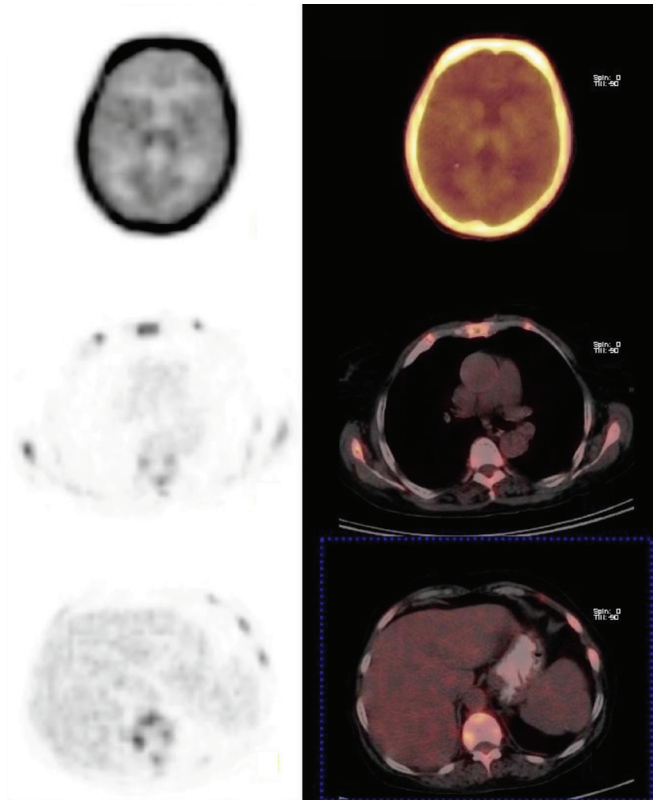

Figure 3. Interestingly the mediastinum, skeletal muscles of the limbs, bowel and especially the brain showed very low FDG uptake on ^{18}F-FDG PET/CT. A parathyroid adenoma failed to be detected by FDG PET. A similar article described by Demir et al. (6) in 2007 reported FDG PET and bone scan results in a patient with primary hyperparathyroidism as showing diffusely increased tracer uptake by the skeleton, reflecting metabolic bone disease. However, to the best of our knowledge, superscan secondary to hyperparathyroidism caused by parathyroid carcinoma has not been reported previously and is described herein

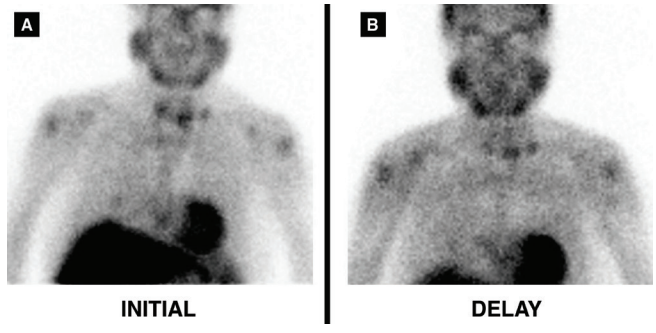

Figure 4. The patient underwent parathyroid scintigraphy for detecting a parathyroid focus, after injection of 740 MBq (20 mCi) MIBI. Three focal MIBI uptakes in the low cervical region were considered as functional parathyroid carcinoma recurrence (A and B). These functional lesions were embolized percutaneously with 95% alcohol under ultrasound guidance in two sessions with an amount of 0.8 cc and 1.5 cc, respectively, by an interventional radiologist experienced in ultrasound guided procedures

Ethics

Informed Consent: Consent form was filled out by all participants.

Peer-review: Internally peer-reviewed.

Authorship Contributions

Surgical and Medical Practices: İ.B.G., S.P., H.T.B., Concept: İ.B.G., S.P., H.T.B., Design: İ.B.G., Data Collection or Processing: İ.B.G., Analysis or Interpretation: İ.B.G., S.P., H.T.B., Literature Search: İ.B.G., Writing: İ.B.G., S.P.

Conflict of Interest: No conflict of interest was declared by the authors.

Financial Disclosure: The authors declared that this study received no financial support.

References

1. Chew FS, Huang-Hellinger F. Brown tumor. AJR 1993;160:752.
2. Wiegemann T, Rosenthall L, Kaye M. Technetium-99m-pyrophosphate bone scans in hyperparathyroidism. J Nucl Med 1977;18:231-235.
3. Buckley O, O'Keeffe S, Geoghegan T, Lyburn ID, Munk PL, Worsley D, Torreggiani WC. 99m Tc bone scintigraphy superscans: a review. Nucl Med Commun 2007;28:521-527.
4. Frankel RS, Johnson KW, Mabry JJ, Johnston GS. "Normal" bone radionuclide image with diffuse skeletal lymphoma. A case report. Radiology 1974;111:365-366.
5. Chakraborty PS, Sharma P, Karunanithi S, Bal C, Kumar R. Metastatic superscan on (99m)Tc-MDP bone scintigraphy in a case of carcinoma colon: Common finding but rare etiology. Indian J Nucl Med 2014;29:158-159.
6. Demir H, Halac M, Gorur GD, Sonmezoglu K, Uslu I. FDG PET/CT findings in primary hyperparathyroidism mimicking multiple bone metastases. Eur J Nucl Med Mol Imaging 2008;35:686.

Interesting Image
Mol Imaging Radionucl Ther 2017;26:120-123 DOI:10.4274/mirt.06025

Two Uncommon Sites of Metastasis: Breast and Hypophysis Metastases of Head and Neck Adenoid Cystic Carcinoma Detected by FDG PET/CT

Baş Boyun Adenoid Kistik Karsinomlu Olguda İki Olağan Dışı Metastaz Alanı: Hipofiz ve Meme

Evrim Sürer Budak[1], Şenay Yıldırım[2], Sevim Yıldız[3], Ali Ozan Öner[4], Şeyda Gündüz[5]
[1]*Antalya Training and Research Hospital, Clinic of Nuclear Medicine, Antalya, Turkey*
[2]*Antalya Training and Research Hospital, Clinic of Pathology, Antalya, Turkey*
[3]*Antalya Training and Research Hospital, Clinic of Radiology, Antalya, Turkey*
[4]*Afyon Kocatepe University Faculty of Medicine, Clinic of Nuclear Medicine, Afyon, Turkey*
[5]*Antalya Training and Research Hospital, Clinic of Medical Oncology, Antalya, Turkey*

Abstract

Adenoid cystic carcinoma (ACC) is a rare epithelial malignancy arising from secretory glands, particularly the salivary glands. It tends to invade nerves and has a high potential for distant hematogenous metastasis, especially to the lungs, bone, liver and brain. The breast and hypophysis are not common sites of ACC metastatic disease. Herein, we report a case of ACC of the head and neck region with two unusual sites of metastases, the hypophysis and breast.
Keywords: PET/CT, adenoid cystic carcinoma, breast, hypophysis, metastasis

Öz

Adenoid kistik karsinom (AKK), sekretuar glandlardan özellikle de tükrük bezlerinden köken alan nadir bir epitelyal tümördür. Sinir invazyonu sıktır ve özellikle akciğer, kemik, karaciğer ve beyin gibi organlara uzak hematojen metastaz yapma potansiyeli yüksektir. Ancak, meme ve hipofiz AKK için tipik metastaz alanları değildir. Bu çalışmada, hipofiz ve meme gibi iki olağan dışı alana metastazı olan baş-boyun AKK olgusunu sunmaktayız.
Anahtar kelimeler: PET/BT, adenoid kistik karsinom, meme, hipofiz, metastaz

Address for Correspondence: Evrim Sürer Budak MD, Antalya Training and Research Hospital, Clinic of Nuclear Medicine, Antalya, Turkey
Phone: +90 242 249 44 00 E-mail: evrimsurer@hotmail.com ORCID ID: orcid.org/0000-0002-8318-0785
Received: 23.03.2017 **Accepted:** 10.07.2017

©Copyright 2017 by Turkish Society of Nuclear Medicine
Molecular Imaging and Radionuclide Therapy published by Galenos Yayınevi.

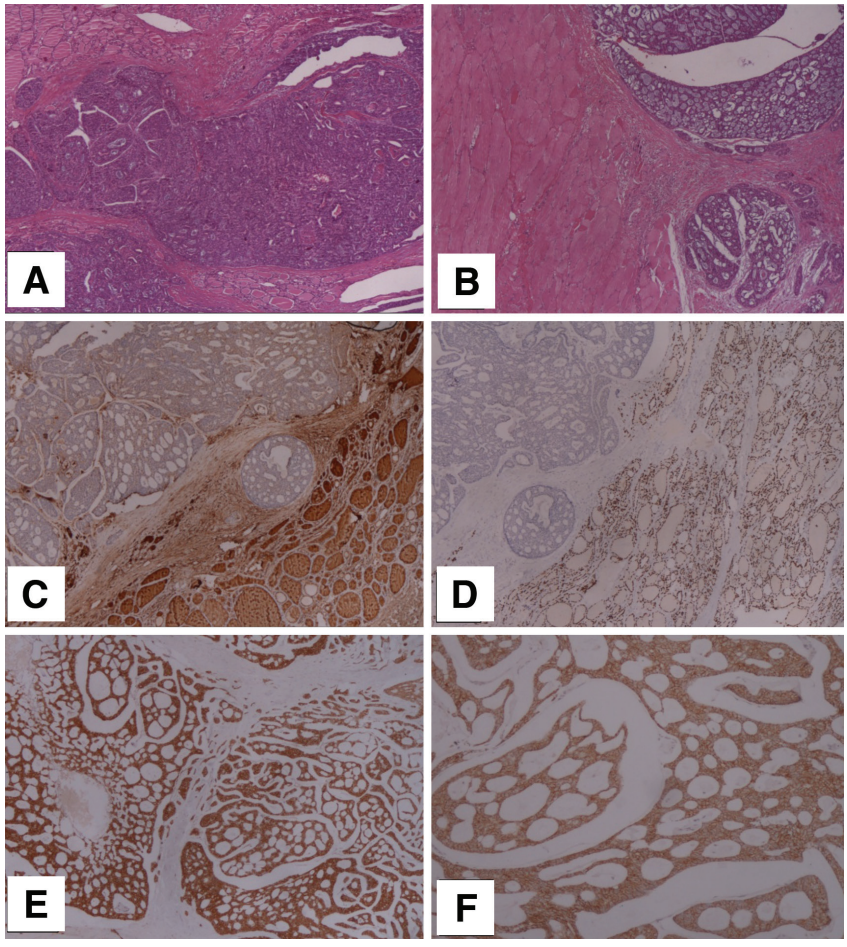

Figure 1. A 49-year-old woman presented with a left cervical mass. The ultrasound examination revealed a gross mass adjacent to the thyroid gland and she underwent total excision of the mass along with total thyroidectomy. Histopathologic examination of the 9.5x10 cm mass revealed adenoid cystic carcinoma (ACC) infiltrating both the thyroid and adjacent smooth muscle tissue. (A, B): Hematoxylin and eosin (H&E) staining of the primary tumor: Tumor cells were arranged in cord-like or acinar-like by atypical hyperplastic epithelial cells forming a cribriform and tubular pattern with a mucoid luminal material (x40). (C, D): Tumor cells were negative for thyroglobulin (C) and TTF-1 (D) excluding thyroid origin (x40). Tumor cells were immune-positive for CD-117 (E) indicating ductal origin and E-cadherin (F) (x100). She was accepted as ACC of the head and neck region. The patient was referred to FDG PET/CT scanning for initial staging. PET/CT images revealed multiple hypermetabolic lung metastasis and a mild FDG uptake in the operation region secondary to surgery. She received radiotherapy and chemotherapy, and was stable for about 20 months follow-up

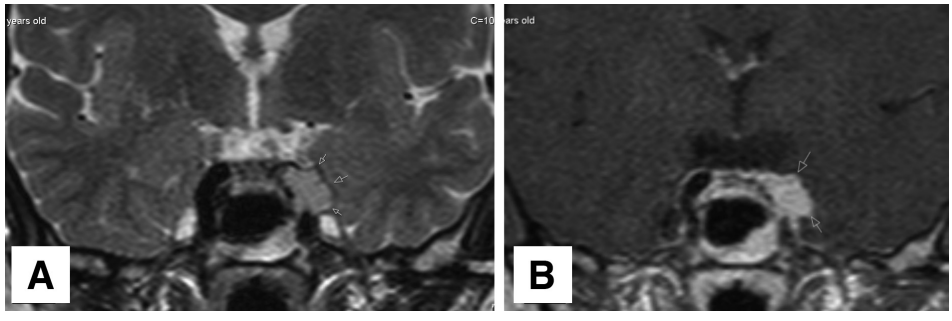

Figure 2. (A, B) Twenty months after the initial diagnosis, the patient developed sudden vision loss. The cranial magnetic resonance imaging T2 and post-contrast T1 weighted coronal images revealed a mildly T2 hyper-intense and homogenously enhancing left parasellar mass compatible with metastasis. The patient received radiotherapy. Pituitary metastasis is very rare, accounting for only about 1% of pituitary surgeries (1). In the literature, although extraordinary metastasis sites of ACC were reported including the kidney (2) and vertebrae (3), there are only two cases reporting hypophysis metastasis (4,5)

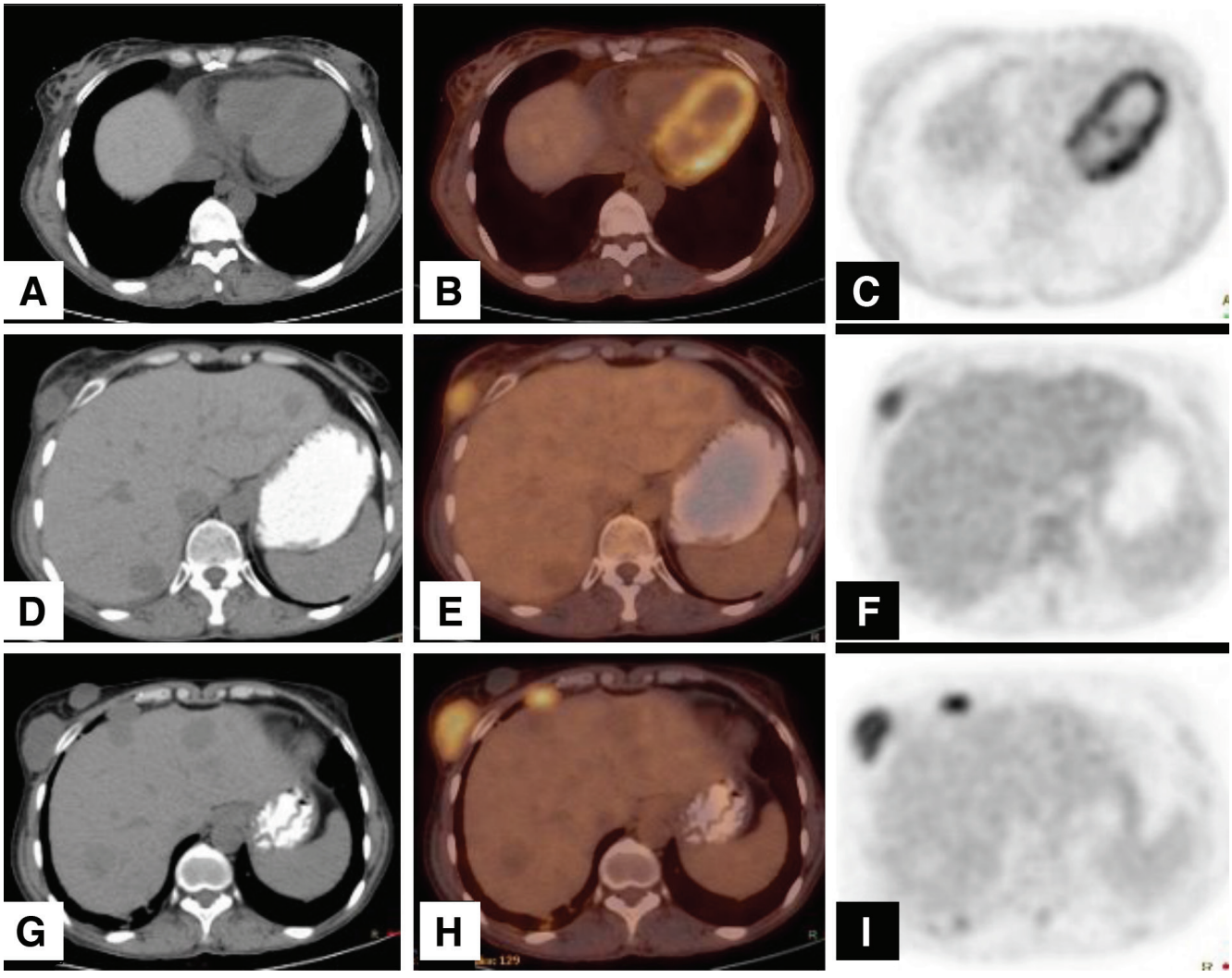

Figure 3. The PET/CT images performed for response evaluation at the 24th month after initial diagnosis showed two new lesions in the right breast. The interval between the last two PET/CT imaging was about one year, and these breast lesions were new findings. (A, B, C): The initial FDG PET/CT images with no lesion both anatomically and metabolically in the breast tissue. (D, E, F): The second year FDG PET/CT examination revealed an unexpected, lobulated hypermetabolic solid mass measuring 19x30 mm with a SUV_{max} of 5.2 in the lower outer quadrant of the right breast. There was also a smaller non-metabolic lesion next to this lesion. The patient underwent incisional biopsy, the histopathologic examination revealed ACC in the lateral lesion while the other one was composed of necrotic material. The histology and immunophenotyping of the breast ACC is similar to that of the salivary gland. Therefore, it is difficult to differentiate metastatic disease from a primary breast ACC by pathologic examination. The diagnosis is usually based on clinical behavior of the tumor. In our case, based on the clinical findings (sudden onset in one year), it was diagnosed as metastasis from the primary tumor. Hypermetabolic right parasternal, anterior diaphragmatic/paracardiac lymph nodes were also detected in the same examination. (G, H, I): In the following FDG PET/CT, her metastatic breast lesion progressed anatomically (24x35 mm) while remaining metabolically stable (SUV_{max}: 5.6). Anterior mediastinal, paracardiac, parasternal and right anterior mediastinal lymph nodes were also detected as new findings while the existing lung metastasis were progressing. (D, G): The patient also had multiple hypodense stable lesions in the liver that did not show any FDG uptake, compatible with hemangiomas. The patient's chemoradiotherapy is still on-going in the third year of diagnosis. In the consecutive follow-up PET/CT images performed at 4 month intervals, her metastatic lung lesions, lymph nodes and breast lesion all have been progressing both in dimension and metabolically.

Breast metastasis from extra-mammary neoplasms is very rare, with a reported incidence of 0.5-3% (6). Also, the incidence of unexpected breast focal uptake in ^{18}F-DG-PET/CT is reported as 0.36-1.12% (7,8,9). The rate of malignancy in incidental FDG-avid breast foci was reported in a range of 37.5-83% (10,11,12). Under these circumstances, it can be concluded that focal FDG-avid breast lesions need further evaluation, especially in cases with known malignancies

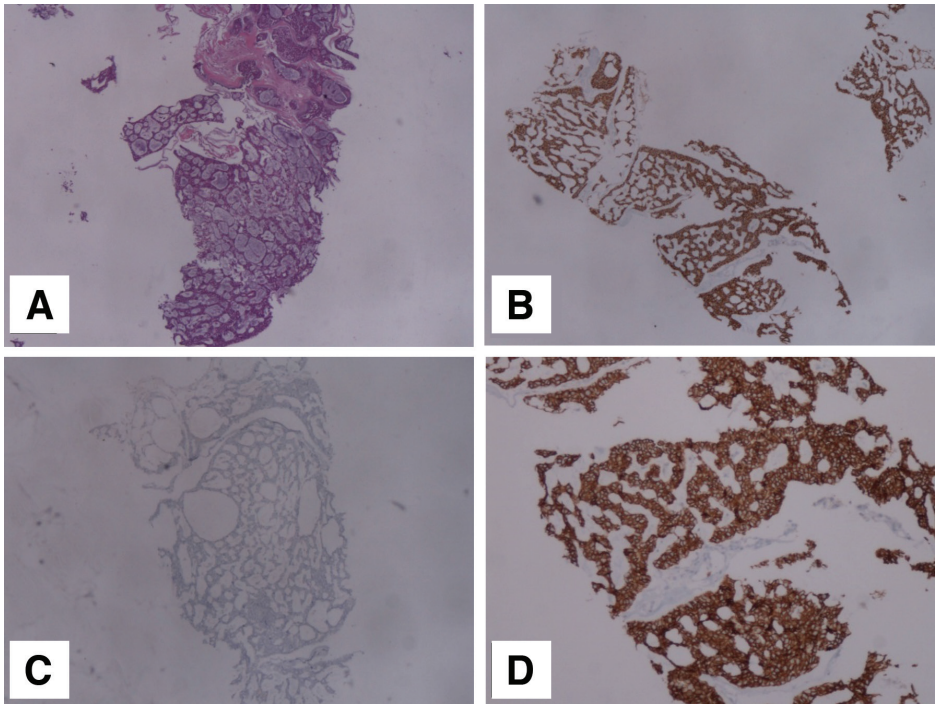

Figure 4. Histopathologic examination of the breast lesion revealed ACC. (A): Invasive tumor cells forming cylindromatous nodules and glandular spaces with basophilic secretion (x40) (B): CD-117 positivity in tumor cells (x40) (C): Tumor cells were negative for Estrogen receptor (x40) (D): Tumor cells were immune-positive for E-cadherin (x100)

Ethics

Informed Consent: Consent form was filled out by all participants.

Peer-review: Internally peer-reviewed.

Authorship Contributions

Surgical and Medical Practices: E.S.B., Ş.Y., S.Y., Ş.G., Concept: E.S.B., Design: E.S.B., Data Collection or Processing: E.S.B., Ş.Y., S.Y., Ş.G., Analysis or Interpretation: E.S.B., A.O.Ö., Literature Search: E.S.B., A.O.Ö., Writing: E.S.B.

Conflict of Interest: No conflict of interest was declared by the authors.

Financial Disclosure: The authors declared that this study received no financial support.

References

1. Fassett DR, Couldwell WT. Metastases to the pituitary gland. Neurosurg Focus 2004;16:E8.
2. Qiu DS, Xu LY, Hu XY. Imaging appearance of a singular metastatic adenoid cystic carcinoma of the right kidney: A case report and literature review. Oncol Lett 2014;8:2669-2671.
3. Feng H, Wang J, Guo P, Xu J, Feng J. C3 Vertebral Metastases From Tongue Adenoid Cystic Carcinoma: A Rare Case Report. Medicine (Baltimore) 2015;94:e1135.
4. Kawamata T, Harashima S, Kubo O, Hori T. Intrasellar remote metastasis from adenoid cystic carcinoma of parotid gland: case report. Endocr J 2006;53:659-663.
5. Hughes DJ, Retzlaff A, Sims J, O'Brien E, Giannini C, Huston J, Van Gompel JJ. Adenoid Cystic Carcinoma Metastatic to the Pituitary: A Case Report and Discussion of Potential Diagnostic Value of Magnetic Resonance Elastography in Pituitary Tumors. World Neurosurg 2016;91:669.e11-14.
6. Lee SK, Kim WW, Kim SH, Kim S, Choi JH, Cho EY, Han SY, Hahn BK, Choe JH, Kim JH, Kim JS, Lee JE, Nam SJ, Yang JH. Characteristics of metastasis in the breast from extramammary malignancies. J Surg Oncol 2010;101:137-140.
7. Litmanovich D, Gourevich K, Israel O, Gallimidi Z. Unexpected foci of (18)F-FDG uptake in the breast detected by PET/CT: incidence and clinical significance. Eur J Nucl Med Mol Imaging 2009;36:1558-1564.
8. Kang BJ, Lee JH, Yoo IeR, Kim SH, Choi JJ, Jeong SH, Yim HW. Clinical significance of incidental finding of focal activity in the breast at 18F-FDG PET/CT. AJR Am J Roentgenol 2011;197:341-347.
9. Dunne RM, O'Mahony D, Wilson G, McDermott R, O'Keeffe SA. The role of the breast radiologist in evaluation of breast incidentalomas detected on 18-fludeoxyglucose positron emission tomography/CT. Br J Radiol. 2013;86:2013003.
10. Litmanovich D, Gourevich K, Israel O, Gallimidi Z. Unexpected foci of (18)F-FDG uptake in the breast detected by PET/CT: incidence and clinical significance. Eur J Nucl Med Mol Imaging 2009;36:1558-1564.
11. Korn RL, Yost AM, May CC, Kovalsky ER, Orth KM, Layton TA, Drumm D. Unexpected focal hypermetabolic activity in the breast: significance in patients undergoing 18F-FDG PET/CT. AJR Am J Roentgenol 2006;187:81-85.
12. Kang BJ, Lee JH, Yoo IR, Kim SH, Choi JJ, Jeong SH, Yim HW. Clinical significance of incidental finding of focal activity in the breast at 18F-FDG PET/CT. AJR Am J Roentgenol 2011;197:341-347.

Interesting Image
Mol Imaging Radionucl Ther 2017;26:124-127 DOI:10.4274/mirt.30592

Cyclosporine and Vancomycin + Amikacin Induced Hot Kidney Appearance in a Young Adult and a Pediatric Patient

Genç Yetişkin ve Pediatrik Bir Hastada Siklosporin ve Vankomisin + Amikasin ile İndüklenen Hot Kidney Görünümü

Derya Çayır, Mine Araz, Mustafa Filik, Mehmet Erdoğan
University of Health Sciences, Dışkapı Yıldırım Beyazıt Training and Research Hospital, Clinic of Nuclear Medicine, Ankara, Turkey

Abstract

The appearance of a hot kidney on bone scintigraphy is rare and can be seen due to various factors. In our clinic, we observed hot kidney appearance in two patients to whom technetium-99m methylene diphosphonate (Tc-99m MDP) whole body scan has been performed: a young male adult at the age of 18 who was diagnosed with acute lymphocytic leukemia with a presumptive diagnosis of avascular necrosis, and a 9-year-old girl with cystitis for a pre-diagnosis of osteomyelitis. The first patient had a history of cyclosporine usage and the second patient was being treated with amikacin + vancomycin. To the best of our knowledge, we present the first cases where hot-kidney appearance on Tc-99m MDP whole body scan due to the use of cyclosporin and amikacin + vancomycin is demonstrated.

Keywords: Kidney, Tc-99m medronate, radionuclide imaging

Öz

Kemik sintigrafisinde hot kidney görünümü nadir olup, çeşitli faktörlere bağlı olarak görülebilmektedir. Kliniğimizde teknesyum-99m metilen difosfanat (Tc-99m MDP) tüm vücut kemik sintigrafisi yaptığımız iki hastada; ilki avasküler nekroz ön tanısı ile 18 yaşında akut lenfositer lösemi tanılı genç erişkin erkekte, diğeri osteomiyelit ön tanısı ile 9 yaşında sistit tanılı kız çocuğunda hot kidney görünümü izledik. İlk hastada siklosporin kullanım öyküsü vardı, ikinci hasta ise amikasin + vankomisin tedavisi altındaydı. Bildiğimiz kadarıyla, Tc-99m MDP tüm vücut kemik sintigrafisinde siklosporin ve amikasin + vankomisin kullanımına bağlı hot kidney görünümünün gösterildiği ilk olguları sunuyoruz.

Anahtar kelimeler: Böbrek, Tc-99m medronat, radyonüklid görüntüleme

Address for Correspondence: Derya Çayır MD, University of Health Sciences, Dışkapı Yıldırım Beyazıt Training and Research Hospital, Clinic of Nuclear Medicine, Ankara, Turkey
Phone: +90 535 568 10 66 E-mail: drderyaors@hotmail.com ORCID ID: orcid.org/0000-0002-7756-3210
Received: 05.05.2017 **Accepted:** 16.07.2017

©Copyright 2017 by Turkish Society of Nuclear Medicine
Molecular Imaging and Radionuclide Therapy published by Galenos Yayınevi.

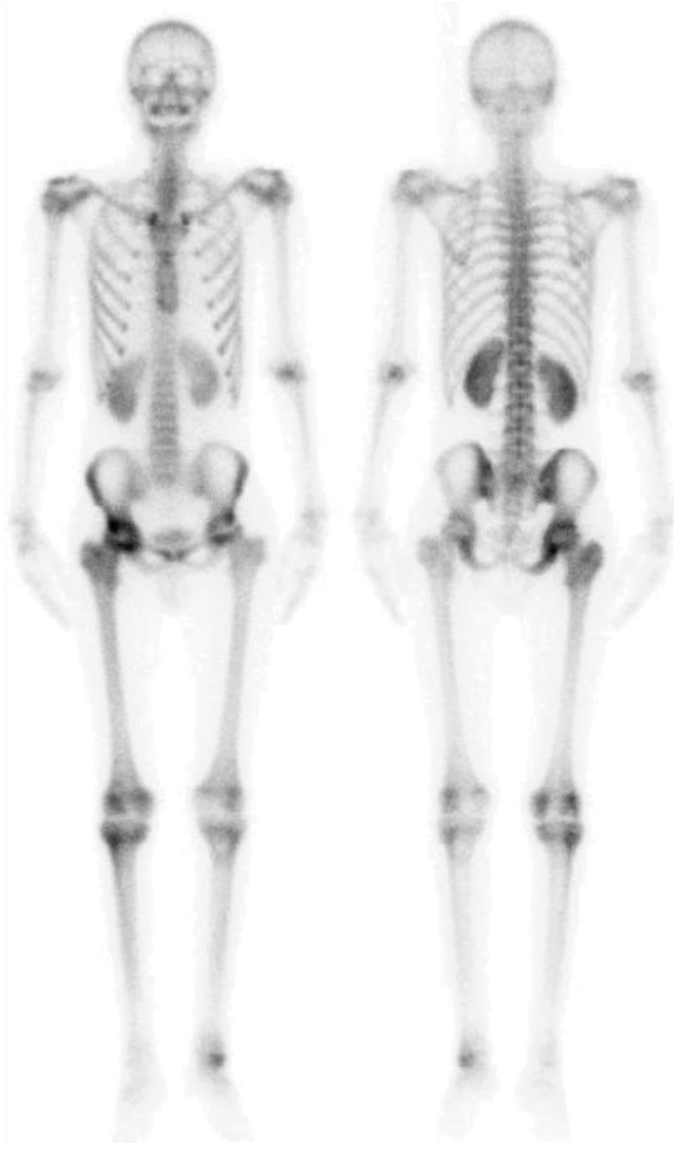

Figure 1. A male patient at the age of 18 who has been diagnosed with acute lymphocytic leukemia was under cyclosporine treatment for 9 months. The patient suffered from hip and right leg pain, and Tc-99m MDP whole-body bone scintigraphy was performed for possible avascular necrosis. There was no pathological finding throughout the skeleton except for increased peripheral osteoblastic activity in the middle of the right femur, hypoactive area in the middle, and mildly increased activity in the femur neck and trochanteric region, findings in accordance with the preliminary diagnosis. As an additional finding, diffuse increased activity was observed in both kidneys. Abdominal ultrasonography performed before immunosuppressive therapy revealed that both kidneys were normal. Following cyclosporine treatment, serum urea level raised to 42 mg/dL (normal range: 11-39 mg/dL) and serum creatinine level was detected as 1.23 mg/dL (normal range: 0.5-1.2 mg/dL). Urinary ultrasonography showed bilateral grade 1 increase in renal parenchymal echogenicity

Figure 2. A 9-year-old girl with a diagnosis of cystitis has been receiving amikacin and vancomycin treatment for a week. She had persistent fever, fatigue and widespread body pain despite normal urinary US findings, and normal blood urea nitrogen and creatinine levels. Tc-99m MDP whole body scintigraphy was performed to rule out osteomyelitis. Scintigraphic findings were normal, but both kidneys were enlarged and showed diffuse increased radiopharmaceutical uptake.

Tc-99m MDP is a highly sensitive method for assessing dissemination of primary skeletal system disorders (1). Tc-99m MDP uptake in the soft tissue can be detected due to various reasons. Diffuse increased radionuclide uptake in the kidneys is defined as 'hot kidneys'. The incidence of hot kidneys on bone scintigraphy was reported to be less than 1% (2). There are several proposed reasons for bilateral diffuse increased kidney uptake on Tc-99m MDP bone scan. It has been suggested that renal damage causes deterioration of secretory or glomerular filtration function (3). Another mechanism of Tc-99m MDP uptake can be calcification of the kidneys due to ischemia caused by injury to the kidney at any time (3,4). The common causes of the appearance of hot kidneys include nephrotoxic drugs (antibiotics, chemotherapeutics, and nonsteroidal anti-inflammatory agents), urinary obstruction, nephrocalcinosis, metastatic calcification, hypercalcemia, hyperparathyroidism, infective pyelonephritis, vascular pathologies, iron overload, radiotherapy, and rhabdomyolysis (3,4,5,6,7,8,9,10,11,12,13,14,15,16). We observed the appearance of "hot kidneys" in our two cases, which may be due to temporary renal damage secondary to the long-term use of cyclosporine and amikacin + vancomycin. Cyclosporin is a calcineurin inhibitor that provides immunosuppression by blocking the production of interleukin-2 by T cells. Cyclosporine reduces glomerular filtration rate by causing vasoconstriction in afferent arterioles in the kidneys (17,18). Aminoglycosides (amikacin) are used in the short-term treatment of infections caused by susceptible strains of gram-negative microorganisms. Vancomycin is used in the treatment of infections caused by gram-positive microorganisms. Nephrotoxicity can be seen in the use of these two drugs in combination, especially in long-term or high-dose use. The glomerular filtration rate may be reduced and the nephrotoxic effect may be caused also by impaired proximal tubular transport.

Tc-99m MDP might sometimes show extra-skeletal uptake in the soft tissue. The urinary system is mildly visualized on a normal bone scan, but symmetrical diffuse increased Tc-99m MDP uptake is almost always pathological and should be mentioned in the reports and etiology should be further investigated

Ethics

Informed Consent: Consent form was filled out by all participants.

Peer-review: Internally peer-reviewed.

Authorship Contributions

Surgical and Medical Practices: D.Ç., M.A., Concept: D.Ç., Design: D.Ç., Data Collection or Processing: D.Ç., M.E., Analysis or Interpretation: M.F., Literature Search: M.E., Writing: D.Ç., M.A.

Conflict of Interest: No conflict of interest was declared by the authors.

Financial Disclosure: The authors declared that this study received no financial support.

References

1. Langsteger W, Rezaee A, Pirich C, Beheshti M. 18F-NaF-PET/CT and 99mTc MDP Bone Scintigraphy in the Detection of Bone Metastases in Prostate Cancer. Semin Nucl Med 2016;46:491-501.
2. Koizumi K, Tonami N, Hisada K. Diffusely increased Tc-99m-MDP uptake in both kidneys. Clin Nucl Med 1981;6:362-365.
3. Ting A, Freund J. Nonsteroidal antiinflammatory-induced acute renal failure detected on bone scintigraphy. Clin Nucl Med 2004;29:318-319.
4. Gentili A, Miron SD, Adler LP, Bellon EM. Incidental detection of urinary tract abnormalities with skeletal scintigraphy. Radiographics 1991;11:571-579.
5. Choy D, Murray IP, Hoschl R. The effect of iron on the biodistribution of bone scanning agents in humans. Radiology 1981;140:197-202.
6. Ozdoğan O, Karahan NP, Sarıoğlu S, Durak H. Acute Kidney Injury Secondary to NSAID Diagnosed on 99mTc MDP Bone Scan. Mol Imaging Radionucl Ther 2013;22:66-69.
7. Siddiqui AR. Increased uptake of technetium-99m-labeled bone imaging agents in the kidneys. Semin Nucl Med 1982;12:101-102.
8. Buxton-Thomas MS, Wraight EP. High renal activity on bone scintigrams. A sign of hypercalcaemia? Br J Radiol 1983;56:911-914.
9. Arbona GL, Antonmattei S, Tetalman MR, Scheu JD. Tc-99m-diphosphonate distribution in a patient with hypercalcemia and metastatic calcifications. Clin Nucl Med 1980;5:422.
10. Datz F. Bone imaging: increased renal uptake-diffuse. In: Gamuts in Nuclear Medicine. St Louis, Mosby, 1995;160-161.
11. Lantieri RL, Lin MS, Martin W, Goodwin DA. Increased renal accumulation of Tc-99m-MDP in renal artery stenosis. Clin Nucl Med 1980;5:305-309.
12. Lamki LM, Wyatt JK. Renal vein thrombosis as a cause of excess renal accumulation of bone seeking agents. Clin Nucl Med 1983;8:267-268.
13. Lutrin CL, Goris ML. Pyrophosphate retention by previously irradiated renal tissue. Radiology 1979;133:207-209.
14. Sheth KJ, Sty JR, Johnson F, Tisdale P. Myoglobinuria with acute renal failure and hot kidneys seen on bone imaging. Clin Nucl Med 1984;9:498-501.
15. Schicha H, Rumpf KW, Kaiser H, Emrich D. Scintigraphy with 99mTc-methylene diphosphonate for the detection and localization of rhabdomyolysis. Nuklearmedizin 1984;23:287-291.
16. Watanabe N, Shimizu M, Kageyama M, Kamei T, Seto H, Kakishita M. Diffuse increased renal uptake on bone scintigraphy in acute tubular necrosis. Clin Nucl Med 1994;19:19-21.
17. Maza A, Montaudié H, Sbidian E, Gallini A, Aractingi S, Aubin F, Bachelez H, Cribier B, Joly P, Jullien D, Le Maître M, Misery L, Richard MA, Ortonne JP, Paul C. Oral cyclosporin in psoriasis: a systemic review on treatment modalities, risk of kidney toxicity and evidence for use in non-plaque psoriasis. J EurAcad Dermatol Venereol 2011;25(Suppl 2):19-27.
18. Feutren G, Abeywickrama K, Friend D, von Graffenried B. Renal function and blood pressure in psoriasis patients treated with cyclosporine. Br J Dermatol 1990;122(Suppl 36):57-69.

Interesting Image
Mol Imaging Radionucl Ther 2017;26:128-130 DOI:10.4274/mirt.37167

Incidental Tc-99m Methylene Diphosphonate Uptake in an Active Thyroid Nodule

Aktif Tiroid Nodülünde İnsidental Tc-99m Metilen Difosfonat Tutulumu

Derya Çayır[1], Mine Araz[1], Şafak Akın[2], Melia Karaköse[2], Erman Çakal[2]
[1]*University of Health Sciences, Dışkapı Yıldırım Beyazıt Training and Research Hospital, Clinic of Nuclear Medicine, Ankara, Turkey*
[2]*University of Health Sciences, Dışkapı Yıldırım Beyazıt Training and Research Hospital, Clinic of Endocrinology and Metabolism, Ankara, Turkey*

Abstract

Tc-99m-methylene diphosphonate (MDP) whole body scintigraphy is the method of choice for detection of metastatic bone diseases. It is primarily used to help diagnose various bone-related conditions such as primary or metastatic cancer of the bone, location of bone inflammation, and fractures that may not be visible on traditional X-ray images, as well as detection of bone damage due to infections and other conditions. In addition, bone scanning is often used for the follow-up or evaluation of response to treatment in some malignancies like prostate and breast cancers. Pathologies of other systems can also be incidentally detected on whole body bone scan. Herein we present an interesting image of an active thyroid nodule that showed Tc-99m MDP uptake in a prostate cancer patient.
Keywords: Thyroid nodule, Tc-99m medronate, radionuclide imaging

Öz

Tc-99m metilen difosfonat (MDP) tüm vücut kemik sintigrafisi kemik metastazlarının araştırılmasında sıklıkla uygulanan bir tetkiktir. Primer ve metastatik kemik kanseri tanısı, kemik enflamasyonunun lokalizasyonu, geleneksel X-ray görüntülerinde izlenemeyen fraktürlerin tanısı, enfeksiyon ve diğer durumlara bağlı gelişebilen kemik hasarının tanısı gibi kemik ile ilişkili çok sayıda durumun teşhisinde yardımcıdır. Ek olarak, kemik sintigrafisi, prostat ve meme kanseri gibi bazı malignitelerin takibinde veya tedaviye yanıtının değerlendirilmesinde sıklıkla kullanılmaktadır. Tüm vücut kemik sintigrafisinde diğer sistemlere ait patolojiler insidental olarak saptanabilir. Bu olguda prostat karsinomu tanısı olan hastada Tc-99m MDP tutan aktif tiroid nodülüne ait ilginç görünümü sunuyoruz.
Anahtar kelimeler: Tiroid nodülü, Tc-99m medronat, radyonüklid görüntüleme

Address for Correspondence: Derya Çayır MD, University of Health Sciences, Dışkapı Yıldırım Beyazıt Training and Research Hospital, Clinic of Nuclear Medicine, Ankara, Turkey
Phone: +90 535 568 10 66 E-mail: drderyaors@hotmail.com ORCID ID: orcid.org/0000-0002-7756-3210
Received: 11.05.2017 **Accepted:** 16.07.2017

Presented in: This case was presented as a poster in National Nuclear Medicine Congress in 2016 in İzmir.

©Copyright 2017 by Turkish Society of Nuclear Medicine
Molecular Imaging and Radionuclide Therapy published by Galenos Yayınevi.

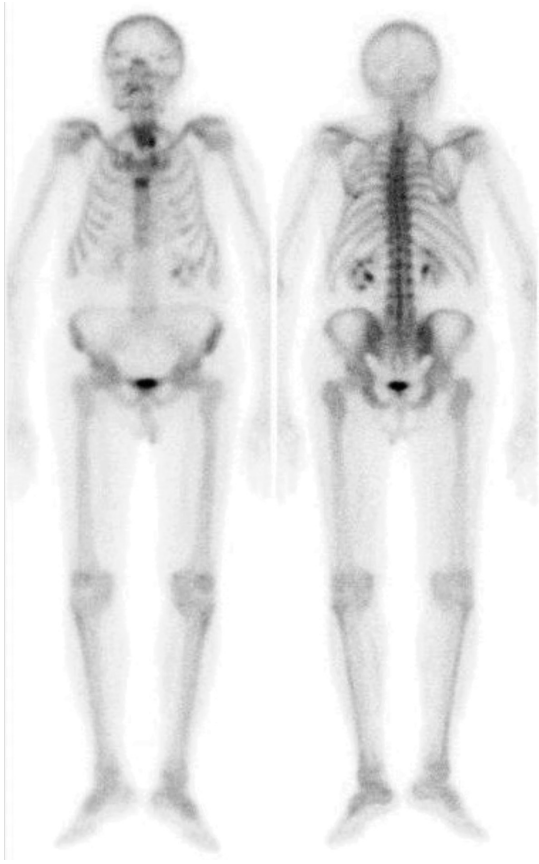

Figure 1. A 84-year-old male patient with prostate adenocarcinoma underwent technetium-99m (Tc-99m) methylene diphosphonate (MDP) whole body bone scintigraphy in order to evaluate bone metastasis. The patient did not have any other known diseases or complaints. The bone scintigraphy showed focal increased activity in the area consistent with the inferior pole of the left lobe of the thyroid gland. The serum thyroid function tests were as follows: TSH 2.45 uIU/mL (N: 0.34-5.60), fT3: 3.52 pg/mL (N: 2.5-3.9), fT4: 0.76 ng/dL (N: 0.58-1.6) and thyroid autoantibodies were negative

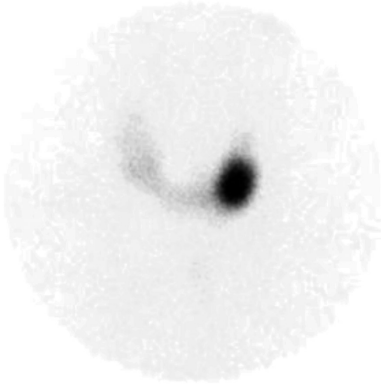

Figure 2. Tc-99m pertechnetate thyroid scintigraphy showed an active nodule in the lower pole of the left lobe, significant suppression was observed in extranodal areas

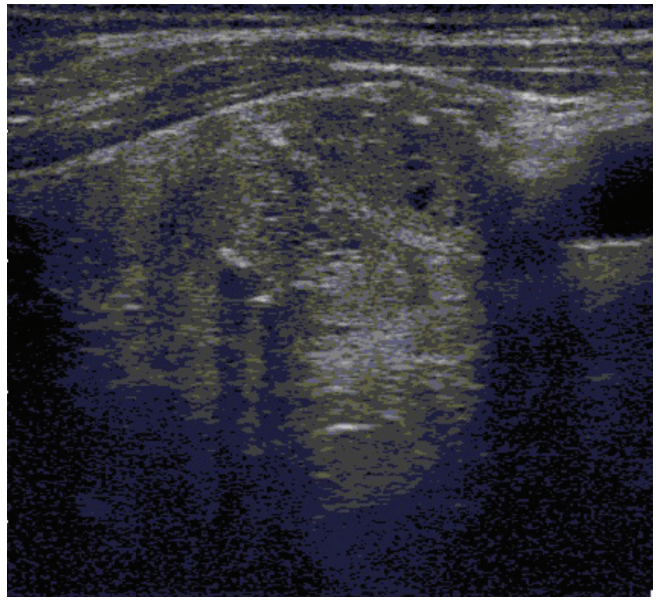

Figure 3. Thyroid ultrasound revealed a 14x14x22 mm nodule with a mixed echo pattern, rough calcification foci and cystic-necrotic areas in the left lobe lower pole. Fine needle aspiration biopsy of this nodule complied with benign follicular nodule.

Bone scintigraphy is usually performed to evaluate a wide variety of skeletal abnormalities (1). Tc-99m-labeled diphosphonates have been used for bone scanning as a major diagnostic tool since the beginning of 1970s (2). Tc-99m MDP has rapid blood clearance, excellent in vivo chemical stability, and a high bone-to-soft tissue ratio, thus, it is ideal for bone imaging (3). In the literature, many cases of incidental Tc-99m-MDP uptake by the soft tissue have been reported due to various reasons, both benign (tumoral calcinosis, myositis ossificans) and malignant (sarcomas, adenocarcinomas, metastases) conditions (4,5). Mechanisms leading to increased extraosseous Tc-99m MDP uptake include extracellular fluid expansion, enhanced local vascularity and permeability, and high tissue calcium concentration. The composition of the calcium deposition and the presence of other elements (e.g. iron and magnesium) are important (4). It is known that there may be incidental Tc-99m MDP uptake in the thyroid gland, in calcific thyroid nodules, secondary to biopsy interventions, anaplastic thyroid carcinoma or metastatic thyroid cancer (4,6). In our case, unexpected incidental Tc-99m MDP involvement was presented in a functionally active thyroid nodule. This appearance of Tc-99m MDP uptake in an active thyroid nodule, first demonstrated in this case, is thought to be secondary to the presence of microcalcifications in the nodule

Ethics

Informed Consent: Consent form was filled out by all participants.

Peer-review: Externally and internally peer-reviewed.

Authorship Contributions

Surgical and Medical Practices: D.Ç., Concept: D.Ç., Design: D.Ç., Data Collection or Processing: Ş.A., M.K., E.Ç., Analysis or Interpretation: D.Ç., M.A., Literature Search: D.Ç., M.A., Writing: D.Ç.

Conflict of Interest: The authors declared that they have no conflict of interests.

Financial Disclosure: The authors declared that this study received no financial support.

References

1. Langsteger W, Rezaee A, Pirich C, Beheshti M. 18F-NaF-PET/CT and 99mTc MDP Bone Scintigraphy in the Detection of Bone Metastases in Prostate Cancer. Semin Nucl Med 2016;46:491-501.
2. Subramanian G, McAfee JG. A new complex for 99mTc for skeletal imaging. Radiology 1971;99:192-196.
3. Subramanian G, McAfee JG, Blair RJ, Kallfelz FA, Thomas FD. Technetium-99m methylene diphosphonate: a superior agent for skeletal imaging: comparison with other technetium cornplexes. J Nucl Med 1975;16:744-755.
4. Peller PJ, Ho VB, Kransdorf MJ. Extraosseous Tc-99m MDP uptake: a pathophy-siologic approach. Radiographics 1993;13:715-734.
5. Bares R. Skeletal scintigraphy in breast cancer management. QJ Nucl Med 1998;42:43-48.
6. Padhy AK, Gopinath PG, Amini AC. Myocardial, pulmonary, diaphragmatic, gastric, splenic, and renal uptake ofTc-99m MDP inpatients with persistent, severe hypercalcemia. Clin Nucl Med 1990;15:648-664.

Interesting Image
Mol Imaging Radionucl Ther 2017;26:131-134 DOI:10.4274/mirt.70883

False Positive Perfusion/Ventilation SPECT Study for Pulmonary Embolism in a Patient with Fontan Circulation

Fontan Dolaşımlı Bir Hastada Pulmoner Emboli için Yanlış Pozitif Perfüzyon/Ventilasyon SPECT İncelemesi

Emmanouil Panagiotidis
Royal Liverpool University Hospital, Clinic of Nuclear Medicine, Liverpool, UK

Abstract

Fontan circulation is the consequence of an operation that results in the flow of systemic venous blood to the lungs without passing through a ventricle. An 18-year old man with a history of congenital heart disease surgically treated with Fontan circulation, presented with pleuritic chest pain and a raised D-dimer level. Perfusion/ventilation SPECT was performed to exclude the possibility of pulmonary embolism (PE) that showed unilateral reduced perfusion of the left lung with a mismatched right upper lobe defect, suspicious of PE. However, subsequent computed tomography pulmonary angiogram and clinical follow-up excluded the possibility of PE, emphasizing the need for knowledge of potential pitfalls to avoid false interpretations. Given the fact that adult congenital heart disease population is growing, with the majority having single ventricle/Fontan circulation and being at risk for thromboembolic disease, knowledge of the perfusion pattern pitfalls is important to avoid false interpretation and preventing the misdiagnosis of PE in patients with Fontan physiology.

Keywords: Fontan circulation, perfusion/ventilation, single-photon emission computed tomography, pulmonary embolism, computed tomography pulmonary angiogram

Öz

Fontan dolaşım sistemik venöz kanın ventrikülden geçmeden akciğere ulaşmasına neden olan cerrahi girişime bağlıdır. Konjenital kalp hastalığı nedeniyle Fontan dolaşım cerrahisi geçirmiş 18 yaşında bir erkek hasta plöretik göğüs ağrısı ve yüksek D-dimer değeri ile başvurdu. Pulmoner emboliyi (PE) ekarte etmek amacıyla perfüzyon/ventilasyon SPECT yapıldı. PE için şüpheli olacak şekilde sol akciğerde unilateral perfüzyon azalması ve sağ üst lobda uyuşma defekti saptandı. Ancak bilgisayarlı tomografi pulmoner anjiyografi ve klinik takip ile PE olasılığı ekarte edildi. Çoğunluğu tek ventrikül/Fontan dolaşım sahibi ve dolayısıyla tromboembolik hastalık riski altında olan erişkin konjenital kalp hastalıklı popülasyonundaki artış göz önünde tutularak, Fontan fizyolojisi olan hastalarda PE yanlış tanısını ve yanlış yorumu engellemek için perfüzyon patern tuzaklarının bilinmesi önemlidir.

Anahtar kelimeler: Fontan dolaşım, perfüzyon/ventilasyon, tek-foton emisyon bilgisayarlı tomografisi, pulmoner emboli, bilgisayarlı tomografi pulmoner anjiyografi

Address for Correspondence: Emmanouil Panagiotidis MD, Royal Liverpool University Hospital, Clinic of Nuclear Medicine, Liverpool, UK
Phone: +44(0)151-706-2000 E-mail: m_panagiotidis@yahoo.com ORCID ID: orcid.org/0000-0002-8501-3905
Received: 19.12.2016 **Accepted:** 24.07.2017

©Copyright 2017 by Turkish Society of Nuclear Medicine
Molecular Imaging and Radionuclide Therapy published by Galenos Yayınevi.

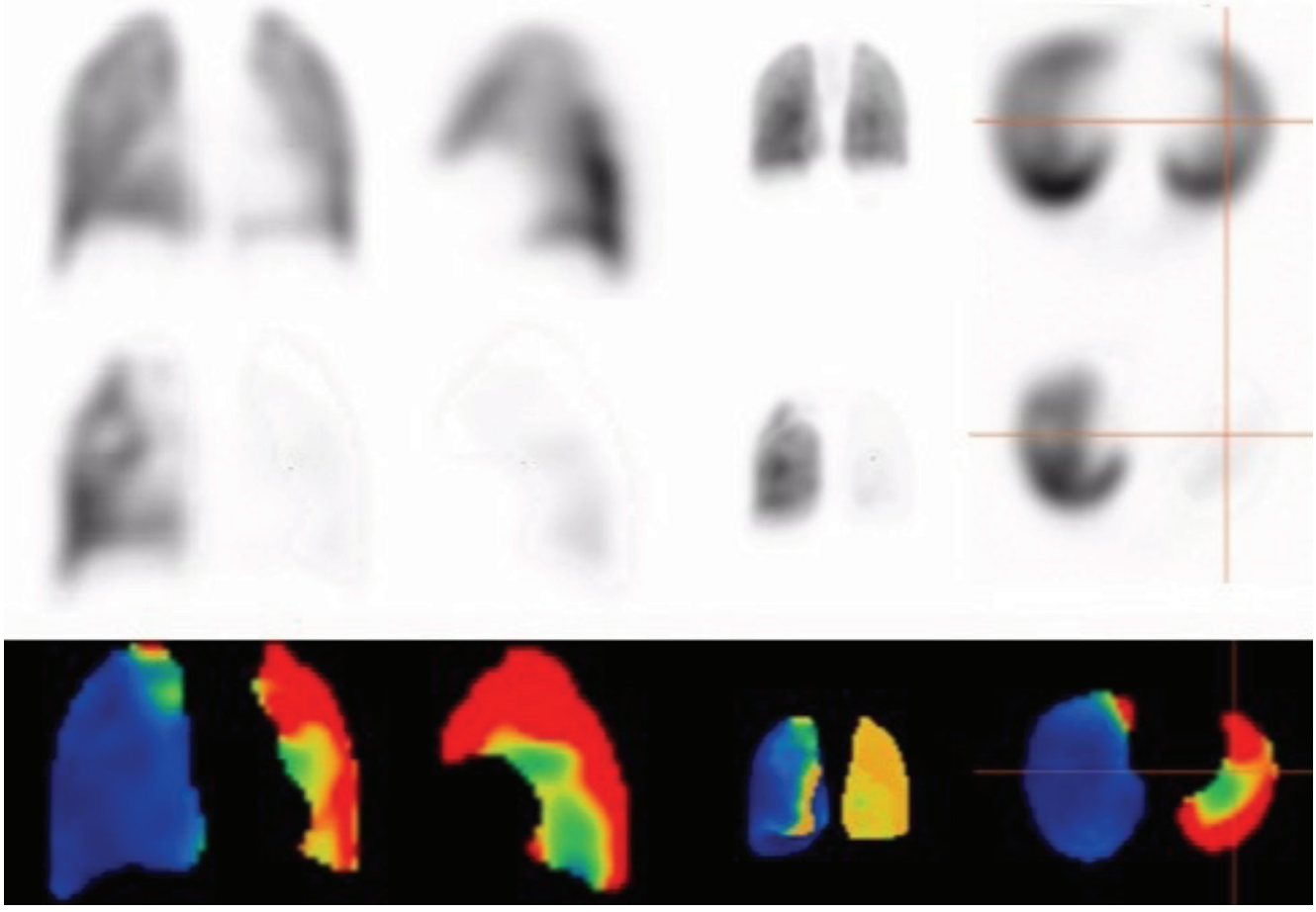

Figure 1. SPECT: First row: Ventilation with technegas, second row: Perfusion with 200 MBq of Tc-99m MAA, and third row: Subtraction of anterior, left lateral, MIP and transaxial images. There is satisfactory ventilation in both lungs. However, there is nearly no perfusion in the left lung (cross in transaxial images). Moreover, there is a subsegmental perfusion/ventilation mismatched defect in the right upper lobe, raising the possibility of pulmonary embolism (PE)

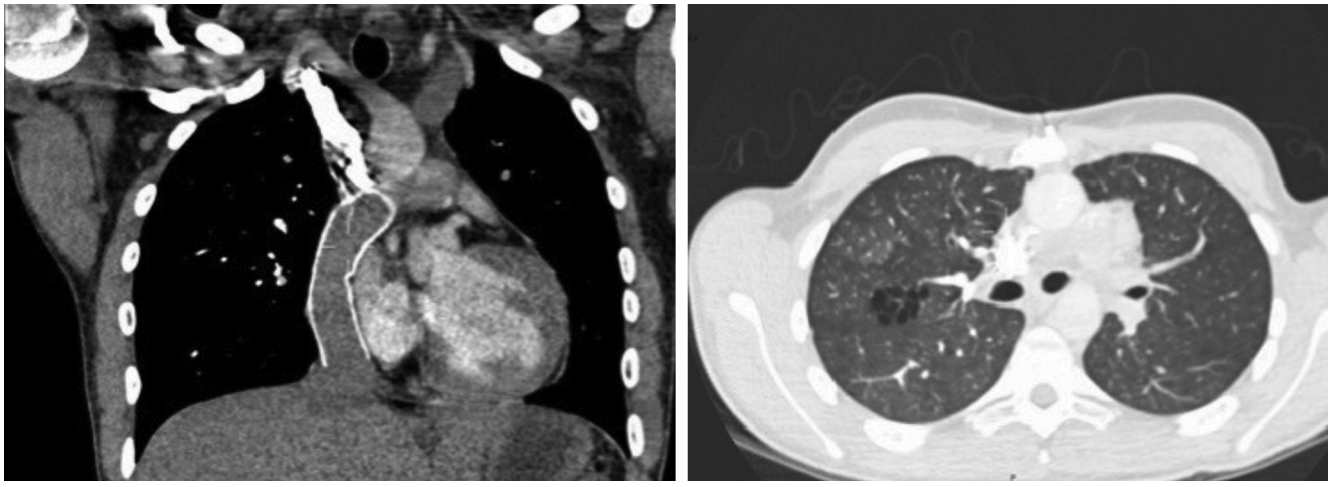

Figure 2. Computed tomography (CT) pulmonary angiogram coronal and transaxial images below the level of the carina. A extra cardiac conduit demonstrated with the superior vena cava (SVC) to pulmonary arteries (PA) and a stent within the intra-thoracic inferior vena cava (IVC) which enters the right PA resulting to single ventricle/Fontan physiology. There is non-opacified blood within the stent as a result of passive venous supply to the lungs in Fontan circulation and IV contrast seen within the stent post upper extremity contrast administration and passive venous supply to the lungs. There is also a hypoplastic right ventricle. The peripheral PA are patent with no evidence of distal PE. There is ground glass shadowing in the right upper lobe with minor cystic changes, which could represent an atypical infection.

The Fontan procedure refers to any surgical procedure that leads to systemic flow of venous blood to the lungs without passing through a ventricle. In 1971, Fontan and Baudet (1) described a surgical procedure for repair of tricuspid atresia that was built on experimental and clinical research since the 1940s. The principle of the Fontan operation is diversion of systemic venous return directly to the PA, thus by-passing the right ventricle when the latter is nonexistent, too small, or dysfunctional (2).

Thromboembolism can be a significant cause of morbidity and mortality after the Fontan operation, with contributing risk factors including low flow state, stasis in venous pathways, right to left shunt, blind cul de sacs, prosthetic materials and/or arrhythmias (3,4,5). It has been demonstrated that the prevalence of silent PE in adult patients with Fontan circulation was 17%, while the long-term hemodynamic implications of this with respect to Fontan attrition over time have been unknown (3). Fontan circulation can mimic PE on perfusion lung imaging. Unilaterally decreased relative lung perfusion is the most common perfusion abnormality seen in patients with congenital heart disease such as congenital absence of PA, wherein ipsilateral lung perfusion occurs through collaterals from bronchial arteries that cannot be assessed by lung perfusion except in patients with a functioning right to left shunt (6). Other differential diagnoses of unilateral absence of lung perfusion include pulmonary aplasia (absence of ipsilateral PA, absence of ipsilateral pulmonary tissue, and bronchus terminating in dilated blind pouch), hyperlucent lung syndrome, and tetralogy of Fallot (7). However, the most common pattern in perfusion scan of congenital heart disease is unilateral decreased lung perfusion, as in our case (8).

Several methods to minimize misdiagnosis of PE in Fontan patients have been proposed. Misinformation regarding pulmonary flow patterns can occur because of preferential blood flow from the SVC to the right PA and from the IVC to the left PA. A proposed protocol to resolve this problem includes injection of macroaggregates for perfusion scanning into the arm and any foot vein. Moreover, the timing of image acquisition with contrast during CT pulmonary angiography is also critical to prevent false positive diagnoses.

Given the fact that adult congenital heart disease population is growing, with the majority having single ventricle/Fontan circulation and being at risk for thromboembolic disease, knowledge of the perfusion pattern pitfalls is important to avoid false interpretation and preventing the misdiagnosis of PE in patients with Fontan physiology

Ethics

Informed Consent: Consent form was filled out by all participants.

Peer-review: Externally and internally peer-reviewed.

Financial Disclosure: The author declared that this study received no financial support.

References

1. Fontan F, Baudet E. Surgical repair of tricuspid atresia Thorax 1971;26:240-248.
2. de Leval MR. The Fontan circulation: what have we learned? What to expect? Pediatr Cardiol 1998;19:316-320.
3. Varma C, Warr MR, Hendler AL, Paul NS, Webb GD, Therrien J. Prevalence of "silent" pulmonary emboli in adults after Fontan operation. J Am Coll Cardiol 2003;41:2252-2258.
4. Balling G, Vogt M, Kaemmerer H, Eicken A, Meisner H, Hess J. Intracardiac thrombus formation after the Fontan operation. J Thorac Cardiovasc Surg 2000;119:745-752.
5. Monagle P, Cochrane A, McCrindle B, Benson L, Williams W, Andrew M. Thromboembolic complications after Fontan procedures-the role of prophylactic anticoagulation. J Thorac Cardiovasc Surg 1998;115:493-498.
6. White RI Jr, James AE Jr, Wagner HN Jr. The significance of unilateral absence of pulmonary artery perfusion by lung scanning. Am J Roentgenol Radium Ther Nucl Med 1971;111:501-509.
7. Wu MT, Huang YL, Hsieh KS, Huang JT, Peng NJ, Pan JY, Huang JS, Yang TL. Influence of Pulmonary Regurgitation Inequality on Differential Perfusion of the Lungs in Tetralogy of Fallot After Repair: A Phase-Contrast Magnetic Resonance Imaging and Perfusion Scintigraphy Study. J Am Coll Cardiol 2007;49:1880-1886.
8. O'Laughlin MP, Slack MC, Grifka RG, Perry SB, Lock JE, Mullins CE. Implantation and intermediate-term follow-up of stents in congenital heart disease. Circulation 1993;88:605-614.

2017 Referee Index - 2017 Hakem Dizini

A. Özgür Karaçalıoğlu
Ahmet Tutuş
Ali Sarıkaya
Ayşe Aktaş
Ayşe Mavi
Aziz Murat Argon
Bengul Gunalp
Bilge Volkan salancı
Bircan Sönmez
Bülent Turgut
Cengiz Taşçı
Çiğdem Soydal
Csaba Juhasz
Doğan Bor
Emel Ceylan Günay
Emre Entok
Erkan Vardareli
Fevziye Canbaz Tosun
Feyza Şen
Fikriye Gül Gümüşer
Funda Aydın
Gonca Kara Gedik
Gülay Durmuş Altun
Hakan Demir
Hamid Amer
Irena Dimitrova Kostadinova
Mahmut Yüksel
Majid Assadi
Meliha Korkmaz
Metin Kır
Murat Tuncel
Murathan Sahin
Nalan Alan Selçuk
Nuri Arslan
Olga Yaylalı
Ömer Uğur
Pelin Arıcan
Seval Erhamamcı
Seyhan Karacavus
Seyhan Karaçavuş
Taner Erselcan
Tansel Ansal Balci
Ülkem Yararbaş
Ümit Özgür Akdemir
Yakup Yürekli

2017 Subject Index - 2017 Konu Dizini

18F-2'-deoxy-2-fluoro-d-glucose/*18F-2'-deoksi-2-fluoro-d-glukoz* 47
18F-FDG/*18F-FDG* 93
18F-fluorodeoxyglucose positron emission tomography/computed tomography/*18F-fluorodeoksiglukoz pozitron emisyon tomografi/bilgisayarlı tomografi* 83,116
18F-fluorodeoxyglucose/*18F-florodeoksiglukoz* 1,78,93
Abscess/*Apse* 47
Adenoid cystic carcinoma/*Adenoid kistik karsinom* 120
Attenuation correction/*Atenüasyon düzeltme* 110
Beta radiation/*Beta radyasyonu* 53
Bone marrow biopsy/*Kemik iliği biyopsisi* 69
Bone scan/*Kemik sintigrafisi* 43
Bone scintigraphy/*Kemik sintigrafisi* 101
Breast/*Meme* 120
Camptodactyly-arthropathy-coxa-vara-pericarditis/*Kamptodaktili-artropati-koksa vara-perikardit* 33
Castration-resistant prostate cancer/*Kastrasyona dirençli prostat kanseri* 63
Computed tomography pulmonary angiogram/*Bilgisayarlı tomografi pulmoner anjiyografi* 131
Diabetes/*Diyabet* 17
Ectopic kidney/*Ektopik böbrek* 43
Endometrial cancer/*Endometrium kanseri* 24
False-positive/*Yanlış-pozitif* 43
Fluorodeoxyglucose positron emission tomography/computed tomography/*Florodeoksiglukoz pozitron emisyon tomografi/bilgisayarlı tomografi* 9
Fontan circulation/*Fontan dolaşım* 131
Gastric emptying/*Mide boşalması* 17
Gastroparesis/*Gastroparezi* 17
Geant4 Monte Carlo simulation/*Geant4 Monte Carlo simülasyonu* 53
Hodgkin's lymphoma/*Hodgkin lenfoma* 9,69
Hypophysis/*Hipofiz* 120
Infection/*Enfeksiyon* 47
Inflammation/*Enflamasyon* 47
Iodine-131/*İyot-131* 43
Iterative reconstruction/*İteratif rekonstrüksiyon* 110
Kidney/*Böbrek* 124
Lu-177-PSMA/*Lu-177-PSMA* 63
Magnetic field/*Manyetik alan* 53
Magnetic resonance imaging/*Manyetik rezonans görüntüleme* 101
Maximum standardized uptake value/*Maksimum standardize tutulum değeri* 24
Metabolic tumor parameters/*Metabolik tümör parametreleri* 83
Metabolic tumor volume/*Metabolik tümör volümü* 9
Metastasis/*Metastaz* 120
Minimum apparent diffusion coefficient/*Minimum görünen difüzyon katsayısı* 24
Myocardial perfusion SPECT/*Miyokard perfüzyon SPECT* 110
Neuroendocrine tumors/*Nöroendokrin tümörler* 38
Non-Hodgkin's lymphoma/*Non-Hodgkin lenfoma* 69
Parathyroid carcinoma/*Paratiroid kanseri* 116
Perfusion/ventilation/*Perfüzyon/ventilasyon* 131
PET/CT/*PET/BT* 93,120
PET/*PET* 93
Positron emission tomography/computed tomography/*Pozitron emisyon tomografisi/bilgisayarlı tomografi* 47,69,78
Positron emission tomography/*Pozitron emisyon tomografisi* 1,93
Primary gastrointestinal lymphoma/*Primer gastrointestinal lenfoma* ... 83
Prone positioning/*Pron pozisyon* 110
Prostate cancer/*Prostat kanseri* 63,78
Prostate incidentaloma/*Prostat bezi insidentaloması* 78
Prostate specific antigen/*Prostat spesifik antijen* 78
Prostate-specific membrane antigen/*Prostat spesifik membran antijen* 63
PSMA/*PSMA* 63
Pulmonary embolism/*Pulmoner emboli* 131
Radionuclide imaging/*Radyonüklid görüntüleme* 124,128
Radionuclide therapy/*Radyonüklit tedavi* 63
Radiosynovectomy/*Radyosinovektomi* 33
Rat/*Sıçan* 47
S. aureus/*S. aureus* 47
Sacroiliitis/*Sakroiliit* 101
Scintigraphy/*Sintigrafi* 17,38
Single-photon emission computed tomography/*Tek-foton emisyon bilgisayarlı tomografisi* 131

2017 Subject Index - 2017 Konu Dizini

Single-photon emission computerized tomography/*Bilgisayarlı-tek foton emisyonlu tomografi*..... 38
SPECT/*SPECT*..... 101
Spondyloarthritis/*Spondiloartrit*..... 101
Standardized uptake value/*Standart tutulum değeri*..... 9
Super scan/*Süper görüntü*..... 116
Tc-99m medronate/*Tc-99m medronat*..... 124,128
Thyroid cancer/*Tiroid kanseri*..... 1,43
Thyroid carcinoma/*Tiroid karsinoma*..... 93
Thyroid incidentaloma/*Tiroid insidentaloma*..... 93
Thyroid nodule/*Tiroid nodülü*..... 128
Turpentine/*Terebentin*..... 47
Von Hippel-Lindau disease/*Von Hippel-Lindau hastalığı*..... 38
Yttrium-90/*İtriyum-90*..... 33,53

2017 Author Index - 2017 Yazar Dizini

Adil Boz 69
Ahmet Polat 43
Akın Yıldız 69
Ali Mahmoud-Pashazadeh 17
Ali Ozan Öner 24,69,120
Ali Sarıkaya 43
Anthony Ciarallo 76,93
Aslan Aygün 62
Atila Gökçek 9
Bahar Akkaya 69
Berna Okudan Tekin 38
Berrin Çavuşoğlu 53
Can Çevikol 24
Cumhur Heper 83
Derya Çayır 1,124,128
Dilek Berker 38
Dimitrios Kassimos 101
Duygu Kuşlu 110
Ebru Tatcı 9
Emel Öztürk 110
Emmanouil Panagiotidis 131
Emre Demirci 62
Emre Karayel 62
Engin Alagöz 9,83
Erman Çakal 128
Esmail Jafari 17
Evrim Sürer Budak 24,69,120
Fırat Güngör 69
Foad Khatib 17
Funda Aydın 24,69
George Angelidis 101
Gül Ege Aktaş 43
Gülgün Oktay 47
Gürses Şahin 9
Hakan Epik 53
Hamid Javadi 17
Hatice Durak 47,53
Hikmet Gülşah Tanyıldız 9
Hüseyin Pehlivanoğlu 62
Hüseyin Tuğsan Ballı 116
Iraj Nabipour 17
İnci Uslu Biner 9
İsa Burak Güney 116
John Koutsikos 101
Kadir Akgüngör 53
Khalid Alismail 33
Kürşat Okuyucu 83
Leila Aghaghazvini 17
Levent Kabasakal 62
Levent Undar 69
Majid Assadi 17
Mehmet Erdoğan 124
Melia Karaköse 128
Meltem Ocak 62
Meral Karaman 47
Mine Araz 1,124,128
Mine Sencan Eren 47
Mohammad Abuqbeitah 62
Murat Kantarcıoğlu 83
Mustafa Filik 124
Nalan Alan Selçuk 62
Nami Yeyin 62
Nora Almutairi 33
Nuri Arslan 83
Orhan Kemal Yücel 69
Ozan Salim 69
Özlem Özmen 9
Pelin Arıcan 38
Rıza Şefizade 38
Selda Sucu 53
Selin Soyluoğlu Demir 43
Semra İnce 83
Semra Paydaş 116
Seniha Naldöken 38
Sevim Yıldız 120
Seyed Masoud Tabib 17
Sulaiman Mohammed Al-Mayouf 33
Suna Emir 9
Şafak Akın 128
Şenay Yıldırım 120
Şeyda Gündüz 120
Şükrü Özaydın 83
Tayfun Toptaş 24,69
Tayup Şimşek 24
Theodoros Pipikos 101
Türkan Ertay 47,53
Türkay Toklu 62
Türker Türker 83
William Makis 76,93
Zeinab Alipour 17

Türkiye Nükleer Tıp Derneği

TİROİD HASTALIKLARI SEMPOZYUMU ve TİROİD ULTRASONOGRAFİ KURSU

18-19 Kasım 2017

THE MARMARA OTEL, İSTANBUL

BİLİMSEL SEKRETERYA

TÜRKIYE NÜKLEER TIP DERNEĞİ

Cinnah Caddesi Pilot Sokak No:
10/12 – 06690, Çankaya ANKARA
Tel: +90 (0312) 441 00 45
Faks : +90 (0312) 441 12 97
E-posta: dernekmerkezi@tsnm.org
Web: www.tsnm.org

ORGANİZASYON SEKRETERYASI

SERENAS ULUSLARARASI TURİZM KONGRE ORGANİZASYON A.Ş.

Hilal Mh. Cezayir Cd.
No:13, 06550 Yıldız,
Çankaya - ANKARA
T: +90 (312) 440 50 11
F: +90 (312) 441 45 62
E-posta: yasemin.cekirdek@serenas.com.tr
Web: www.serenas.com.tr